Co-operative Programme for Monitoring and Evaluation of the Long-Range Transmission of Air Pollutant in Europe

EMEP

Long-Range Transport of Selected Persistent Organic Pollutants

Part I

Development of Transport Models for Lindane, Polychlorinated Biphenyls, Benzo(a)pyrene

M.Pekar, N.Pavlova, L.Erdman, I.Ilyin,
B.Strukov, A.Gusev, S.Dutchak

With contributions from: W.A.J. van Pul, RIVM, The Netherlands

EMEP/MSC-E Report 2/98

August 1998

METEOROLOGICAL SYNTHESIZING CENTRE - EAST

Kedrova str.8-1, Moscow, 117 292, Russia

Tel.: 007 095 124 47 58

Fax: 007 095 310 70 93

e-mail: msce@glasnet.ru

Preface

The report “Long-range transport of selected POPs” was prepared for the twenty second session of the Steering Body of Co-operative Programme for Monitoring and Evaluation of the Long-Range Transmission of Air Pollutant in Europe (EMEP).

The environment pollution by persistent organic pollutants (POPs) is of a great concern at national and international levels. This problem is being attacked by a number of International organizations like AMAP, UNEP, HELCOM, PARCOM and others. The most extensive efforts in this field are made within the framework of the Convention on Long-Range Transboundary Air Pollution. The latest achievement in this field is the adoption and signing of the Persistent Organic Pollutants Protocol (Arhus, Denmark, June 1998). Under this Protocol, EMEP should provide countries with information on the long-range transport of POPs. Nowadays investigations of physical-chemical properties of selected POPs, their behaviour in different compartments and the evaluation of POPs transport on the regional level are in progress under EMEP. This activity is oriented to devising mathematical models describing POPs transport in the atmosphere and exchange processes between different compartments. Modelling results will provide information on deposition and exposure required for effect-oriented approach and abatement strategy.

This report is prepared under the EMEP work-program and dedicated to the simulation of selected POPs transport and to study of factors, impacting the distribution and accumulation of these species in the environment. Part I of this report contains a description of POPs transport model coupled with atmosphere-surface exchange blocks and calculation results of lindane, polychlorinated biphenyls (PCB) and benzo(a)pyrene (B(a)P) airborne transport.

For better understanding of the POPs behaviour in different compartments the global model, described in *A.Strand and Ø.Hov* [1996] and provided with MSC-E, was launched. Some results are included in this report.

In addition the sensitivity study of the POPs transport model has been performed in order to evaluate the model response to variations of a number of physical-chemical parameters of POPs.

Part II of the report contains a detail description of physical-chemical properties of polychlorinated dibenzo-p-dioxins and dibenzofurans. Some consideration on the atmosphere/vegetation exchange, based on the available information on POPs air concentration and accumulation in plants are presented. Taking into account the importance of POPs re-distribution and accumulation in the marine environment the consideration of sea currents is included in this report.

Results of the studies included in Part II will provide the basis for the further development of POPs models.

Contents

Introduction

The Part I of the report “Long-range transport of Persistent Organic Pollutant” deals with a description of the structure and main modules of the persistent organic pollutants (POPs) model and results of simulation of POPs transport within the EMEP grid.

The basic model used for calculations of POPs transport is described in chapter 1. The model contains an atmospheric module based on the transport model ASIMD [*Pekar,* 1996] and modules of the atmosphere/soil and atmosphere/sea exchange developed in RIVM [*Jacobs and van Pul,* 1996].

In chapter 2 physical-chemical properties of lindane and modelling results of its transport and exchange with other compartments are considered. In addition exchange processes between different media on the global level were considered using the model described in [*Strand and Hov,* 1996].

Chapter 3 contains a description of PCB physical-chemical properties and simulation results of PCB transport in the atmosphere and its exchange with soil and sea compartments.

Chapter 4 is devoted to the description of B(a)P physical-chemical properties, and modelling results of B(a)P transport.

Chapter 5 deals with a study of model sensitivity to variations of main physical-chemical parameters of POPs.

Chapter 1 Description of the transport model for POPs

Calculations of lindane, PCB and B(a)P transport in the environment are made by the modified three-dimensional Eulerian model ASIMD [*Pekar,* 1996] conjugated with the atmosphere-soil and atmosphere-sea exchange modules described in the work [*Jacobs and van Pul,* 1996]. The basic model ASIMD (ASymmetric Improved MoDel) originally was developed for calculations of radioactive species transport, then it was used for modelling of acid compounds. Later it was modified for modelling of heavy metals transported on aerosol particles and as such it has participated in Pb model intercomparison study. The present version of the model is modified for calculation of POPs transport.

1.1 Description of the airborne transport model

Formulation of problem and space discretization

The modelling domain covers Europe, parts of the Atlantic and Polar Oceans and part of Greenland Island. Spatial resolution 150x150 km is used. In the vertical direction a grid with a variable gridsize of 100 m, 300 m, 700 m and 1000 m (Figure 1.1) is used. The time-step is 1 hour. When necessary a variable time-step is used.

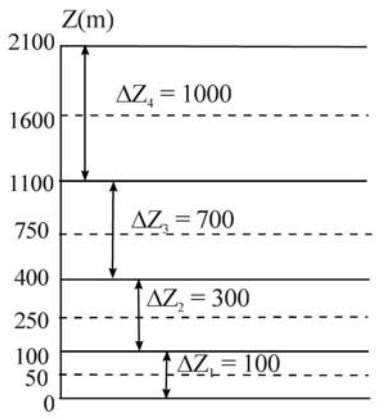

Figure 1.1 Vertical structure of the model

Advection - diffusion equation in Cartesian co-ordinates for passive pollutants is:

$$\frac{\partial C}{\partial t} = -u\frac{\partial C}{\partial x} - v\frac{\partial C}{\partial y} + K_{xy}\left(\frac{\partial^2 C}{\partial x^2} + \frac{\partial^2 C}{\partial y^2}\right) + \frac{\partial}{\partial z}\left(K_z \frac{\partial C}{\partial z}\right) + \\ + E - Deg - Dep_{A/O} - Dep_{A/S} - Wet \qquad (1.1)$$

where: C - concentration of passive pollutants, ng/m^3;

K_{xy} - horizontal coefficient of turbulent diffusion, m^2/s;

K_z - vertical coefficient of turbulent diffusion, m^2/s;

E - rate of pollutant input to the atmosphere due to emissions, ng/m^3/s;

Deg - rate of pollutant degradation in the atmosphere, ng/m^3/s;

$Dep_{A/O}$ - rate of atmosphere/sea surface pollutant exchange, ng/m^3/s;

$Dep_{A/S}$ - rate of atmosphere/soil surface pollutant exchange, ng/m^3/s;

Wet - rate of pollutant scavenging from the atmosphere due to precipitation, ng/m^3/s.

Eq.(1.1) is solved numerically.

The first 2 terms in the right side of Eq.(1.1) describe the airborne transport of a pollutant. The finite-difference scheme approximating the advection terms is described below in the section entitled «Horizontal transport».

The next 2 terms describe horizontal and vertical diffusion of a substance in the atmosphere. For the approximation of diffusion terms an explicit finite-difference scheme in a non-uniform grid is used. The coefficients of turbulent diffusion are calculated on the basis of the boundary atmospheric layer model. This model is described in section “Parametrizaiton of the boundary layer”.

A separate module operates with emissions (E) in such a way that at each time-step the pollutant mass is added depending on spatial and temporal distribution of the emissions.

The degradation (*Deg)* is also calculated in a separate module, which considers pollutant mass decrease in accordance with the life-time of the pollutant considered in the compartments mentioned above.

The exchange of a pollutant with the ocean ($Dep_{A/O}$) and the soil ($Dep_{A/S}$) (including dry deposition and re-emission processes) is calculated by the model of *C.M.J.Jacobs and W.A.J.van Pul* [1996]. The modules of the exchange with the soil and ocean are described in subsection 1.2 «Surface-atmosphere exchange module».

Wet deposition module (Wet) is described in section «Wet deposition».

Hence the total mass balance of pollutants has the form:

$$Q = \sum E = M_A + M_O + M_S - Deg_A - Deg_O - Deg_S - M_{OUT} \qquad (1.2)$$

where $\sum E$ - total emissions;

M_A, M_O, M_S - pollutant mass in the air, ocean and soil;

Deg_A, Deg_O, Deg_S - pollutant mass degraded in the air, ocean and soil;

M_{OUT} - pollutant mass transported outside the grid.

Gas-aerosol partitioning of POPs is described in section “Distribution of gaseous and aerosol POPs ”.

Horizontal transport

Finite - difference approximation is realized within the framework of classical “upwind scheme” for which numerical diffusion is well known. Compensation of numerical diffusion is realized by correcting of advection velocities depending on the local gradients. The resulting velocity and real velocity are connected by a non-linear equation.

Let us consider the one-dimensional equation (symbols are commonly accepted):

$$\frac{\partial C}{\partial t}+\frac{\partial (uC)}{\partial x}=0 \tag{1.3}$$

and apply it to grid element $C_i^n = C(x_i, t_n), x_i = (i+1/2)\Delta x, t_n = n\tau$ (Δx - grid-size, τ-time step). The method used for devising difference approximations is complying with distribution:

$$\Delta C_i^k = p_i^k C_i^n \tag{1.4}$$

where:

p_i^k = weights determining the contributions of element C_i^n to the neighbouring *k*-th cells.

In this presentation a standard scheme of directed differences for Eq.(1.3) is ($R_i = u_i\,\tau/\Delta x,\ u_i > 0$):

$$\begin{aligned} p_i^i &= 1-R_i, \\ p_i^{i+1} &= R_i. \end{aligned} \tag{1.5}$$

Scheme (1.5) has artificial viscosity with coefficient:

$$\chi=\frac{1}{2}\left(u\Delta x-u^2\tau\right) \tag{1.6}$$

In order to compensate this viscosity we are to find an approximation for the equation:

$$\frac{\partial C}{\partial t}+\frac{\partial}{\partial x}\left\{C\left(u+\frac{\tilde{\chi}}{C}\frac{\partial C}{\partial x}\right)\right\}=\tilde{\chi}\frac{\partial^2 C}{\partial x^2} \tag{1.7}$$

where:

$$\tilde{\chi}=\frac{1}{2}\tilde{u}\Delta x-\frac{1}{2}\tilde{u}^2\tau,\ \tilde{u}=u+\frac{\tilde{\chi}}{C}\frac{\partial C}{\partial x} \tag{1.8}$$

In Eq.(1.8), $\tilde{\chi}$ and $\tilde{u}$ are interrelated; exclusion of $\tilde{\chi}$ from Eq.(1.8) results in a non-linear equation for $\tilde{u}$ depending on *u* and a local gradient:

$$\tilde{u}=u+\frac{1}{2}\left(\tilde{u}\Delta x-\tilde{u}^2\tau\right)\frac{1}{C}\frac{\partial C}{\partial x} \tag{1.9}$$

Assuming for the *i*-th element:

$$\left(\frac{1}{C}\frac{\partial C}{\partial x}\right)_i = \frac{2}{\Delta x}\frac{C_{i+1}-C_i}{C_{i+1}+C_i} \quad \text{if } u_i > 0;$$

$$\left(\frac{1}{C}\frac{\partial C}{\partial x}\right)_i = \frac{2}{\Delta x}\frac{C_{i-1}-C_i}{C_{i-1}+C_i} \quad \text{if } u_i < 0; \tag{1.10}$$

and solving (1.9), we obtain:

$$\tilde{R}_i = \frac{-1+\sqrt{1+\left(a_i^2-1\right)R_i}}{a_i-1} \quad \text{if } a_i \neq 1;$$

$$\tilde{R}_i = R_i \quad \text{if } a_i = 1; \tag{1.11}$$

Here, $R_i = u_i\tau/\Delta x, \tilde{R}_i = \tilde{u}_i\tau/\Delta x, a_i = C_{i\pm1}/C_i$ (signs +/- correspond to velocity).

The second formula of Eq.(1.11) shows the lack of compensation of artificial viscosity in the region where $\partial C/\partial x = 0$, in smooth parts of the field. In such a way we obtain an analogue to "upwind" scheme ($u_i > 0$):

$$p_i^i = 1-\tilde{R}_i,$$
$$p_i^{i+1} = \tilde{R}_i. \tag{1.12}$$

where $\tilde{R}_i$ is determined by formulae (1.11).

Parametrization of the boundary layer

A system of parameters required for the description of local conditions of pollution dispersion consists of friction velocity u_* (m/s), Monin-Obukhov length scale L(m), mixing layer height h (m) and vertical diffusion coefficient profiles $K_z(z)$ (m^2/s) which were derived on the basis of the data on 1000 mb wind, temperature and roughness z_0. The roughness data were taken from the article "Global Data Set for Land-Atmosphere Models" received in "International Satellite Land Surface Climatology Project" (ISLSCP). The database contains global data on roughness with resolution $1^0\times1^0$ averaged over a month. Monthly data for 1988 were used in the model.

A meteorological pre-processor is based on the method of energetic balance evaluation with further application of results to similarity theory [*Holtslag and van Ulden*, 1983; *van Ulden and Holtslag*, 1985]. The parameter calculations were made for each 6-hour interval (0003, 0009, 0015, 0021 UTC).

The procedure is as follows:

1. The solar inclination angle φ is calculated for each point with geographical co-ordinates λ, ϕ (longitude, latitude) for a day of the year and time of the day.
2. According to φ a flux of solar short-wave radiation is calculated as follow:

   $$K^* = (990\cdot\sin\varphi - 30)\cdot(1-0.75N^{3.4})(1-r), \tag{1.13}$$

   where N - cloud coverage fraction; r - albedo, $K^* = 0$, if $\varphi < 1.7^0$.

   It was assumed that $N = 1$ with precipitation events, $N = 0.4$ in all other cases.

3. Balance of solar short-wave radiation and long-wave radiation of the atmosphere and ground surface determines the positive flux of sensible heat in the atmospheric surface layer in the daytime:

$$H_0 = 0.4(K^* - 91 + 60 \cdot N) \geq 0 \tag{1.14}$$

At night ($H_0 < 0$) the heat flux cannot be presented in such a simple form since it is in a complicated relationship with friction velocity u_*. Here we take rougher estimate of heat flux than in [*van Ulden and Holtslag*, 1985], where the calculation gives the dependence of temperature scale θ_* on u_* for night conditions. Taking into account that at velocities $u_* > 0.1$ m/s, θ_* is slightly dependent on u_* we take constant value $\theta_* = 0.065\ ^0K$ for negative fluxes.

4. Monin-Obukhov length scale is expressed as:

$$L = -\frac{\rho C_p T u_*^3}{kgH_0} = \frac{u_*^2 T}{kg\theta_*}, \tag{1.15}$$

where ρ is air density, C_p is the specific heat of dry air, k is von Karman`s constant, g is acceleration due to gravity.

Friction velocity, u_* determines universal wind profile in the surface layer:

$$u(z) = \frac{u_*}{k}\left[\ln(z/z_0) - \psi_m(z/L) + \psi_m(z_0/L)\right], \tag{1.16}$$

where:

$$\psi_m(z/L) = -17(1 - \exp(0.29\ z/L)), \quad \text{if} \quad L>0 \tag{1.17}$$

$$\psi_m(z/L) = (1 - 16z/L)^{1/4} - 1, \quad \text{if} \quad L<0 \tag{1.18}$$

(function (1.17, 1.18) are presented in [*van Ulden and Holtslag*, 1985], as approximations valid for a wider range than $z<L$). When wind and temperature data are available at two levels z iteration method [*Berkowicz and Prahm*, 1982] can be applicable to the solution of two highly non-linear equations (1.15, 1.16) with allowance for (1.17, 1.18). We used less accurate technique. For this purpose supplementary empirical data of power dependence of wind on height making up for the absence of data from the second level were invoked:

$$u(z) = u_r(z/z_r)^p, \tag{1.19}$$

where $u_r = (u_{1000}^2 + v_{1000}^2)^{1/2}$, $z_r \cong 200$ m

According to data of *J.S.Irwin* [1979] the following values for exponent p depending on stability is assumed:

$$p = \begin{cases} 0.10, if\ L > -200m \\ 0.16, if\ L > 200m \\ 0.32, if\ L < 200m \end{cases} \tag{1.20}$$

All calculations are made for z = 50 m. An appropriate exponent profile also defines wind speeds at lower 100 m layer. The wind rotation with height is neglected.

The stability over the sea was assumed to be neutral and then [*Lindfors et al*, 1991]:

$$\begin{aligned} &u_* = \sqrt{C_d}\,u_{10}, \\ &C_d = 0.0012, \text{if } u_{10} \le 11 m/s, \\ &C_d = \left(0.49 + 0.065 u_{10}\right)\cdot 10^{-3}, \text{if } u_{10} > 11 m/s, \end{aligned} \tag{1.21}$$

here C_d - friction coefficient, u_{10} - wind speed at 10 m.

5. The mixing layer height is a significant parameter for the evaluation of the coefficient of vertical diffusion K_z (z). The temporal variation in the mixing layer height makes it possible to reproduce fumigation process.

   For the mixing layer height (h) under stable and neutral conditions the well known expression is used:

$$h = C_1 u_* / f\,, \tag{1.22}$$

   where f - Coriolis parameter.

   For coefficient C_1 there is a great choice from 0.07 to 0.4. It was accepted that C_1 = 0.2.

   For the convective layer, there are no similar diagnostic formulas since under these conditions, the mixing layer height h_C is progressively varying with time though for strong convection, a simple formula is suggested [*Sorbjan*, 1994]:

$$\overline{(w'\theta')}_s = 0.75 \cdot h_C \cdot \frac{\Delta\theta}{\Delta t}, \tag{1.23}$$

   where $\overline{(w'\theta')}_s$ - temperature flux near the surface, $\overline{(w'\theta')}_s = H_0 / \rho C_p, \Delta\theta/\Delta t$ - temporal variation in potential temperature in the convective layer, h_C - convective layer height of mixing. Further it is supposed to investigate a possibility of the application of (1.23).

   There are several methods for the determination of the convective mixing layer and some of them are based on non-linear equation of type:

$$\frac{\partial h_C}{\partial t} = f\left(h_C, \overline{(w'\theta')}_s, \gamma, L, u_*\right)$$

   (γ - gradient of potential temperature above the mixing layer).

   For lack of some required data as well as due to inefficient application of a numerical solution of this equation each grid point, following direct dependence h_C on the surface heat flux was derived while testing the algorithm suggested by *G.H.L.Verver and M.P.Scheele* [1989]:

$$h_C = 150 + 7 \cdot H_0 \tag{1.24}$$

   where h_C in [m], H_0 in [W/m^2].

6. Profiles of vertical diffusion coefficient in the surface layer are derived from locally determined u_* and L means [*Businger*, 1973] for 6-hour interval:

$$K_z(z) = \frac{ku_* z}{\phi(z/L)}, \tag{1.25}$$

where $\phi(z/L)$ - similarity function for heat:

$$\begin{aligned} &\phi(z/L) = 0.74(1-9z/L)^{-1/2}, \quad \text{if } L<0 \\ &\phi(z/L) = 0.74 + 4.7\, z/L, \qquad \text{if } L>0 \end{aligned} \tag{1.26}$$

The profiles K_z(z) were extended along the vertical of the boundary layer in the following way:

a) for the neutral layer the formula given by *C.C.Shir* [1973] is used:

$$K_z(z) = ku_* z e^{-4z/h}, \tag{1.27}$$

b) for stable layer *K.S.Rao and H.F.Snodgrass* profile [*Rao and Snodgrass*, 1976]:

$$K_z(z) = \frac{ku_* z}{\phi(z/L)}\ e^{-0.9z/h}, \tag{1.28}$$

c) a profile similar to (1.27) was used for the convective layer:

$$K_z(z) = \frac{ku_* z}{\phi(z/L)}\ e^{-4z/h_C}, \tag{1.29}$$

which may lead to the underestimation of vertical diffusion under convective conditions.

Distribution of gaseous and aerosol POPs

The model assumes that the coefficient of the equilibrium distribution of gaseous and aerosol B(a)P, K_{pg}, is determined by Junge's formula [*Junge*, 1977]:

$$K_{pg} = \frac{C_{part}}{C_{tot}} = \frac{C\theta}{\mathrm{P_{0l}} + c\theta}$$

where $C_{tot} = C_{part} + C_g$ - total POP concentration in the atmosphere (ng/m^3); C_{par} and C_g - particulate and gaseous POP concentrations, respectively (ng/m^3); c - the constant equal to 0.17 Pa·m; θ (m^2/m^3) - specific aerosol surface; P_{0l} - saturated vapour pressure for overcooled liquid (Pa).

The data on the specific aerosol surface for different regions have been taken from [*Whitby,* 1978].

Data on specific aerosol surface for various regions [*Whitby,* 1978]

	Clean continental background	Average background	Average background & local sources	Urban
θ (m^2/m^3 air)	$4{\cdot}2{\cdot}10^{-5}$	$1.5{\cdot}10^{-4}$	$3.5{\cdot}10^{-4}$	$1.1{\cdot}10^{-3}$

Wet deposition

The quantity of pollutants washed out with precipitation was calculated on the assumption:

$C_A = K_H \cdot C_W$

$C_W = W \cdot C_A$;

C_A - air concentration;

C_W - concentration in rain water;

W – washout ratio;

$W = W_g = 1/K_H$ – for seasonal gaseous phase;

$W = W_p$ – for particle phase;

K_H – dimensionless Henry coefficient.

The dissolution rate of species in precipitation is not considered and it is assumed to be instantaneous.

In the calculation model containing 4 vertical layers of height 100, 300, 700 and 1000 m a layer-by-layer washout is used.

Washout in the N^{-th} upper calculation layer of Δz_N thickness is calculated in the following way:

$$\frac{\partial C_A}{\partial t} = \frac{h \cdot W \cdot C_A}{\Delta z_N}, \tag{1.30}$$

where h - precipitation intensity, m/s;

In the following layers ($1 \le k \le N$-1) the dissolution in precipitation is calculated taking into account the pollutant amount dissolved in the upper layer and existing there. Washout in the $k^{-\text{th}}$ layer of Δz_k thickness is calculated through formula:

$$\frac{\partial C_A}{\partial t} = \frac{h \cdot W \cdot (C_A - C_W^{k+1} \cdot K_H)}{\Delta z_k} \tag{1.31}$$

where $C_W^{k+1} = \sum_{j=N}^{k+1} F_k / h$ - pollutant concentration in precipitation upon its dissolution in the upper layers, and F_k - pollutant flux with precipitation from the $k^{-\text{th}}$ layer.

Dry deposition of particles

The current version of the model, like model [*Pekar*, 1996], includes the ordinary assumption that downward aerosol flux is proportional to the dry deposition velocity V_d, and the concentration in the lower model layer, C_1:

$F = V_d \cdot C_1$

In parameterizing dry deposition, the data on the spectral distribution are considered, with MMD equal to 0.84 μm being only taken into account as an «effective» size of the particles.

In accordance with model [*Pekar,* 1996], the velocities of dry deposition on the land, V_d^{land}, are calculated by the formulae based on *G.A.Sehmel's* [1980] results:

$$V_d^{land}(cm/s) = \left(0.04u_*^2 + 0.02\right)\cdot\left(Z_0/10^{-3}\right)^{0.33}\ **.$$

The velocity of dry deposition on the sea, V_d^{sea}, also calculated by the formula from model [*Pekar,* 1996] based on the results of *V.Lindfors et al.* [1991] and *R.Williams* [1982].

$$V_d^{sea}(cm/s) = 0.15u_* + 0.023\ **.$$

In the two expressions V_d is dry deposition velocity, u_* is friction velocity, Z_0(m) is roughness length.

A reasonable character of the formulas presented is supported by the actual coincidence of mean deposition velocities calculated by these formulas with those obtained by *J.van Jaarsveld* [1992] using data of [*van den Hout,* 1994] on the size distribution of cadmium - carrying aerosols [*Pekar*, 1996].

** adapted for B(a)P

Degradation in various compartments

It is assumed that degradation in all considered compartments is described by reaction of 1th order.

1.2 Surface-atmosphere exchange module

Fluxes of POP in the atmospheric surface layer

The gaseous exchange of POP at soil and sea surfaces is parameterized using a resistance analogy in the atmosphere. The flux of a POP, F_g at the surface is driven by the difference between the POP concentration at the reference level, C_{zr} and the concentration in the top layer of the soil or sea, $C_{soil,sea}$ and is controlled by a set of resistances assumed to operate in series:

$$F_d = \frac{C_{zr} - C_{soil,sea}}{r_a + r_b + r_s}. \qquad (1.32)$$

Here, r_a is the aerodynamic resistance between a reference level and the aerodynamic roughness length, z_0, r_b is the quasi-laminar boundary layer resistance that applies between z_0 and the average sink or source height of the substance, z_{0c} and r_s is the surface resistance. The aerodynamic and quasi-laminar boundary layer resistances (r_a and r_b) are calculated in the usual way [e.g., *Monteith and Unsworth,* 1990].

Soil-atmosphere exchange

In the case of soil, a formulation for r_s and C_{soil} can be derived that is consistent with (1.32) and with the theory of transport and storage of POPs in the soil. In the description of the transport and storage of POPs in the soil we follow *Jury et al.* [1983, 1991]. It is assumed that concentrations of POP in the solid, liquid and gas phases of the soil are in equilibrium. The

total concentration, C_T, is partitioned over the solid phase (C_s), the liquid phase (C_l) and the gas phase (C_g) as follows:

$$C_T = \rho_s C_s + \theta C_l + a C_g , \tag{1.33}$$

where ρ_s is the density of the solid material per cubic meter of soil volume, θ is the volumetric water content of the soil and a is the volumetric air content of the soil. The pollutant is assumed to obey Henry's law, so that:

$$C_g = K_H C_l , \tag{1.34}$$

where K_H is the dimensionless Henry coefficient. This coefficient depends on temperature and here, we use the parameterization as suggested in *GESAMP* [1989]. The ratio of C_s to C_l is assumed to be equal:

$$C_s = f_{oc} K_{oc} C_l , \tag{1.35}$$

where K_{oc} is the organic carbon distribution coefficient and f_{oc} is the fraction of organic carbon in soil. Using (1.33)-(1.34), partition coefficients for the liquid phase, the adsorbed phase and the gas phase (R_l, R_s and R_g, respectively) can be defined such that:

$$C_T = R_l C_l = R_s C_s = R_g C_g . \tag{1.35}$$

The flux of POP in the soil is given by:

$$J_T = V_E C_T - D_E \frac{\partial C_T}{\partial z} \tag{1.37}$$

where: $V_E = J_w / R_l$ is the solute velocity with J_w = convective water flux

D_E is the so-called effective gas-liquid diffusion coefficient:

$$D_E = \frac{\xi_g D_g}{R_g} + \frac{\xi_l D_l}{R_l} \tag{1.38}$$

Here, D_g and D_l are the molecular diffusion coefficients of the POP in gas and water, respectively. Furthermore, ξ_g and ξ_l are the so-called gas and liquid tortuosity factors, by which the effect of the reduced flow area and the longer diffusion path in the soil is accounted for.

The gas exchange is assumed to occur between the atmosphere and a thin top layer, having thickness Δz_1 and a mid-layer concentration $C_{T,1}$. Furthermore, we assume a constant flux between the reference level and halfway the top layer. Then, it can be shown that r_s and C_{soil} are defined by :

$$r_s \equiv \frac{1}{R_g \left(\frac{2 D_E}{\Delta z_1} + p V_E \right)} ; \qquad C_{soil} \equiv \frac{C_{T,1}}{R_g} \frac{\left(\frac{2 D_E}{\Delta z_1} - q V_E \right)}{\left(\frac{2 D_E}{\Delta z_1} + p V_E \right)} \tag{1.39}$$

where: $p = 1$ and $q = 0$ if $V_E > 0$ and $p = 0$ and $q = 1$ if $V_E < 0$.

For example, in the case of lindane, r_s may vary between about 500 s m^{-1} for cool, wet soils and 10000 s m^{-1} or more in the case of warm soils at moderate values of the water content. For completely dry soils $r_s \approx 1300$ s m^{-1}. The value of r_s is independent of f_{oc} whilst C_{soil} increases strongly with increasing f_{oc} due to the increased adsorption of material to the solid phase (Eq.1.35).

Sea-atmosphere exchange

For water surfaces a similar approach can be applied to define r_s and C_{sea}. Here, we follow the theory presented by *P.S.Liss and P.G.Slater* [1974]. Surface waters are assumed to be well-mixed and have concentration C_w. For the depth of the surface water layer a typical value of 25 m is used. At the top of this water surface layer, a thin water layer, directly adjacent to the atmosphere, is present where transport is dominated by molecular diffusion. r_s and C_{sea} are then defined by:

$$r_s = K_H r_w \;; \qquad C_{sea} = K_H C_w \tag{1.40}$$

where r_w is the resistance to POP transport in this thin water layer given by:

$$r_w = \frac{\Delta Z_{top}}{D_l} \tag{1.41}$$

Here, ΔZ_{top} is the depth of the molecular layer. *P.S.Liss and P.G.Slater* [1974] found that $\Delta Z_{top} \approx 4\times10^{-5}$ m for oxygen, whose value is assumed to be valid for POPs as well. For example, for lindane the r_s value for water is small as compared to the other resistances (< 10 s m^{-1}). This means that the exchange of lindane at the water surface is primarily controlled by atmospheric transport. For PCB-153, r_s is much larger (> 500 s m^{-1}) because the Henry coefficient is much larger due to a lower water solubility.

Numerical aspects of soil-atmosphere exchange

The theory described above was implemented in a numerical model. In the soil five layers are defined with depths of 0.5, 0.5, 1, 2, and 11 cm. Small layers at the top of the soil are defined to be able to simulate the saturation of POP in the soil. As a first approximation the soil is assumed to be homogeneous, so that each layer is equal with respect to soil characteristics, temperature (taken to be the 2m air temperature) and soil moisture content (θ = 0.3 in the simulations presented here). The fraction of soil organic matter, f_{oc}, per grid cell was taken from the European database by *D.Fraters et al.* [1993].

The concentrations are defined halfway of each layer and fluxes at the interfaces between layers. The sum of the average dry deposition or re-emission flux (F_d) and the wet deposition flux (see next section) is taken as the boundary conditions at the top of the soil model domain. It is assumed that no pollutant escapes out of the model domain i.e. J_T (15cm) = 0. A simple explicit numerical scheme proved to be sufficiently accurate. The module is operated with a time step of 6 hours.

1.3 Geophysical information

Meteorology

Meteorological information prepared by Hydrometeorological Centre of the Russian Federation at MSC-E request using procedure described in [*Shapiro*, 1981] for 1987-1993 and in [*Frolov et al.*, 1994] for 1994-1996 is used in calculations. In model calculations the following values are used: orthogonal components of the wind speed at 1000 and 850 mb levels, temperature at 1000 mb and precipitation, with the time step of 6 hours. In addition to data prepared by Hydrometeorological Centre a number of meteorological parameters (mixing layer height, coefficients of vertical turbulent diffusion, dry deposition velocities) are prepared by the meteorological pre-processor in course of modelling [*Pekar*, 1996].

Surface information

The ASIMD model considers three types of the surface: sea, land and coastal zone. Data on the surface roughness are taken from the archive "Global Data Set for Land-Atmosphere Models" (ISLSCP). Data on the organic matter content in soil based on the work [*Fraters et al.*, 1993] were prepared by RIVM and made available to MSC-E.

The European Land Use Data Base received from RIVM is planned to be used in the modelling. This data base includes eight types of the underlying surfaces with spatial resolution 50×50 km^2 and covers the whole EMEP grid. The application of these data will allow the dry deposition scheme to be refined. Information on vegetation, soil type and sea currents is planned to be added.

References

Berkowicz R. and Prahm L.P. [1982] Evaluation of the profile method for estimation of surface fluxes of momentum and heat. *Atm.Env.*, v.16, pp.2809-2819.

Businger J.A. [1973] Workshop in Micrometeorology. Am. Met. Soc., pp.67-100.

Fraters D., Bouwman A.F. and Thewessen T.J.M. [1993] Soil Organic Matter of Europe. Estimates of soil organic matter content of the topsoil of FAO-Unesco soil units. Report 481505004, National Institute of Public Health and the Environment, Bilthoven. (Dutch text).

Frolov A., Vazhnic A., Astakhova E., Alferov Yu., Kiktev D., Rosinkina I., Rubinshtein K. [1994] System for diagnosis of the lower atmosphere state (SDA) for pollution transport model, EMEP/MSC-E Technical report 6/94.

GESAMP [1989] The Atmospheric Input of Trace Species to the World Ocean. Rep.Stud.GESAMP, v.38, pp.1-111, World Meteorological Organization, Geneva, Switzerland.

Holtslag A.A.M. and van Ulden A.P. [1983] A simple scheme for daytime estimates of the surface fluxes from routine weather data. *J.Climate Appl.Meteor.*, v.22, pp.517-529.

van den Hout ed. [1994] The impact of atmospheric deposition of non-acidifying Pollutants on the Quality of European forest soils and the North sea, Main report of the ESQUAD project, RIVM rep.722401003, IMW-TNO rep.R93/329.

Irwin J.S. [1979] A theoretical variation of the wind profile power-low exponent as a function of surface roughness and stability. *Atm.Env.*, v.13, pp.191-194.

van Jaarsveld J.A. [1992] Estimating atmospheric inputs of trace constituents to the North Sea: methods and results. Proc. 19th Technical Meeting of NATO-CCMS on Air Pollution and Its Applications, September 29-October 4, in Crete, Greece

Jacobs C.M.J. and van Pul W.A.J. [1996] Long-range atmospheric transport of persistent organic pollutants, I: Description of surface-Atmosphere exchange modules and implementation in

EUROS. National Institute of Public Health and the Environment, Bilthoven, The Netherlands. Report No.722401013.

Junge C.E. [1977] Basic considerations about trace constituent in the atmosphere is related to the fate of global pollutant. In: Fate of pollutants in the air and water environment. Part I, I.H. Suffet (ed.) (Advanced in environmental science and technology, v.8), Wiley-Interscience, New York.

Jury W.A., Spencer W.F. and Farmer W.J. [1983] Behavior Assessment Model for Trace Organics in Soil. *J. Environ. Qual*., v.12, pp.558-564.

Jury W.A., Gardner W.R. and Gardner W.H. [1991] Soil Physics. 5th edition. John Wiley and Sons Inc., New York.

Lindfors V., Joffre S.M., Damski J. [1991] Determination of the wet and dry deposition of sulphur and nitrogen compounds over the Baltic sea using actual meteorological data. Finnish Meteorological Institute Contributions N 4, Helsinki.

Liss P.S. and Slatter P.G. [1974] Fluxes of gases across the air-sea interface. *Nature*, v.247, pp.181.

Monteith J.L. and Unsworth M.H. [1990] Principles of environmental physics. 2nd edition. Arnold, London.

Pekar M. [1996] Regional models LPMOD and ASIMD. Algorithms, parametrization and results of application to Pb and Cd in Europe scale for 1990 MSC-E Report 9/96, September.

Rao K.S. and Snodgrass H.F. [1979] Some parametrization of the nocturnal boundary layer. *Boundary Layer Meteorology*, v.17, pp.15-28.

Sehmel G.A. [1980] Particle and gas deposition: a review. Atm.Env., v.14, pp.983-1011.

Shapiro M.Ya. [1981] Wind field objective analysis based in geopotential and wind data, EMEP/MSC-E Technical report 3/1981.

Shir C.C. [1973] A preliminary numerical study of atmospheric turbulent flows in the idealized boundary layer. *J.Atmos. Sci*., v.30, pp.1327-1339.

Sorbjan Z. [1994] Toward evaluation of heat fluxes in the convective boundary layer. *J. of Appl. Meteor*., v.34, pp.1092-1098.

Strand A. and Hov Ø. [1996] A model Strategy for the Simulation of Chlorinated Hydrocarbon Distribution in the Global Environment. Water, Air and Soil Pollution, v.86, pp.283-316.

van Ulden A.P. and Holtslag A.A.M. [1985] Estimation of atmospheric boundary layer parameters for diffusion applications. *J.Climate Appl.Meteor*., v.24, pp.1196-1207.

Verver G.H.L. and Scheele M.P. [1989] Influence of non-uniform mixing height on dispersion simulations following the Chernobyl accident, in Air Pollution Modelling and Its Application VII (ed.Han van Dop), p.111-121, Proc. 17th technical Meeting of NATO-CCMS, Cambridge, England, 1988, Plenum Press, New York.

Whitby K.T. [1978] The physical characteristics of sulphur aerosols. Atmospheric Environment, v.12, pp.135-195.

Williams R.M. [1982] A model for the dry deposition of particles to natural water surfaces. Atm.Env. 16, pp.1933-1938.

Chapter 2 Lindane modelling

Introduction

Lindane is γ-isomer of hexachlorocyclohexane (γ-HCH) which was widely used all over the world, when the application of DDT was decreased. Lindane is an effective agent for the control of many pests. It is applied during sowing and germination of agricultural plants, for treating forest and gardens, to control locust and sprayed cotton plants, beat roots and potatoes during the growing season and for other purposes. It is used as dust, granules, oil solutions, emulsions and suspensions by spraying, surface application or ploughing in the soil [*Gruzdev,* 1987]. By estimation, in the 80s, 5900 tonnes of lindane were annually used in the world and 4000 tons - in the 90-s [*Li et al.,* 1996]. The part of lindane released directly to the atmosphere is dictated by the way of its application.

2.1 Physical-chemical properties of lindane

Molecular formula

$C_6H_6Cl_6$

Molecular weight

290.85

Melting (T_m) and boiling (T_b) temperature

$T_m = 113^0$C, $T_b = 323.4^0$C [*Howard,* 1991]

Solubility

Solubility (S) at 25^0C

Solubility is 2.6×10^{-2} mol/m^3 = 7.5 mg/l [*Schwarzenbach et al.,* 1993]

Solubility dependence on temperature [*Kucklik et al.,* 1991]

for t = 15-45^{0}C:

$$\log S\ (\text{mol/m}^3) = -(1918 \pm 656)/T(K) + (4.75 \pm 2.16)$$

for sea water at t = 0.5 - 23^{0}C:

$$\log S\ (\text{mol/m}^3) = -2787/T(K) + 8.03$$

for deionized water at t = 0.5-45^{0}C:

$$\log S\ (\text{mol/m}^3) = -3108/T(K) + 9.18$$

Solubility dependence on the organic matter content in the water

Lindane solubility remains practically constant when concentrations of humic and fulvic acids increase from 0 to 100 mg/l and it does not depend on the nature and concentrations of the dissolved organic matter [*Choiu et al.,* 1986].

Saturated vapour pressure (P_{OS}, Pa)

for t = 15-45^{0}C:

$\log P_{OS} = -(5290 \pm 222)/T(K) + (15.65 \pm 0.74)$ [*Kucklik et al.* 1991]

for t = -30-+30^{0}C:

$\log P_{OS} = -5490/T(K) + 16.72$ [*Wania et al*., 1994]

Vapour pressure/temperature dependence for a subcooled liquid:

$\log P_{OL} = -3680/T(K) + 11.15$ [*Hincley et al.,* 1990]

Henry`s law constant (H, Pa·m^3/mol)

Temperature dependencies:

for deionized water in the range from 0.5 to 45 ^{0}C:

$\log H = -(2382 \pm 160)/T + (7.54 \pm 0.54)$ [*Kucklik et al.,* 1991]

for sea water in the range from 0.5 to 23 ^{0}C:

$\log H = -(2703 \pm 276)/T + (8.68 \pm 0.96)$ [*Kucklik et al.,* 1991]

$\ln(H) = 19.99 – 6225/T$ [*Strand and Hov*, 1996]

for fresh water in the range from 0.5 to 45 ^{0}C:

$\ln(H) = 17.36 – 5486/T$ [*Strand and Hov*, 1996]

$H = 0.073 \cdot \exp(25.88-7329/T)$ [*Jacobs and van Pul*, 1996]

Sorption by soil, sediments and suspended particles

The sorption value is determined by the following coefficients: K_{oc} (dm^3/kg) – organic carbon distribution coefficient; K_{ow} (dm^3/kg) – octanol-water distribution coefficient.

$\log K_{oc} = 2.99$ [*Kushi et al.,* 1990], $\log K_{oc} = 2.96$ [*Kenaga and Goring*, 1980], $\log K_{oc} = 3.03$ [*Lyman,* 1982].

$\log K_{ow} = 2.96$ [*Kenaga and Goring,* 1980], $\log K_{ow} = 3.30$-3.89 with average value 3.60 [*Isnard and Lambert*, 1988].

Degradation half-life in the soil (mainly due to biodegradation)

267 days	[*Jacobs and van Pul*, 1996]
253 days	[*Strand and Hov*, 1996]
2 years	[*Mackay et al.,* 1991]

Lindane degradation half-lives in soils measured in the field experiments after the surface application varied in the range of 150-350 days [*Kononiuk,* 1986; *Lyman,* 1982; *Tzukerman* 1985]. However, under field conditions volatilization of lindane to the atmosphere plays a significant role for the evaluation of the lindane content in the soil. Therefore the degradation rate constant for this pesticide can be determined only under laboratory conditions where volatilization is supressed or controlled. Based on the laboratory experiments data the lindane half-life in the soil was estimated to be 600 days [*Laskovski et al.,* 1984].

Degradation half-life in the water (mainly due to hydrolysis and photolysis)

4.7 years in surface water	[*Strand and Hov*, 1996]
28 years in deep water	[*Strand and Hov*, 1996]
2 years	[*Mackay et al.,* 1991]

At pH = 7 and 25^0C the hydrolysis half-life is 6 years [*Ellington et al.,* 1987].

Estimated values of the degradation half-live in the water due to the reaction with hydroxyl radical are 1.3, 27, 530 days for fresh water, coastal sea water and open ocean, respectively [*Vozhzennikov et al.*, 1997].

Degradation half-life in the air (mainly due to reaction with hydroxyl radicals in the air)

32 days	[*Jacobs and van Pul*, 1996]
170 days	[*Mackay et al.,* 1991]

2.2 Model assumptions and parametrization

The modelling was performed using the model of gaseous POP transport (ASIMD) coupled with atmosphere-soil and atmosphere-sea exchange modules provided by RIVM [*Jacobs and van Pul,* 1996].

The following model assumptions were used at this stage:

1. Lindane is presented in the atmosphere only in the gaseous phase.
2. Sedimentation, sea currents and lindane diffusion to deeper sea layers are not taken into account.
3. Processes of lindane exchange with vegetation are not considered.

The model parametrization associated with the processes of exchange between the atmosphere and surface is largely taken from *C.M.J.Jacobs and van W.A.J.Pul* [1996].

Model parametrization [Jacobs and van Pul, 1996]

HENRY`S LAW CONSTANT $K_H = \frac{0.073}{8.314 \cdot T} \exp\left(-7329\left(\frac{1}{T} - \frac{1}{283.15}\right)\right)$ (Dimensionless)

DISTRIBUTION COEFFICIENT $K_d = f_{oc} \times K_{oc}$

f_{oc} - fraction of organic carbon in the soil f_{oc} (from data base)

K_{oc} - organic carbon distribution coefficient $K_{oc} = 1.3$ m^3/kg

DEGRADATION:

SOIL	$K_s = 3.0 \cdot 10^{-8}$, s^{-1}	
SEA	$K_w = 4.66 \cdot 10^{-9}$, s^{-1}	taken from [*Strand and Hov*, 1996]
ATMOSPHERE	$K_a = 2.5 \cdot 10^{-7}$, s^{-1}	

MOLECULAR DIFFUSION COEFFICIENT:

AIR	$D_g = 5.0 \cdot 10^{-6}$, m^2/s
WATER	$D_w = 5 \cdot 10^{-10}$, m^2/s

VOLUMETRIC FRACTION:

POROSITY $\varphi = 0.5$

VOLUMETRIC AIR CONTENT $a = 0.3$

VOLUMETRIC WATER CONTENT $\theta = 0.2$

SOIL BULK DENSITY $\rho_s = 1300$ kg/m^3

AERODYNAMIC RESISTANCE $$r_a = \frac{\ln(Z_r/Z_0) - \psi(Z_r/L) + \psi(Z_0/L)}{ku_*}, \text{ s/m}$$

QUASI-LAMINAR BOUNDARY LAYER RESISTANCE $$r_b = \frac{2}{ku_*}\left(\frac{Sc}{Pr}\right)^{2/3}, \text{ s/m}$$

MOLECULAR DIFFUSION LAYER THICKNESS $d_{zwm} = 4.0 \cdot 10^{-5}$, m

AND ACCUMULATING LAYER DEPTHS FOR WATER $d_{wz} = 25$, m

CHARACTERISTICS OF THE CALCULATION GRID FOR SOIL:

NUMBER OF LAYERS $K_{max} = 5$

DEPTHS OF LAYERS: DSZ(1) = 0.005, m
DSZ(2) = 0.005, m
DSZ(3) = 0.01, m
DSZ(4) = 0.02, m
DSZ(5) = 0.11, m

2.3 Input data

Emissions

In model calculations emission data for 1990 prepared in the framework of the UBA project are used [*Berdowski et al.,* 1997] (Table 2.1). Figure 2.1 presents a map of the lindane emission distribution with 150x150 km^2 resolution over the EMEP grid in 1990. Total lindane emissions amount to 1307 t/yr. In the calculations it was assumed that 10% of lindane emissions take place in February, 15% - in March and 25% - each month from April to June [*Jacobs and van Pul,* 1996].

The uncertainty of the emission data can be around 5 times [*Berdowski et al.,* 1997].

Table 2.1 Lindane emission estimates [*Berdowski et al.*, 1997]. Units: t/yr.

Country	Emissions	Country	Emissions
Albania	3.50	Latvia	13.6
Austria	13.3	Lithuania	25.1
Belarus	47.2	Luxembourg	0
Belgium	54.3	The FYR of Macedonia	0.760
Bosnia&Herzegovina	6.23	Republic of Moldova	13.2
Bulgaria	0	Netherlands	15.0
Croatia	11.0	Norway	4.10
Cyprus	-	Poland	0
Czech Republic	0.210	Portugal	4.40
Denmark	3.80	Romania	51.4
Estonia	7.45	Russian Federation *	348
Finland	8.80	Slovakia	0.090
France	211	Slovenia	1.23
Germany	-	Spain	0
Greece	19.4	Sweden	0
Hungary	0.300	Switzerland	0.800
Iceland	0	Ukraine	265
Ireland	0.900	United Kingdom	114
Italy	44.9	Yugoslavia	18.6
Total			1307

* within the EMEP grid

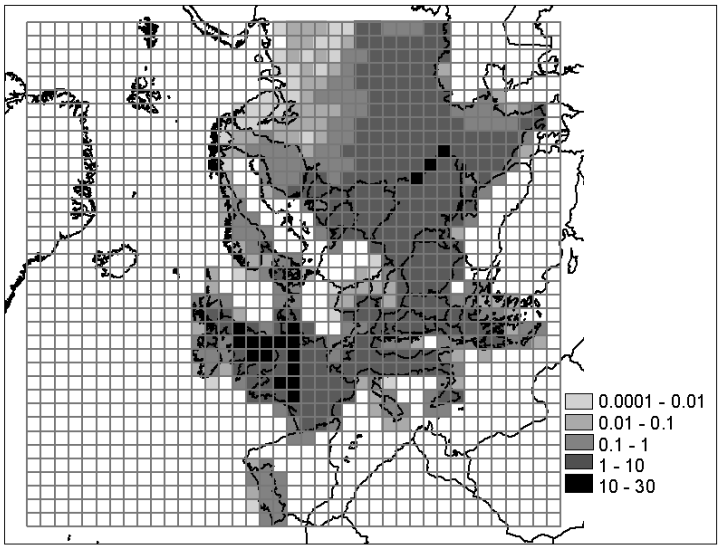

Figure 2.1 Map of lindane emissions within the EMEP region for 1990. Units: t/yr

Meteorology

Meteorological information prepared by Hydrometeorological Centre of the Russian Federation at the request of the MSC-E using the procedure described in [*Shapiro*, 1981] for 1987-1993 and in [*Frolov et al.*, 1994] for 1994-1996 is used in calculations.

2.4 Calculation results

Calculations of the lindane transport within the geographical scope of the EMEP grid for a decade (1987-96) have been performed using a modified version of the ASIMD model and the atmosphere-soil and atmosphere-sea exchange modules coupled to it.

Modelling of the lindane transport for the ten-year period was performed in order to trace tendencies of lindane accumulation in the soil and ocean alongside the lindane degradation and re-emission.

In calculations of 10-year period the total emissions of lindane were as much as 13070 tons.

Figure 2.2 presents the diagrams showing the mass balance of lindane in the soil (a) and in the sea (b) for 10-year calculation period.

The diagram shows that the input of dry deposition (71%) predominates over wet deposition over the sea, and over the land wet deposition prevails over dry deposition (62%). Thus dry deposition processes compared to wet deposition are more important for the marine environment than for soil.

During 10 years, the degradation of lindane in the soil amounts to 78% of the total mass entered the soil. In the surface layer of the ocean the degradation is 48% of the total mass. It is explained by the difference of degradation constants for the soil and for the upper layer of the ocean during the simulation period.

16% of lindane entered the soil and 10% of lindane entered the sea were re-emitted to the air.

The remaining mass of lindane in the soil is 8% of the total input, whereas the mass remained in the sea is about 44%.

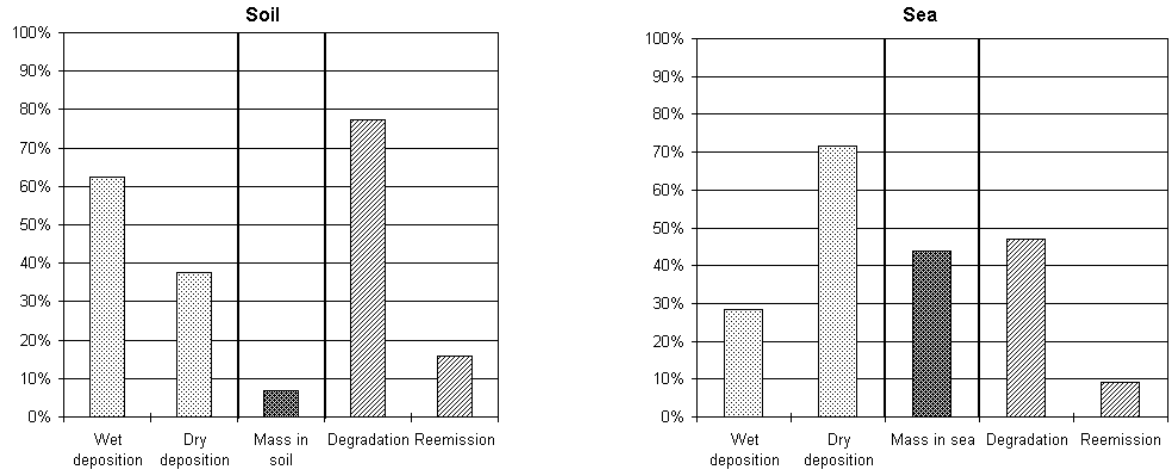

Figure 2.2 Input of dry and wet deposition to total deposition over land and sea after 10-year simulation period. The fraction of the matter remained in the soil and in the sea, degraded and re-emitted from the soil and the sea

Figure 2.3 shows the annual variations in the mean air concentrations (averaging is made over the whole EMEP grid) over the land and sea and annual variations in the net gaseous flux and wet deposition for the soil and ocean for 1987, 1990 and 1996.

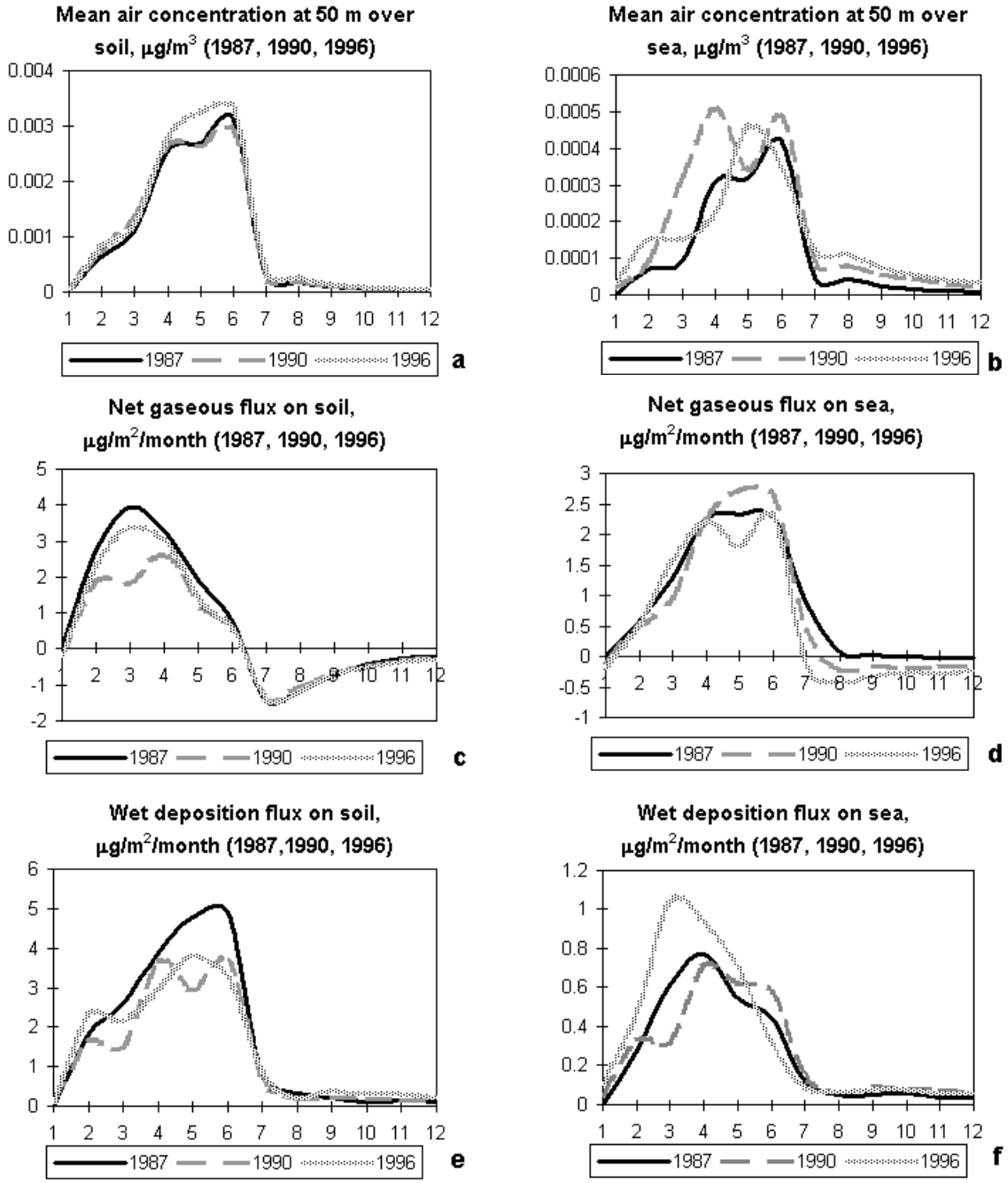

Figure 2.3 Annual variations of the mean air concentrations of lindane over the land (a) and over the sea (b); annual variations in the net gaseous flux over the land (c) and over the sea (d); annual variations in mean wet deposition flux over the land (e) and over the sea (f)

Due to the proximity to emission sources mean concentrations over the land were found to exceed concentrations over the sea by a factor of 6. For the same reason wet deposition flux over land exceeds wet deposition flux over sea (about 5 times). The net gaseous flux over the sea and land are approximately equal.

Air concentrations over the land (Figure 2.3a) are maximum in April-June (the period of maximum emissions). Since July emissions have been terminated. Re-emission processes predominate and continue up to the time of new emissions reaching maximum values in July-August (Figure 2.3c).

Mean concentrations over the sea (Figure 2.3b) varies like mean concentrations over the land except for local maxima associated obviously with peculiarities of meteorological conditions. In July-August the mean concentration decreases and re-emission processes become more important over the sea (Figure 2.3d). During the first calculation year (1987) re-emission from the oceanic surface is zero. During subsequent years when the ocean accumulated a substantial amount of lindane re-emission increases from year to year.

Figure 2.4 demonstrates the map of the total deposition over the land and sea within the EMEP grid (averaging was made over 10 years). The region of the maximum deposition density (150 μg/m^2/yr) coincides with the region of the maximum emission density.

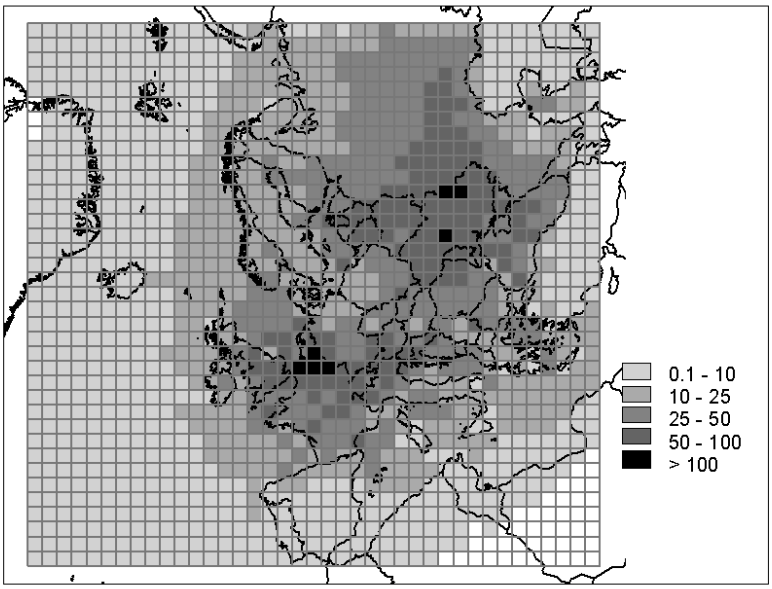

Figure 2.4 Map of total deposition over the land and the sea within the EMEP grid (averaged over 1987-96). Units: μg/m^2/yr

In addition to the map of total deposition mean air concentration fields of lindane in four calculation vertical layers have been obtained. These concentration fields for 1990 are presented in Figure 2.5 over Europe. In the region of maximum emissions air concentrations are maximum. The maximum lindane concentration decreases with height from 4 ng/m^3 at 50 m to 3.5 ng/m^3 at 250 m, 2.5 ng/m^3 at 750 m, and 0.8 ng/m^3 at 1600 m.

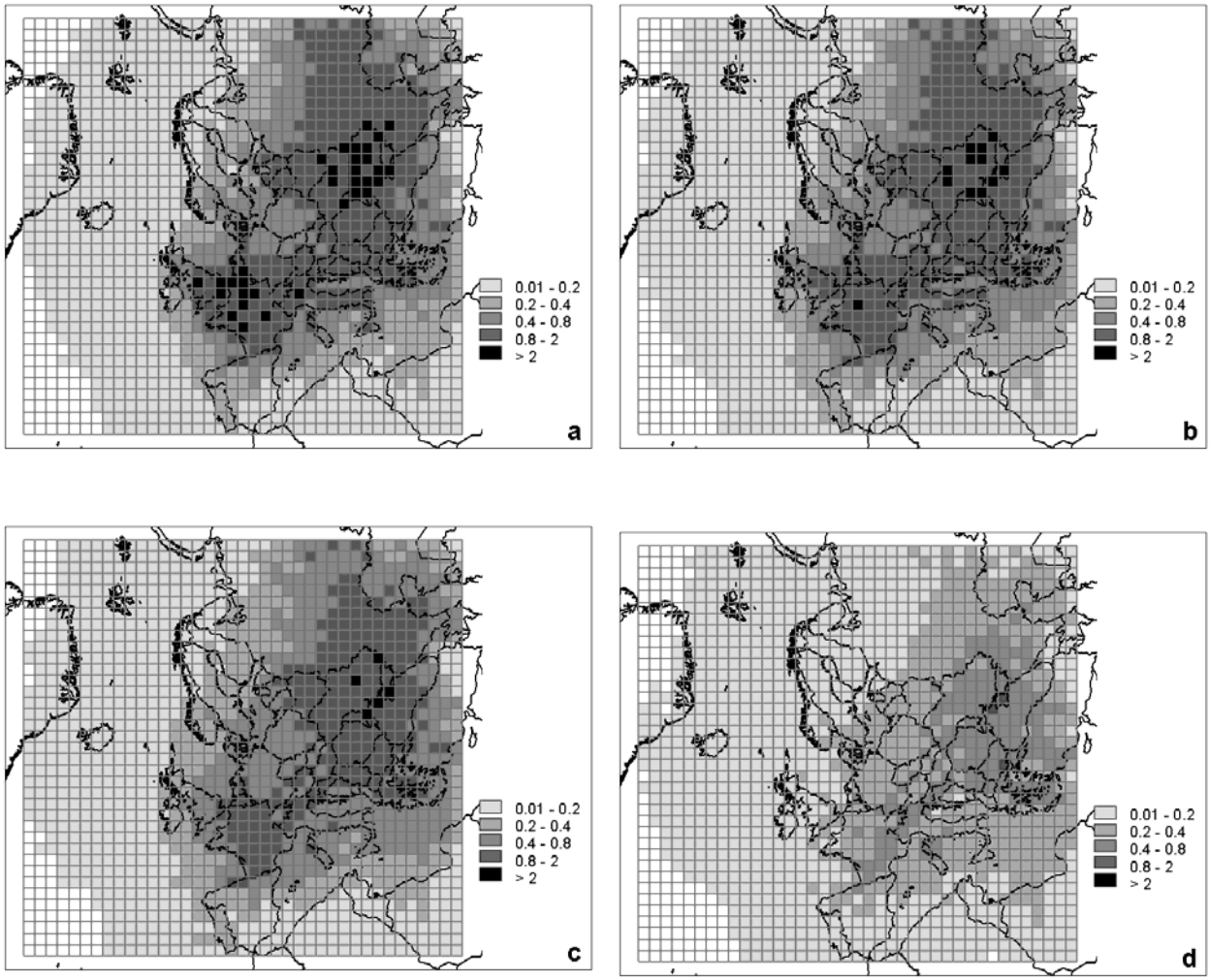

Figure 2.5 Mean annual concentrations of lindane in the air for 1990, ng/m^3: a) at height 50 m; b) at height 250 m; c) at height 750 m; d) at height 1600 m

Figure 2.6a,b demonstrates lindane mass accumulated and degraded in the soil and in the sea during 10-year period at constant annual emission 1307 tons. As evident from Figure 2.6a,b in oceanic waters lindane mass grows steadily during this period whereas the soil mass remains constant from year to year but it varies with emission and re-emission variations round the year. Lindane mass degraded in the soil accounted for 3900 tons (30% of total emissions by the end of 10-year calculation period).

The degradation in the ocean is slower than accumulation. For this reason lindane mass in oceanic waters grows steadily during 10 years. Lindane mass degraded in the ocean during 10 years is 840 tons (about 6% of the total emissions for 10 years). Lindane mass in the ocean after 10-year calculation period is about 800 tons (about 6% of total emissions).

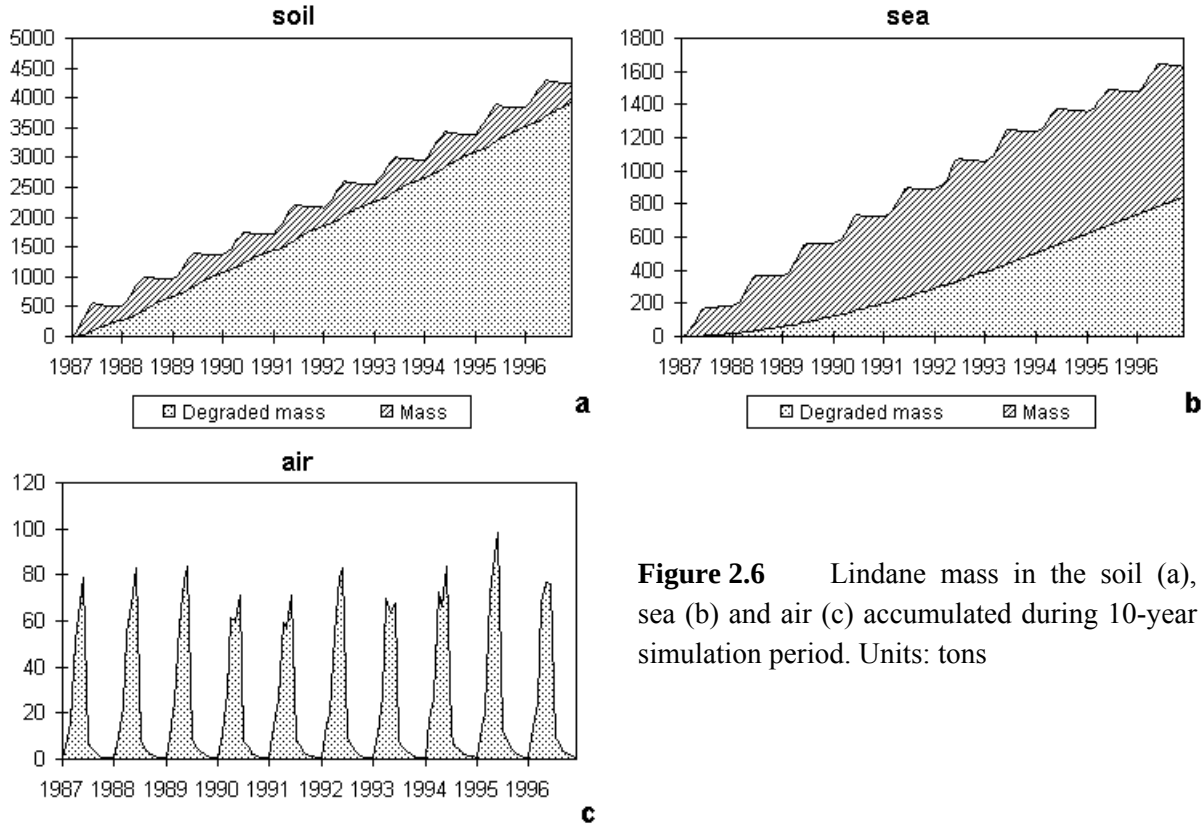

Figure 2.6 Lindane mass in the soil (a), sea (b) and air (c) accumulated during 10-year simulation period. Units: tons

Comparison with measurements

The comparison of calculated versus observed values has been made. The comparison results for lindane concentrations in the air and precipitation are given in Figure 2.7 and Figure 2.8. The correlation coefficient of calculated and observed concentrations of lindane in precipitation is 0.6; the correlation coefficient of measured and calculated concentrations of lindane in the air is 0.8. Perhaps the value of the coefficients is connected with a small number of measurement data referring to different years.

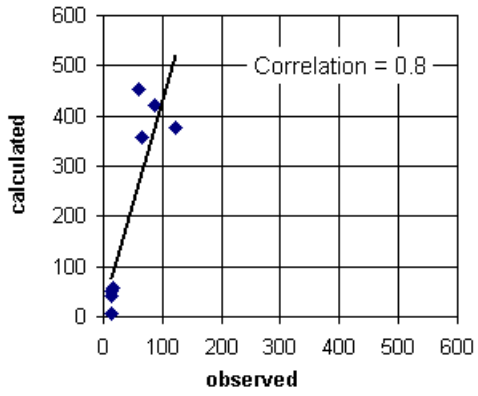

Figure 2.7 Comparison results of calculated and measured lindane concentrations in the air. Units: pg/m^3

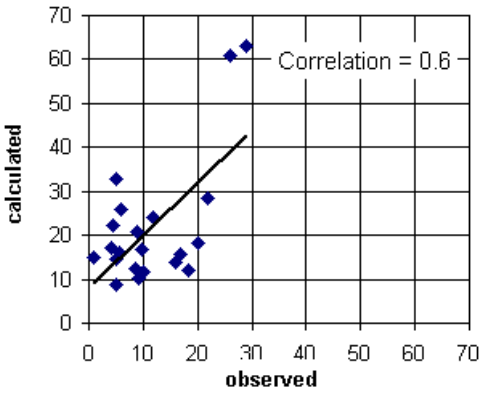

Figure 2.8 Comparison results of calculated and measured lindane concentrations in precipitation. Units: ng/l

Measurement data on mean annual concentrations in precipitation along with calculated values are given in Table 2.2. Data on measured mean annual concentrations of lindane in the air are given in Table 2.3 [*Berg et al.*, 1996].

As seen from Figures 2.7 and 2.8 the calculated concentrations exceed measured ones in 2-3 times. It can be explained by a simplified parametrization of physical-chemical processes of lindane behaviour in the atmosphere and in other compartments and by the emission uncertainty and scarce measurement data.

Table 2.2 Calculated and measured on mean annual concentrations in precipitation along with calculated values

Station code	Year	Mean annual lindane concentrations in precipitation. Units: ng/l	
		Measured	Calculated
DE1	90	4.54	22.1
DK31	90	16.98	15.6
GB1	91	22	28.5
GB2	91	29	62.9
GB3	91	10	11.5
DK31	91	11.91	24.2
NO99	91	4.05	17.2
GB1	92	20	18.3
GB2	92	26	60.8
GB3	92	0.8	14.9
DE1	92	18.22	11.9
DK31	92	15.82	13.9
NO99	92	5.02	8.8
GB1	93	9	20.9
GB2a	93	6	26.0
GB3	93	5	14.5
GB5	93	5	32.9
DE1	93	9.28	10.2
NO99	93	8.45	12.4
NO99	94	9.88	16.7
NO99	95	5.54	16.1

Table 2.3 Calculated and measured on mean annual concentrations in precipitation along with calculated values

Station code	Year	Mean concentrations of lindane in the air. Units: pg/m^3	
		Measured	Calculated
NO99	92	86.25	421
NO42	93	14.41	6.07
NO99	93	58.52	454
NO42	94	16.06	57.8
NO99	94	122.89	376
IS91	95	14.19	51.2
NO42	95	13.13	42.9
NO99	95	64.98	358

Mass balance

On the basis of calculation results it is possible to trace the re-distribution of the total mass of lindane within the EMEP grid with allowance made for the transport outside the grid.

Figure 2.9 presents diagrams of lindane mass balance inside the EMEP grid for the 1, 5 and 10-year simulation periods and for the middle of the last year of each period.

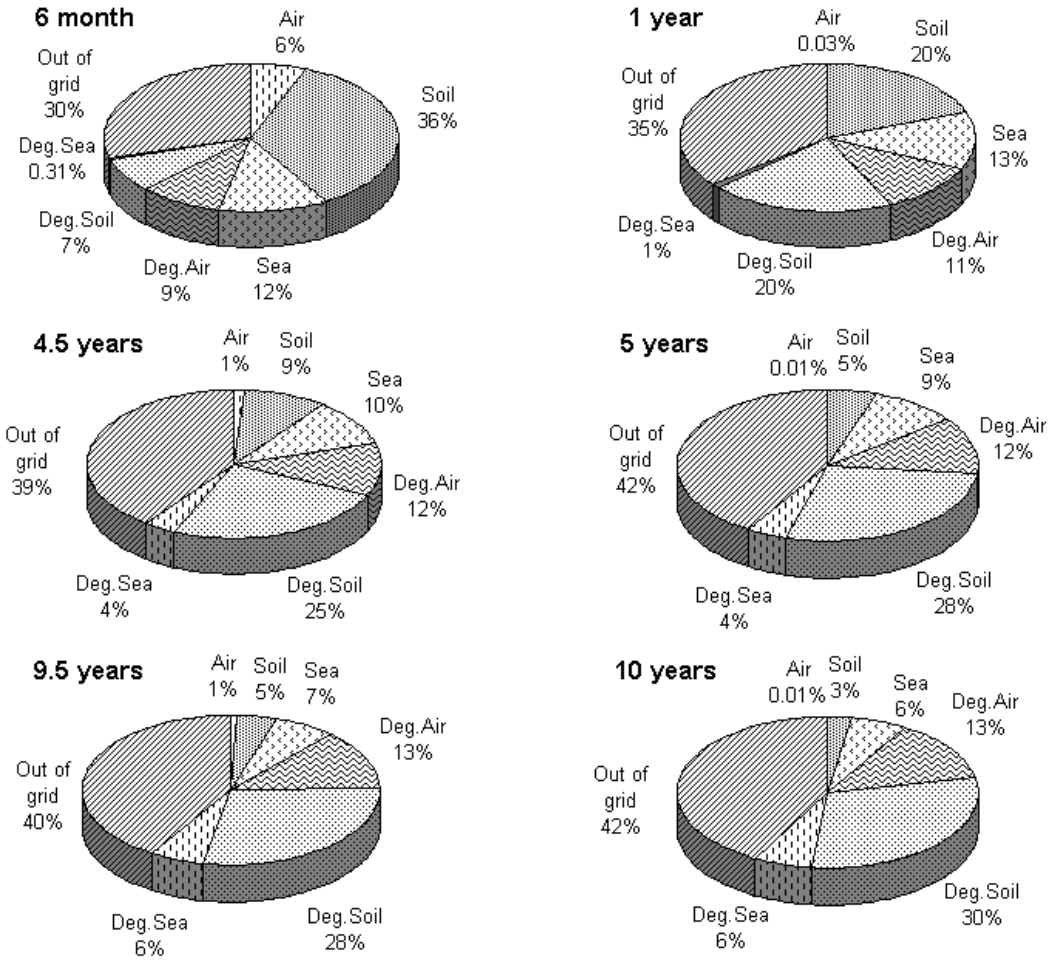

Figure 2.9 Lindane mass balance within the EMEP grid: after calculations for the period of 6 months; 1 year; 4 years and 6 months; 5 years; 9 years and 6 months; 10 years. Air%, Sea%, Soil% - lindane fraction contained in the air, sea and soil within the EMEP grid; Deg. Air%, Deg.Sea%, Deg.Soil% - lindane fractions degraded in the air, sea and soil; Out of grid% - lindane fraction transported outside the EMEP grid

As seen from Figure 2.9 the fraction of lindane in the air is a minor part of total emissions. In the middle of the first year it is 6% and 0.01-1% in the subsequent years. Lindane mass in the soil (accumulation plus degradation) varies within 43-33% of the total emissions during the calculation period. Lindane mass in the marine environment (accumulation + degradation) is about 12-14% of the total emissions. The share of lindane mass transported outside the grid is growing. After the first calculation year it is 35%, after 10 years - 42%. Obviously the increase of this value is conditioned by re-emission of lindane from the soil and the ocean.

Then, in order to follow the fate of lindane accumulated during 10-year period, it was assumed that no further emissions took place during the next 10 years.

Figure 2.10 presents changes in the lindane mass in the soil and in the upper ocean layer within the EMEP grid during next 10-year simulation period upon emissions termination. As seen from Figure 2.10a almost all lindane accumulated in the soil degraded during 10 years. During this period the total amount of lindane in the soil (plus degradation) increased by 32 tons even when there were no emissions. Obviously, it happens on account of re-emission from the ocean surface.

With regard to the total mass of lindane in the oceanic surface layer (Figure 2.10b), at the beginning of the calculations lindane content in the surface ocean layer was 870 tons. During the next 10 years 540 tons degraded and 220 tons re-emitted and 110 tons remained in the water.

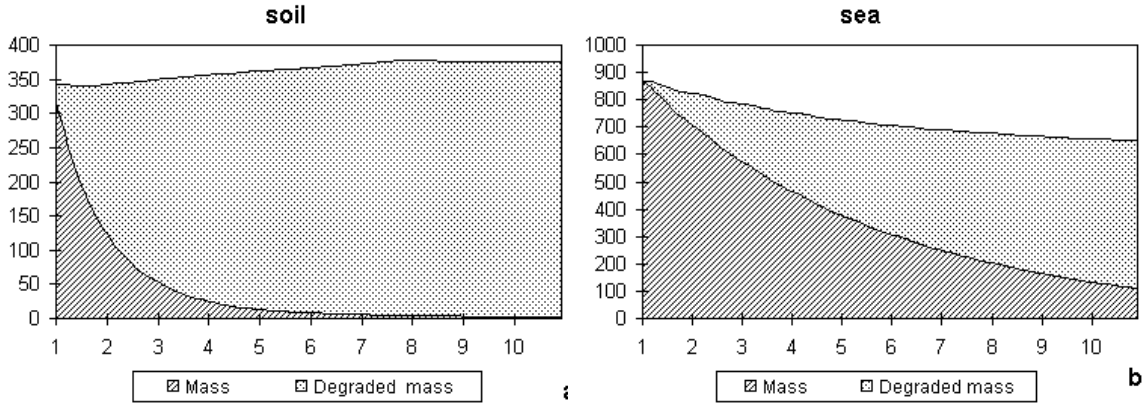

Figure 2.10 Lindane mass in the soil and in the sea during 10-year simulation period after the termination of emissions. Units: tons

Figure 2.11a shows the evolution of lindane mass in the air upon emission termination. In the air lindane mass decreases from year to year due to the degradation (38 tons) and transport outside the grid (143 tons). The degradation in the air and the transport outside the EMEP are shown in Figure 2.11b.

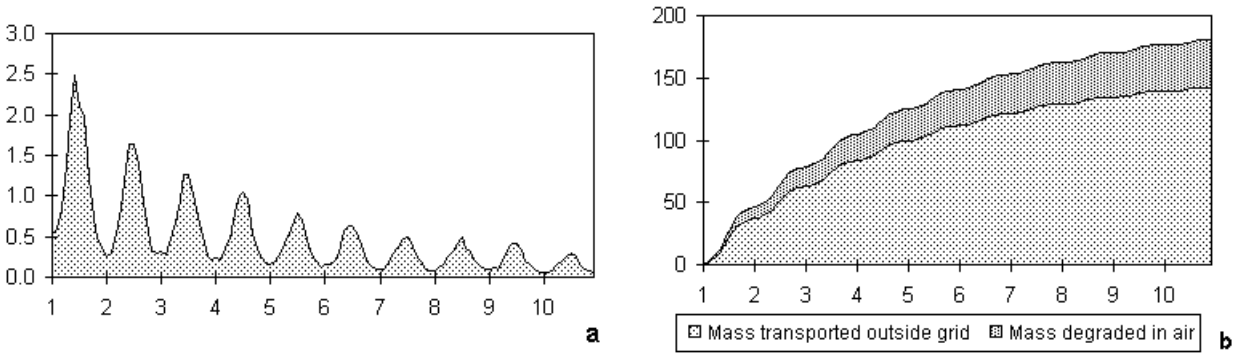

Figure 2.11 Lindane content in the air (a), masses degraded in the air and transported outside the EMEP grid (b) over 10-year simulation period without emissions.. Units: tons

Figure 2.12 presents lindane air concentrations over land (a) and over sea (b), net gaseous fluxes and wet deposition fluxes over land (c,e) and over sea (d,f) for the first, fourth and tenth years under the condition that lindane emissions were stopped.

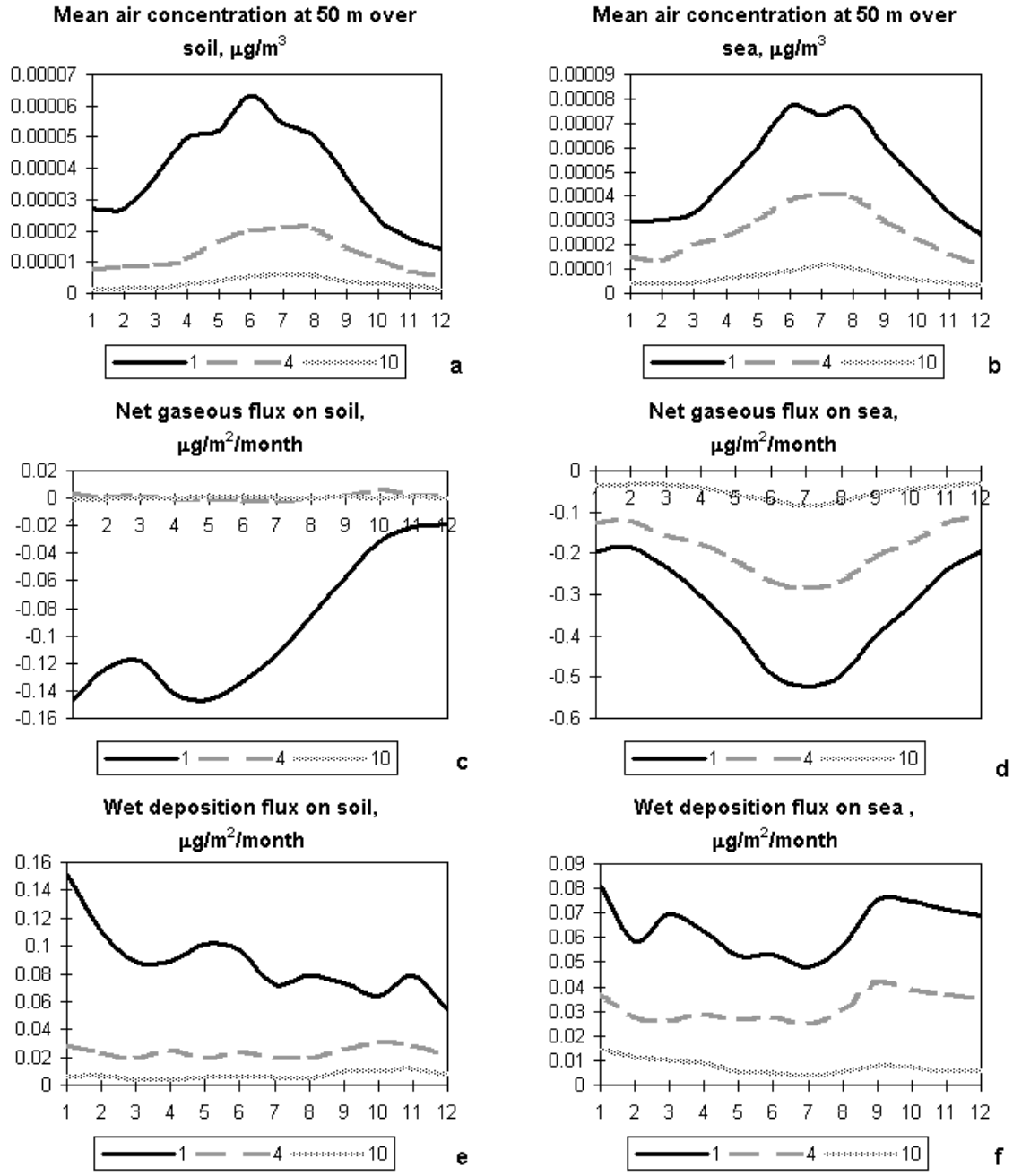

Figure 2.12 Mean annual concentration variations in the air over land (a) and over sea (b); mean annual variations of mean net gaseous flux over land (c) and over sea (d); annual variations of mean wet deposition flux over land (e) and over sea (f)

Exchange fluxes between air and soil (Figure 2.12c) and between air and sea (Figure 2.12d) are negative, i.e. lindane re-emission from the sea and soil surfaces takes place. The lindane flux from the sea is higher than from the soil surface. Maximum negative fluxes over land

and sea are observed in summer months and during the first simulation year. Lindane concentration over the sea (Figure 12b) slightly exceeds the concentration over land (Figure 12a). During the last simulated year lindane flux from the soil surface is inessential but lindane flux from the sea surface is still noticeable and amounts to 0.04 μg/m^2/month.

2.5 Global modelling of lindane

Model description

This section deals with modelling of lindane distribution with different compartments on the global level. The model for this simulation was kindly provided to MSC-E by Dr.Ø.Hov (NILU, Norway). Full description of the global model is presented in [*Strand and Hov*, 1996].

The model is meant for the evaluation of global circulation of persistent toxic chemicals in the environmental compartments: the atmosphere, ocean and soil with allowance made for the exchange between these compartments. The model is two-dimensional considering the exchange only in the zonal and vertical directions. In the longitudinal direction mean values are used.

The model operates on the assumption that the atmospheric mixing is faster along the parallels than along meridians. Input parameters of the model are the following:

- emissions;
- field of wind speed;
- field of the vertical and horizontal diffusion coefficients;
- parameters describing exchange processes at the interface of the atmosphere-ocean and atmosphere-soil;
- parameters describing transport processes in oceanic waters;
- data on precipitation and evaporation;
- rates of lindane degradation.

In the model the globe surface is divided into 6 equally spaced latitude zones with spatial resolution 30^0. Each zone is divided into 2 compartments: oceanic and continental ones. In its turn, the continental compartment is also splitted into two compartments: cultivated and uncultivated land. The area of each zone and fractions of appropriate compartments are given in Table 2.4 (where R – radius of the Earth, ϕ - latitude, A – latitudinal zone area, y – co-ordinate along longitude).

Table 2.4 Characteristics of latitudinal zones in the global model

Zone No.	1	2	3	4	5	6
ϕ	90^{0}S-60^{0}S	60^{0}S-30^{0}S	30^{0}S-EQ	EQ-30^{0}N	30^{0}N-60^{0}N	60^{0}N-90^{0}N
y/R	-1.57÷-1.05	-1.05÷-0.52	-0.52÷0	0÷0.52	0.52÷1.05	1.05÷1.57
A/R^2	0.84	2.29	3.14	3.14	2.29	0.84
Continental fraction	0.372	0.057	0.229	0.286	0.500	0.499
Fraction of cullivaled land	0.0	0.0	0.025	0.025	0.025	0.0

In the global model the atmosphere is divided into 4 vertical layers (Table 2.5). In Table 2.5: p – atmospheric pressure (hPa), z – layer height above the ground surface; Δz – layer depth.

Table 2.5 Characteristics of vertical layers in the global model

Layer No	1	2	3	4
P, hPa	1000-835	835-500	500-110	110-10
z, m	0-1300	1300-5000	5000-15900	15900-33200
Δz, m	1300	3700	10900	17300

Pollution sources of the atmosphere are direct emissions from natural or anthropogenic sources and the input from the ocean and soil resulted from exchange processes.

The whole ocean in the global model is divided into 2 layers: surface layer and interior deep-water reservoir. The surface layer depth is 75 m.

In the model the soil is assumed to be a homogeneous layer of 0.15 m depth divided into cultivated and uncultivated soil.

The emission of lindane to the environment is calculated from the total annual consumption of lindane for recent 3 decades.

Table 2.6 Approximate consumption of lindane. Units: t/yr

Period / Zones	1960-69	1970-79	1980-89
30S-EQ (3)	20	280	240
EQ-30N (4)	130	2000	2200
30N-60N (5)	600	6000	3200

In the soil lindane is lost due to degradation. Under various conditions the half-life of lindane in the soil is 200-300 days (time decrease in e-times is assumed as τ=1 year).

The half-life of 5 years in the surface layer of 75 m depth is assumed (the corresponding life-time is 6.8 years).

In deep oceanic waters the degradation (mainly due to hydrolysis) occurs with the half-life of 30 years for lindane (the corresponding life-time is 41 years).

Calculation results

Some calculations have been carried out using the global model [*Strand and Hov,* 1996]. The first run was fulfilled with global data on lindane consumption (Table 2.6). The second run was fulfilled with the UBA project emissions released in the 5-th latitude zone. It was done to trace the transport of European emissions over the globe.

Lindane calculation (global consumption of lindane)

The first run covered the period of 1960-89. Consumption data presented in Table 2.6 were used. It was assumed that 50% of lindane was applied to cultivated soils and 50% was emitted to the atmosphere. Emissions took place in the 3-d, 4-th and 5-th latitude zones.

Figure 2.13 (a-c) shows the mass balance of lindane after 1-year, 10-year, and 30-year simulation periods. As seen from these diagrams the relative content of lindane in the soil (including degradation) is slightly decreased, and the relative content of lindane in the water (including degradation) is slightly increased during 30-year simulation period. The degradation in the sea and soil predominates over other processes and accounts to (69%). The most part of the remaining fraction of lindane accumulates in the deep water reservoir (23%) and in the surface ocean layer (6%). Only two percent of lindane remains in the soil.

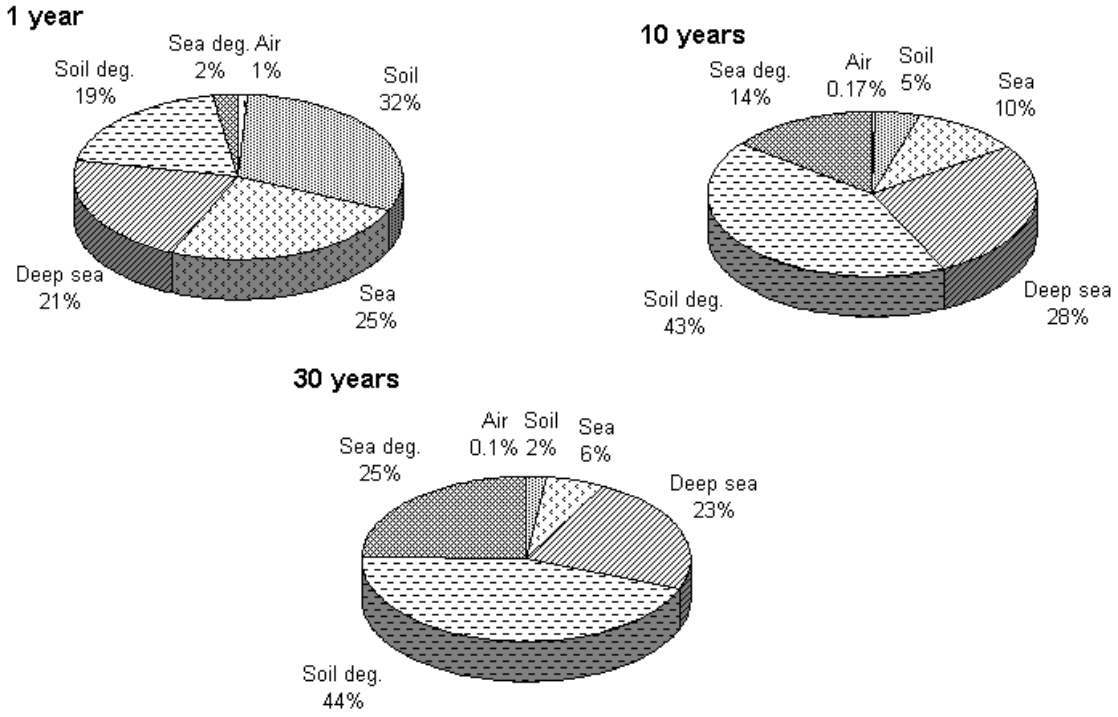

Figure 2.13 Lindane mass balance after modelling 1-year period (a); 10-year (b) and 30-year periods (c) using the global model. Air (%), Soil (%), Sea (%) - the share of lindane in the air, soil and surface marine water; Deep sea (%) - the fraction of lindane in deep oceanic reservoir; Soil degr. (%), Sea degr. (%) - the fraction of lindane mass degraded in the soil and ocean water

Figure 2.14 (a-d) represents annual variations of lindane mass in the air, in the soil, surface sea water and deep water reservoir for each latitude zone over 30-year period of simulation. This figure shows the total mass accumulation, reduction and annual variations in each of the listed above compartments.

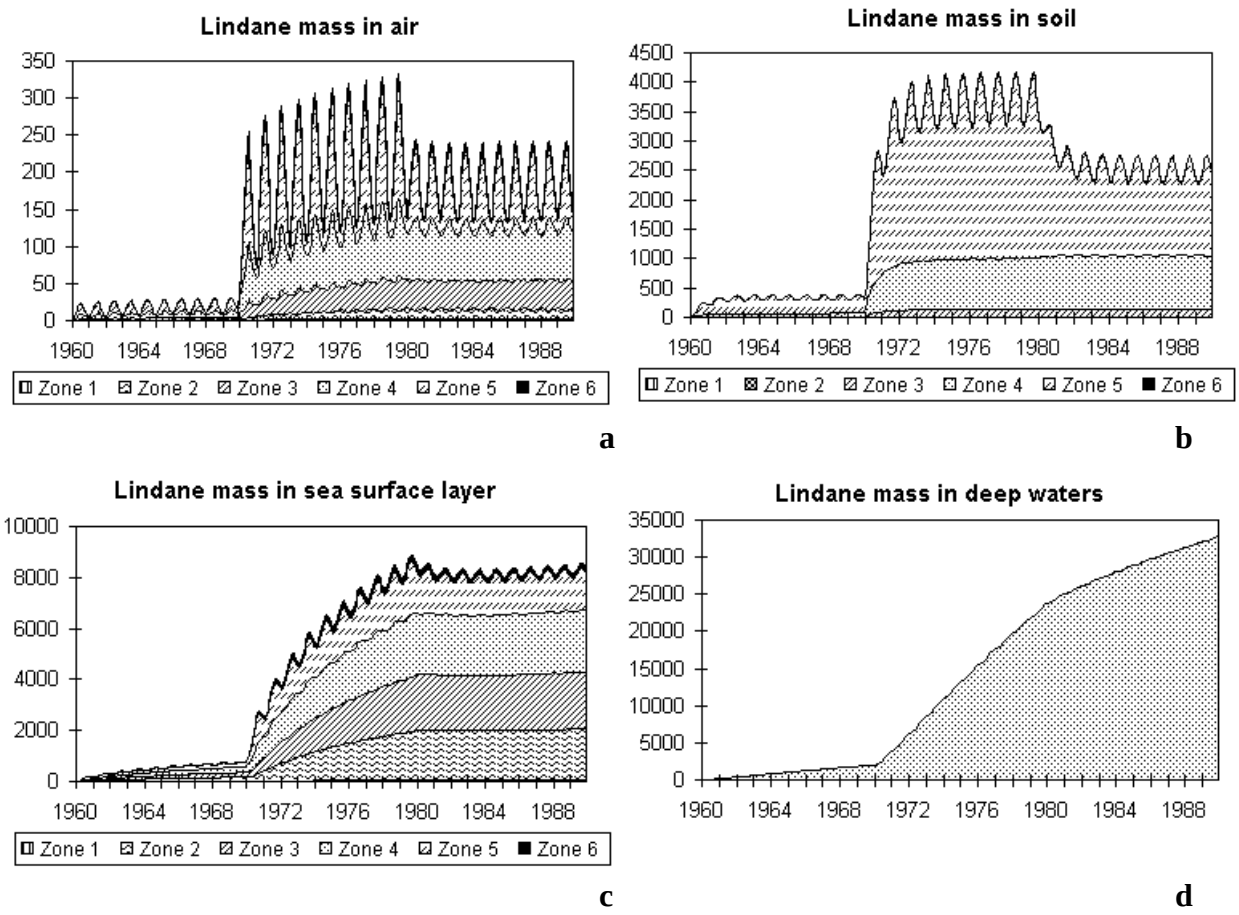

Figure 2.14 Annual variation of lindane mass (tons) in the atmosphere (a); in the soil (b); in surface ocean water (c) in deep ocean reservoir (1-6 latitude zones) (d). Units: tons

Figure 2.14 (a-c) shows mean annual mass of lindane in the air, in the soil and sea for each latitude zone. Figure 2.14 (d) displays lindane mass in the deep ocean reservoir. Lindane mass in the air is mainly associated with the emission values. As a result of lindane emissions reduction in the 80-s lindane content in the air and soil of the 5-th zone cut down. A different situation is observed in the marine environment. Lindane mass increases at the constant emissions and it remains the same when emissions decrease. At the same time after 30 years 2000 tons of lindane were accumulated in the surface water of the 2-d latitude zone (free from emissions). In the deep ocean reservoir the lindane mass also grew during 30-year period.

As evident from Figure 2.14 during 30 years in the surface water 8000 tons of lindane were accumulated, in deep ocean reservoir - 35000 tons, in the soil - 2500 tons and in the atmosphere - 150 tons (the rest of lindane degraded in the marine environment and in the soil). Consequently the ocean has the highest capacity of accumulation.

Then in order to follow the fate of lindane accumulated during 30-year period it was assumed that no further emissions took place during the next 10 years.

Figure 2.15 shows the mass balance after 10-year simulation period without emissions. As seen from the figure 82% of lindane degraded in the soil and marine environment. The remaining part of lindane is retained in the surface sea water (2%) and in ocean deep waters (16%).

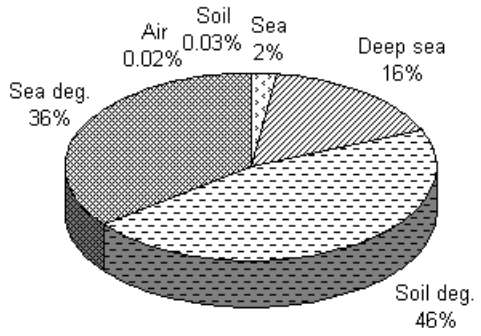

Figure 2.15 Lindane mass balance after 10-year simulation period by the global model upon emission termination

Figure 2.16 (a-c) displays lindane mass in air, soil and surface marine water in all latitude zones after 10-year simulation period with no emissions. Figure 2.14d shows lindane mass in the deep ocean reservoir.

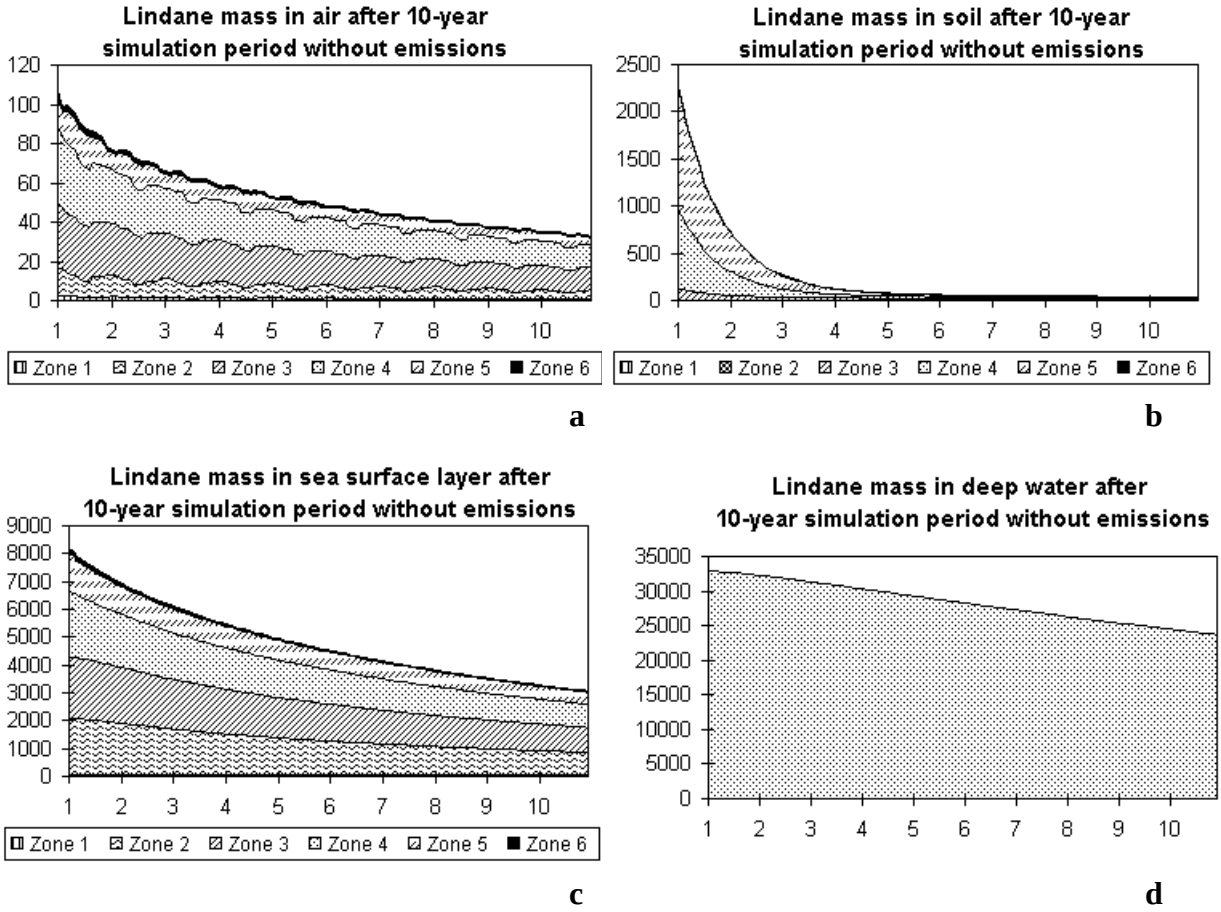

Figure 2.16 Annual variation of lindane mass calculated by the global model: in the atmosphere (a); in the soil (b) and in sea surface water for 1-6 latitude zones (c) and in the deep ocean reservoir (d) after 10-year simulation period with no emissions. Units: tons

The figure indicates that after 10-year of the emission termination the lindane mass reduced in the soil from 2500 tons to 36 tons (in 69 times) in the atmosphere - from 150 tons to 33 tons (in 4.5 times). The lindane mass in the surface ocean water decreased from 8000 tons to 3068 tons (only in 2.6 times). The lindane mass in the deep ocean reservoir reduced from

35000 tons to 24000 tons (less than in 1.5 time). Lindane mass in ocean water remains abundant even after 10 years without emissions.

Lindane calculations with emissions of European countries

In the second numerical experiment calculations were performed only with emission of 1307 t/y (UBA project) in the 5-th zone where most of European countries are situated. Emissions were uniform from year to year. It was assumed that 50% of lindane is emitted to the atmosphere and 50% enters the soil. (Other parameters were the same as in the previous experiments).

Figure 2.17 (a-d) presents annual variation of lindane mass in the atmosphere, in the soil and ocean surface water for 1-6 latitude zones and in deep ocean reservoir. Calculations were made for 30-year period.

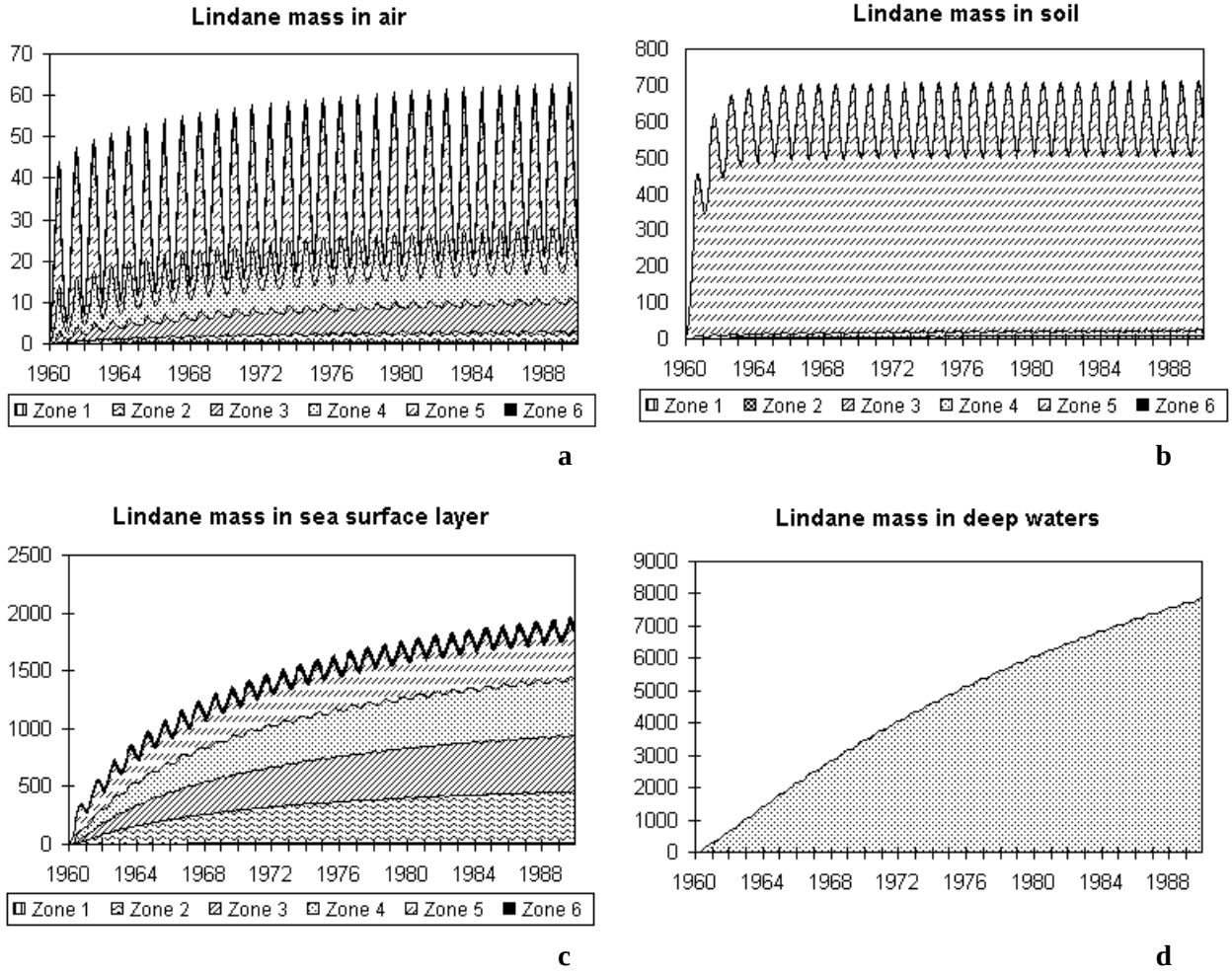

Figure 2.17 Annual variation of lindane mass in the atmosphere (a); in the soil (b); in ocean surface water for 1-6 latitude zones (c) and in deep ocean reservoir (d) for simulation of 30-year period using the global model and UBA project emissions. Units: tons

As seen from Figure 2.17a lindane mean annual mass in the air resulted from UBA emissions is about 35 tons. It is also seen that an essential part of air mass enters other than 5-th latitude

zone. Figure 2.17a clearly shows seasonal variations of lindane mass in the air and its continuous relatively small growth in the 4-th and 5-th latitude zones.

Figure 2.17b indicates that mean annual mass of lindane in the soil is 600 tons concentrated mainly in the 5-th zone. At constant emissions lindane mass in the soil is remained approximately the same during 30-year simulation period. Figure 2.17b clearly indicates seasonal variations of the lindane mass in the soil.

Figures 2.17c and 2.17d show that lindane mass in oceanic waters is growing from year to year at constant emissions. By the end of 30-year simulation period the lindane mass in surface ocean water is 2000 tons and in the deep ocean reservoir - 8000 tons. Figure.2.17c shows that in the 5-th and 4-th latitude zones the lindane mass varied in the surface ocean water.

Figure 2.18 (a-c) presents the mass balance for the 5-th latitude zone after 1-year simulation, 10-year and 30-year simulation periods.

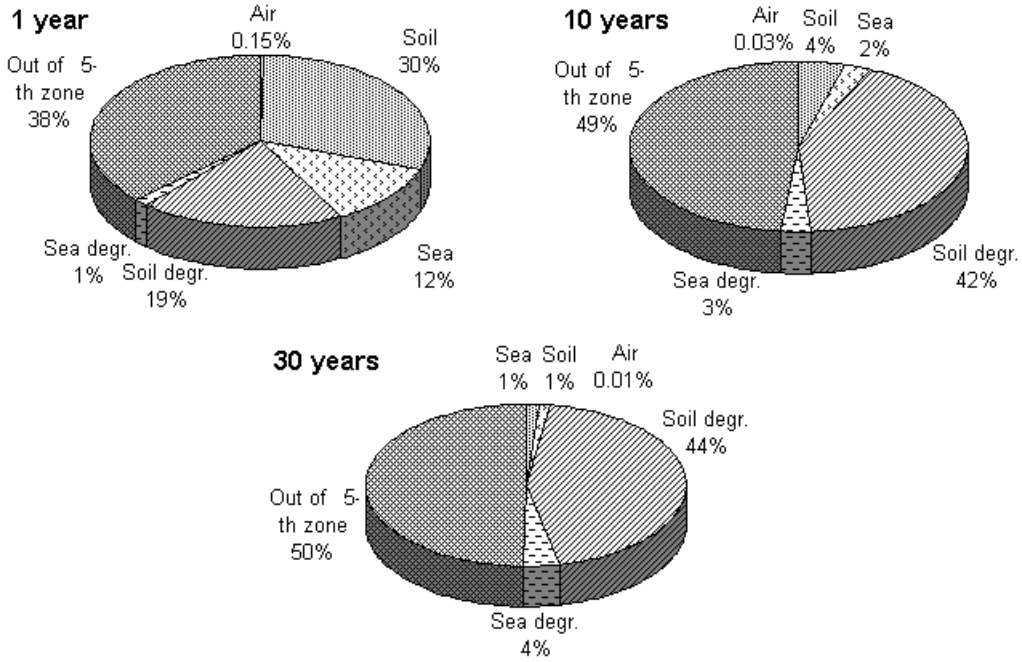

Figure 2.18 Mass balance for lindane after 1-year, 10-year and 30-year simulation periods for 5-th latitude zone. Air %, Soil %, Sea % - lindane fraction in the air, in the soil and sea; Soil degr.%, Sea degr.% - lindane fraction degraded in the soil and surface water; Out of 5-th zone % - lindane fraction transported to other zones

The fraction of lindane in the air is insignificant in the total mass balance. The share of lindane in the soil (including degradation) is from 49% after 1-year to 45% after 30-year of integration periods. The fraction of lindane in the surface oceanic layer (including degradation) is 13% after 1-year and 5% after 10-year and after 30-year integration periods. The transport outside the 5-th latitude zone is 38% after 1-year and about 50% after 10-year and 30-year simulation periods. (Lindane mass transported outside the gird includes lindane of other than 5th latitude zones and of the deep ocean reservoir.)

In the calculation run covering 30-year period it was obtained that 11000 tons of lindane was accumulated over the globe (the total emission mass for this period was assumed to be 39000 tons).

Reasoning from calculation results discussed above the following conclusions can be drawn:

- Emissions in the 5-th latitude zone due to airborne transport result in a continuous growth of lindane mass in oceanic waters in all latitude zones.
- 50% of total lindane mass emitted in the 5-th latitude zone is transported to other latitude zones due to the airborne transport.
- Surface oceanic waters and the deep ocean reservoir have the highest capacity of lindane accumulation.

2.6 Consideration of the calculation results obtained by different models

In this section calculation results obtained by the MSC-E regional model, by the regional model described in [*Jacobs and van Pul*, 1996] and by the global model [*Strand and Hov*, 1996] are considered.

Calculation results obtained by the MSC-E regional and by global models

The regional MSC-E model differs much from the global one in terms of describing the atmospheric and oceanic transport. The MSC-E regional model of the atmospheric transport is three-dimensional, while the global model considered is two-dimensional. Both models incorporate modules of the exchange with soil and sea surfaces. The regional model, however, covers only Europe and therefore we cannot know what is happening to lindane outside the EMEP grid. An undoubted advantage of the global model is an availability of the ocean transport unit while the regional model considers only the upper ocean layer. Therefore, the penetration of lindane into the lower ocean layers and its transport by ocean currents are not taken into account.

We have performed some similar calculations with both models using the same annual lindane emission of 1307 t/year. In the regional model the total emissions were distributed over the EMEP grid in accordance with the data on the annual lindane consumption by individual countries, while in the global model, the total emissions were evenly distributed throughout the 5-th latitude belt (30^{o}N-60^{o}N) where most of European countries are located.

The diagrams of the mass balance after 10-year modelling period by the two models are shown in Figure 2.19a,b.

In the regional model, 5500 t (42%) were transported outside the EMEP grid and in the global model, 6100 t (49%) were transported outside the 5-th latitude zone. Degradation in the soil was 4000 t (30%) for the regional model and 5300 t (42%) for the global model for the 5-th latitude zone. In the regional model after 10-year modelling period the soil mass of lindane accounts for 340 t (3%), in the global model the soil accumulation of lindane is 560 t (4%).

The lindane accumulation in the surface ocean waters after the ten-year integration period was 785 t (6%) for the regional model, for the global model, in the surface ocean waters of the 5-th latitude zone, it was 300 t (2%).

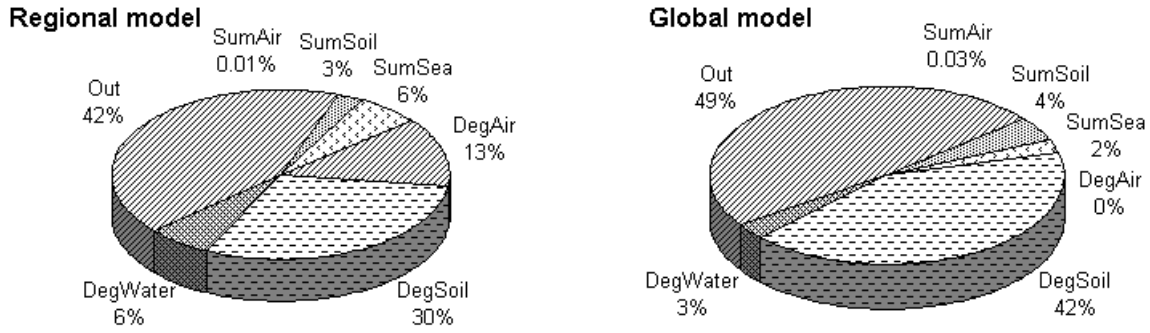

Figure 2.19 Lindane mass balance after modelling of 10-year period calculated by the regional model and by the global model

Consideration of calculation results obtained by MSC-E and EUROS models

C.M.J.Jacobs and W.A.J.van Pul [1996] performed calculations of lindane transport for the ten-year period using the EUROS regional model. The calculation domain of the EUROS covers 52x55 cells in horizontal direction with spatial resolution of 60x60 km^2 i.e. one third of the EMEP area. In the vertical direction it operates with 3 km layer. The model employs a daily variation in the height of the atmospheric boundary layer. The height of the lower atmospheric level where emissions are discharged is 50 m.

Both models incorporate the same module of exchange with soil and ocean [*Jacobs and van Pul*, 1996]. In the MSC-E model lindane degradation in the sea with life-time 6.8 years is considered. In the EUROS model lindane degradation in the sea is not taken into account.

The relationships of lindane masses in different compartments obtained by the two models are found to be close enough (Table 2.7).

In our calculations, mean lindane concentrations in the air over the land and sea are 3-4 times as low as those calculated by the EUROS model, which is associated with a large area where the averaging is made (the area of our calculation grid is three times larger than that of the EUROS grid).

On the whole, the calculational results of the lindane transport within the EMEP grid of both models are in a reasonable agreement.

Table 2.7 Results of lindane transport obtained by the MSC-E model and EUROS models

	MSC-E	EUROS
Maximum mean lindane concentration in the air over the land, μg/m^3 (averaging is made over the EMEP grid)	0.0035	0.010
Maximum mean lindane concentration in the air over the sea, μg/m^3 (averaging is made over the EMEP grid)	0.0005	0.002
Portion of dry deposition in the total deposition over the land, %	25	25
Portion of dry deposition in the total deposition over the sea, %	75	69
Maximum total net deposition, μg/m^2/yr	150	400
Ratio of lindane mass going out the model grid to emission mass after 10-year simulation period, %	42	53.2
Ratio of lindane mass in the soil to emission mass after 10-year simulation period, %	3	3
Ratio of lindane mass degraded in the soil to emission mass after 10-year simulation period, %	30	27
Ratio of lindane mass in surface ocean layer to emission mass after 10-year simulation period, %	6	9.8
Ratio of lindane mass degraded in surface ocean layer to emission mass after 10-year simulation period, %	6	-
Ratio of lindane mass degraded in air to emission mass after 10-year simulation period, %	13	6.9

Conclusions

1. A model for lindane transport with incorporated modules of atmosphere-soil and atmosphere-sea exchange has been developed.
2. The mean concentrations of lindane in the atmosphere for 1990 (annual averaging) at the height of 50 m were 4 ng/m^3 and at 1600 m - 0.8 ng/m^3.
3. Total deposition was maximum in the regions of maximum emissions and accounting for about 150 μg/m^2/year.
4. Annual variations of wet depositions complied with air concentrations over the sea and land and reached the value of 5 μg/m^2/month over land and 1 μg/m^2/month over sea.
5. Dry deposition prevails over wet deposition and accounts to 60% of the total deposition on the soil. Over the marine environment dry deposition predominates over wet deposition accounting for 70%.
6. The analysis of mean net gaseous flux variations over land and sea shows that in the first half of the year these fluxes are positive and account for 3-4 μg/m^2/month over land and 2-3 μg/m^2/month over sea. In the second half of the year net gaseous fluxes over land are negative and about 1 μg/m^2/month. Over the sea in the second half of the year net gaseous

fluxes are also negative and the flux value increases from year to year accounting for 0.5 μg/m^2/month after 10-year simulation period.

7. The simulation results of 10-year period show that about 40% of total lindane emissions were transported outside the EMEP grid, about 30% degraded in the soil, 13% degraded in the atmosphere; 6% accumulated in the soil and 3% in ocean water.
8. The degradation of lindane in the atmosphere and transport outside the EMEP grid are approximately constant from year to year.
9. The analysis of lindane mass variation in the soil and sea show that lindane content in the soil is stabilized after 1-year of simulation period. Lindane content in the marine environment growth steadily during 10-year simulation period.
10. The mass balance in the soil for 10-year simulation period shows that the bulk of lindane mass (75%) degraded in the soil, 15% re-emitted back to the atmosphere and 10% accumulated in the soil.
11. The analysis of the mass balance in sea for 10-year simulation period shows that the bulk of lindane mass about 50% degraded, 10% re-emitted to the atmosphere and 40% accumulated in ocean waters.
12. Calculations of lindane redistribution between different compartments at regional level upon emission termination give the following results:
    - Lindane in the soil is decreased approximately as much as 10 times during 3-year simulation period. In the sea degradation processes are considerably slower;
    - The analysis of net gaseous fluxes over the sea and land show that these fluxes are negative (re-emission) over the whole calculations period. Net gaseous fluxes have annual variations over the land and sea with the peak in summer months. Net gaseous fluxes decrease from year to year and over the land this decrease is considerably more rapid.
13. Runs of the global POP model [*Strand and Hov*, 1996] have been made for 30-year simulation period. The following results were obtained:
    - The lindane mass distributed with different compartments in the following way: maximum quantity of lindane degraded in the soil (44%). The degradation in the sea accounted to 25%;
    - Lindane accumulation in deep waters is 23% after 30-year simulation period.
14. The evaluation of lindane distribution from European sources at the global level was made.
15. Results obtained by two regional models (ASIMD and EUROS) have been compared. The mass balances obtained by both models are in a good consistency.

References

Berdowski J.J.M., Baas J., Bloos J.-P.J., Vesschedijk A.J.H. and Zandveld P.Y.J. [1997] The European Emission Inventory of Heavy Metals and Persistent Organic Pollutants. TNO, Report UBA-FB, UFOPLAN-Ref. No. 104.02 672/03, Apeldoorn, p.239

Berg T., A.-G. Hjellbrekke and J.E. Skjelmoen [1996]: Heavy metals and POPs within the ECE region. EMEP/CCC-Report 8/96. Norwegian Institute for Air Research.

Choiu C.T., Malcolm R.L., Brinton T.I., Kile D.E. [1986] Water solubility enhancement of some organic pollutants and pesticides by dissolved humic and fulvic acids. Environ. Sci. Technol., v.20, pp. 502-508.

Ellington J.J., Stansil F.E., Payne W.D., Trusty C. [1987] Measurements of hydrolysis rate constants for evaluation of hazardous waste land disposal. US Environmental Protection Agency, EPA Report /600/3-87/019.

Frolov A., Vazhnic A., Astakhova E., Alferov Yu., Kiktev D., Rosinkina I., Rubinshtein K. [1994] System for diagnosis of the lower atmosphere state (SDA) for pollution transport model, EMEP/MSC-E Technical report 6/94.

Gruzdev G.S. [1987] Plants chemical protection., Agropromizdat. (in Russian)

Hincley D.A., Bidleman T.F., and Foreman W.T. [1990] Determination of vapor pressures for non-polar and semi-polar organic compounds from gas chromatographic retention data. Journal of Chemical and Engineering Data, v.35(3), pp.232-237.

Howard P.H. [1991] Handbook of environmental fate and exposure data for organic chemicals. Pecticides, v.III, Lewis Publishers Inc., Chelsea, Michigan.

Isnard P., Lambert S. [1988] Estimating bioconcentration factors from octanol-water partition coefficients. Chemosphere, v.17, pp.31-34.

Jacobs C.M.J. and van Pul W.A.J. [1996] Long-range Atmospheric transport of Persistent Organic Pollutants, 1: Description of surface - atmosphere exchange modules and implementation in EUROS. Report N722401013 RIVM, Bilthoven, The Netherlands.

Kenaga E.E., Goring C.A.I. [1980] Relationship between water solibuluty, soil sorption, octanol-water partitioning, and concentration of chemicals in biota. In: Aquatic Toxicology (Eaton J.G., Parrish P.R., Hendricks A.C.(Eds), ASTM, Philadelphia, PA, pp.78-115.

Kononiuk V.F. [1986] About destruction of pesticides in the environment. In: The use and protection of nature water, O, pp.47-54. (in Russian)

Kucklik J.R., Hinckley D.A., Bidleman T.F. [1991] Determination of Henry's low constants for hexachlorocyclohexanes in distilled water and artificial sea water as a function of temperature. Mar. Chem., v.34. pp.197-209.

Kushi M., Kogure N., Hashimoto Y. [1990] Contribution of soil constituents in adsorption coefficient of aromatic compounds, halogenated polycyclic and aromatic compounds to soil. Chemosphere, v.21, pp.867-876.

Laskovski D.A., Swan R.L., McCall P.J., Bidlack H. D., Dishburger H.J. [1984] Characteristics of soil degradation studies for predicting pesticide behaviour. In: Prediction of pesticide behaviour in the environment. Proc. of USA-USSR Symposium, Erevan 1981. EPA-600/9-84-026. Athens, Georgia, USA, pp.90-101.

Li Y.-F., McMillan A. and Scholtz M.T. [1996] Global HCH usage with 10x10 longitude/latitude resolution. Environ.Sci.Technol., v. 30(12), pp.3525-3533.

Lyman W.J. (ed.) [1982] Handbook of chemical properties estimation methods- environmental behaviour of organic compounds. New York, McGraw-Hill Book Co., Inc.

Mackay D., Shiu W.-Y. And Ma K.-C. [1991] Illustrated handbook of phisical-chemical properties and environmental fate for organic chemicals. New York.

Schwarzenbach R.P., Gschwend P.M., [1993] Imboden D.M. Environmental organic chemistry. John Wiley&Sons Inc., New York.

Shapiro M.Ya. [1981] Wind field objective analysis based in geopotential and wind data, EMEP/MSC-E Technical report 3/1981.

Strand A. and Ø.Hov [1996] A model Strategy for the Simulation of Chlorinated Hydrocarbon Distribution in the Global Environment. Water, Air and Soil Pollution, v.86, pp.283-316.

Tzukerman V.G. [1985] Modeling of HCH isomers and simazin behavior in different types of Kazakh SSR soils. In: Pollutions migration in soils and boundary environments. Proceedings of IV Allunion Meeting, Obninsk, L. Hydrometeoizdat, 1985, pp. 31-35, (in Russian).

Vozhzennikov O.I., Bulgakov A.A., Popov V.E. et al. [1997] Review of migration and transformation parameters of selected POPs, EMEP/MSC-E Report 3/97.

Wania F., Shiu W.Y., Mackay D. [1994] Measurement of the vapour pressure of several low volatility organochlorine chemicals at low temperature with gas saturation method. J. Chem. Eng. Data v.39, pp.572-577.

Chapter 3 Polychlorinated biphenyls (PCBs) modelling

3.1 General information on PCBs

Polychlorinated biphenyls (PCBs) were synthesized in the USA in 1929. Since then PCBs have been widely used in various industrial and commercial products (plasticizers, additives to hydraulic liquids and dielectrics and flameretardants) [*Schlatter*, 1994]. The content of PCBs in the environmental compartments is a result of industrial activity.

The current information on PCBs transport, air concentrations, depositions, vertical distribution and behaviour in different compartments is very limited.

The data on the total amount of produced PCBs are rather similar:

$1.2 \cdot 10^9$ kg [*Background monitoring*… , 1990; *Surnina and Tarasov*, 1992; *Vit Long*, 1992; *Rovinsky et al*., 1992];

$1.5 \cdot 10^9$ kg - $2.0 \cdot 10^9$ kg [*Klyuev et al*., 1990].

About 35% of total PCBs production enters the environment [*Kisselev et al*., 1997; *Surnina and Tarasov*, 1992].

In the lower atmosphere PCB isomers occur in the gaseous phase and bound on the particles of submicron size. In the air, PCBs mainly occur in the gaseous phase, over the ocean up to 100% of PCBs are in the gaseous phase and over the land - 50-90% [*Background monitoring...*, 1990; *Surnina and Tarasov*, 1992].

Some data on concentrations and depositions of PCBs are included in table 3.1.

Table 3.1 Mean concentrations of PCBs in the air C_a (ng/m^3), precipitation C_{pr} (ng/l) and fluxes deposition – re-emission D (μg/m^2/yr) (positive flux – from the atmosphere) [*Rovinsky et al.*, 1990; *Izrael and Tsyban*, 1989; *van Oss and Duyzer*, 1996]

	C_a (ng/m^3)	C_{pr} (ng/l)	D (μg/m^2/yr)	
Western Europe (1975 – 1985)	0.3 (0.01 – 1)	30 (1 – 50)	7.2 ÷ 120 5 ÷ 11	(1970 – 1971) (1979 – 1980)
North America (1976 – 1985)	3 (1 – 5)	60 (10 – 390)	3.6 ÷ 360 -80 ÷ -20 -7 ÷ -3 up to – 400	(1973 – 1974) (mid–80s) (1991 – 1993) (summer, 1989)
Arctic (1980 – 1983)	0.005 – 0.02			
Antarctica (1980 – 1982)	0.061	0.2		
Atlantic Ocean (1973 – 1978)	0.1			
Pacific Ocean Northern part (1976)	0.41 – 1	0.6	15 (1990)	

The PCBs content in the atmospheric precipitation in different regions of the globe varies within wide ranges: over the European continent it amounts to 50 ng/l, in the region of the Great Lakes (USA) - 100-130 ng/l [*Larsson*, 1984; *Travis et al.,* 1987; *Manchester et al.*, 1990; *Estimating exposure ...*, 1994]. The PCBs removal from the atmosphere to the underlying surface is due to precipitation and dry deposition. Dry deposition is predominant [*Background monitoring...*, 1990]. According to calculations PCBs deposition on the underlying surface is in the range from 7.2 to 120 $\mu g/m^2/yr$ [*Maistrenko et al.*, 1996].

PCBs are accumulated in surface layer of soil as deep as 30 cm. The half-life of PCBs in the soil varies from 2.5 to 45 years [*Prokofiev*, 1990; *Rovinsky et al*., 1992; *Fischer*, 1989; *Bergen*, 1993; *Klissenko*, 1988]. The half-life is most likely to be 20 years [*Maistrenko et al.*, 1996].

PCBs are weakly soluble. Mean global level of the PCBs content in fresh water and sea basins is $2 \cdot 10^{-6}$ - $20 \cdot 10^{-6}$ mg/l [*Background monitoring...*, 1990; *Rovinsky et al*., 1992]. PCBs are accumulated in organic and inorganic particles. Data on concentrations of PCBs in surface water, bottom sediments, soil and vegetation are given in table 3.2.

Table 3.2 Concentrations of PCBs in the surface water, bottom sediments, soil and vegetation [*Rovinsky et al*., 1992; *Izrael and Tsyban,* 1989]

	Surface water, ng/l	Bottom sediments, ng/kg	Soil, ng/kg	Vegetation, ng/kg
Western Europe	10 (1 – 90)	70	1 – 100 (10)	10 – 300
North America	5 (1 – 10)	75 (1 – 340)	10 - 40	10 – 170
Pacific Ocean	0.1 – 0.3	0.5 – 9.5		
Atlantic Ocean	0.3 – 8			
Antarctica	0.03 – 0.07			

When PCBs ceased to be manufactured (in Sweden since 1971, in Norway - 1977, in Japan - 1972, in USA - 1978) PCBs level in biota slowly decreased [*Kisselev et al.*, 1997]. Mean global level of PCBs in plant tissues is 9 ng/kg; in tissues of wild animals - 90 ng/kg; and in tissues of fresh-water and sea fish from 200 to 2000 ng/kg [*Background monitoring...*, 1990]. Content of PCBs in environment is presented in table 3.3.

Table 3.3 Content of PCBs in the environment [*Fischer*, 1989]

Object	PCB concentration
Atmospheric air, ng/m^3:	
urban area	5.0
agricultural region	0.5
over ocean	0.05
Antarctic	0.05
Atmospheric precipitation, ng/l:	
over land	10-100
over ocean	10-100
Antarctic	10-100
Hydrosphere, ng/l	
surface water of land	1-10
seas, oceans	0.2-9
ocean near Antarctic (bottom sediments) μg/kg	0.2-100
Soil, μg/kg:	
reserves far from agricultural regions	2-20
Land biota, μg/kg:	
plants	2-40
wild animals	20-400
Aquatic biota, μg/kg:	
zooplankton	10-50
freshwater fish	10-300
fish of seas and oceans	10-100
marine mammals (underskinfat)	100-10000

3.2 Physical-chemical properties of polychlorobyphenil – 153 (PCB-153)

In accordance with the recommendation of the EMEP workshop [*Moscow*, 1996] physical-chemical properties of PCB-153 could be used as model parameters to simulate the PCBs long-range transport at the first stage.

PCB-153 is a PCB hexaisomer (2,2', 4,4', 5,5'- hexachlorobiphenyl). There are 42 hexachloroisomers in total. PCB-153 is a reference compound because it is incorporated into the calibration mixture used for the identification and quantification of all 209 PCB congeners. PCB-153 is not coplanar (the angle between the planes of phenyl nuclei is 50^0) and toxic compound. However, it is a modulator of the toxic impact of other pollutants. Moreover PCB-153 is present practically in all produced technical mixtures in a significantly high quantities – from 5 to 17% (on the average - about 10%).

Melting (T_m) and boiling (T_b) temperature

$T_m = 103^0$C [*Yalkowsky et. al.,* 1983]

$T_b = 405^0$C [*Estimating exposure*…, 1994]

Solubility (S)

Solubility at 25^0C

The PCB-153 solubility data at 25^0C found in literature are listed below

Reference	S, mol/m^3	S, mg/l
Pal et al., 1980	24×10^{-6}	8.8×10^{-3}
Shiu and Mackay 1986*	2.8×10^{-6}	1×10^{-3}
Haque and Schmedding 1975	2.6×10^{-6}	0.95×10^{-3}
Choiu et al., 1977	2.6×10^{-6}	0.95×10^{-3}
Yalkovsky et. al., 1983	3.6×10^{-6}	1.3×10^{-3}
Opperhulzen et al., 1988	3.3×10^{-6}	1.15×10^{-3}
Dunnivant and Elzrmann, 1988	2.4×10^{-6}	1.3×10^{-3}
Mackay et al., 1991	3×10^{-6}	1.1×10^{-3}

* Selected value

Solubility dependence on temperature

The following equation is calculated using dissolution enthalpy data [*Doucette and Andren,* 1988]:

$$\log S\ (mol/m^3) = -2435/T + 2.65$$

Solubility dependence on salinity

PCB-153 solubility in sea water can be assessed as 20% of its solubility in distilled water.

Solubility dependence on organic matter content in the water

Solubility of the chlorinated biphenyls increases 5-7 times as the concentration of the humic acid increases from 0 to 100 mg/l, while the increase of fulvic acid concentration in the same range does not considerably affect the PCB-153 solubility [*Choiu et al.,* 1986].

Saturated vapour pressure at $25(20)^0$C

Saturated vapour pressure for solid (P_{OS}) at $25(20)^0$C for PCB-153 is as follows: $P_{OS} = 3.2\times10^{-5}$ Pa [*Dunnivant and Elzerman*, 1988]; $P_{OS} = 4.2\times10^{-5}$ Pa (20^0C) [*Murphy et al.*, 1987]; $P_{OS} = 2.6\times10^{-5}$ Pa [*Harner et al.*, 1995]; 1.2×10^{-4} Pa [*Mackay et al.,* 1991].

Temperature dependence of vapour pressure for solid P_{OS} is written as follows:

$$\log P_{OS}\ (Pa) = -5851/T(K) + 15.10$$ [*Vozhzennikov et al.*, 1997]

The dependence of saturated vapour pressure for the subcooled liquid P_{OL} is written as follows:

$$\log P_{OL}\ (Pa) = -4798/T(K) + 12.30$$ [*Vozhzennikov et al.*, 1997]

Henry`s law constant (H)

Henry`s law constant H values at 25^0C for PCB-153:

References	t, ^{0}C	H, Pa·m^3/mol
Murphy et al., [1987]	20	9.9
Dunnivant and Elzerman, [1988]	25	13.2
Harner et al., [1995]*	25	20
Mackay et al., [1991]	25	42

* Assessment

Dependence of H on temperature is as follows:

$$\log H\ (Pa \cdot m^3/mol) = -3416/T(K) + 12.61$$ [*Vozhzennikov et al.*, 1997]

E.Atlas et al. [1982] showed that average ratio of Henry`s law constants of tetra- and penta-chlorobiphenyls in sea to that in fresh water is 5.

Sorption by soil, sediments and suspended particles

The sorption value is determined by the following coefficients: K_{oc}(dm^3/kg) – organic carbon distribution coefficient; K_{ow}(dm^3/kg) – octanol-water distribution coefficient

$\log K_{oc}$ = 6.07 [*Karikhoff et al.,* 1979], $\log K_{oc}$ = 4.78-6.87 with average value equal to 5.70 [*Horzempa and DiToro,* 1983]. For modelling, K_{oc} = 130 m^3/kg was chosen.

$\log K_{ow}$ = 7.00 [*Shiu and Mackay,* 1986], $\log K_{ow}$ = 7.55 [*Miller et al.,* 1984], $\log K_{ow}$ = 6.9 [*Bayona et al.,* 1991], $\log K_{ow}$ = 6.9 [*Risby et al.,* 1990].

Degradation rates in soils

The measurements of PCB-153 degradation rate constant are complicated by its stability to the action of soil microorganisms. For purposes of the short-term modelling it is reasonable to consider PCB-153 as undegradable substance; for long-term modelling its degradation half-life can be assumed, as for DDT, equal to 10 years. Recommended half-life time for hexachlorobiphenyls is 6 years [*Mackay et al.*, 1991].

Degradation rate in the water

The main mechanism of PCB-153 degradation in natural waters is reaction with hydroxyl radical. Considered half-life values are 4, 80 and 1600 days for fresh water, coastal sea water and open ocean, respectively. These estimations were made for the water-soluble PCB-153 fraction. To calculate the degradation half-lives of the total (dissolved and sorbed by suspended matter and bottom sediments) PCB-153, it could be necessary to divide them by fractions. Recommended half-life time for hexachlorobiphenyls is 6 years [*Mackay et al.*, 1991].

Degradation rate in the atmosphere

Assessment of the degradation half-life of PCB-153 in the atmosphere due to reaction with the OH radical is: 13 days in summer, 34 days in spring/autumn, 300 days in winter. These estimations were made for gaseous PCB-153 fraction. For the calculation of the degradation

half-lives of the total (gaseous and sorbed on particles) PCB-153 it could be necessary to divide them by fractions [*Vozhzennikov et al.*, 1997]. Half-life time for hexachlorobiphenyls is 8 months [*Mackay et al.*, 1991]. For modelling half-life time equal to 10 months was chosen.

3.3 Model assumptions and parametrization

The simulation of PCBs transport was fulfilled for 40 years period with emissions and for the next 10 years without emissions to evaluate the behaviour of PCBs under different conditions.

On the basis of the considered physical-chemical properties of PCB-153 the parametrization of the basic processes contributing to the transport of PCBs in the atmosphere and other environmental compartments was developed.

Modelling was performed using the basic atmospheric transport model (ASIMD) coupled with the atmosphere/soil and atmosphere/sea exchange modules provided by RIVM [*Jacobs and van Pul*, 1996].

At this stage the following model assumptions were made:

1. PCBs are presented in the atmosphere only in the gaseous phase.
2. Initial and background concentrations in the environmental compartments are assumed to be zero.
3. PCBs exchange with soil surface is fully described by the approach developed by [*Jacobs and van Pul*, 1996]. The module of PCBs exchange with sea is supplemented by the additional block of the vertical diffusion in sea. This block calculates the vertical diffusion of PCBs in 5 layers of 25 m depth each.
4. Sedimentation of PCBs in ocean waters and transport by sea currents are not considered.
5. The model parametrization was made using data mentioned above (section 3.2).

Model parameterisation

HENRY`S LAW CONSTANT $\log H = 12.61-3416/T^0$ Pa m^3/mol [*Vozhzennikov et al.*, 1997]

DISTRIBUTION COEFFICIENT $K_d = f_{oc} \times K_{oc}$

f_{oc} - fraction of organic carbon in the soil f_{oc} [from data base [RIVM]]

K_{oc} - organic carbon distribution coefficient $K_{oc} = 130$ m^3/kg [see section 3.2]

DEGRADATION:

SOIL	$K_s = 3.66 \cdot 10^{-9}$ s^{-1}	[*Mackay et al.*, 1991]
SEA	$K_w = 3.66 \cdot 10^{-9}$ s^{-1}	[*Mackay et al.*, 1991]
ATMOSPHERE	$K_a = 2.67 \cdot 10^{-8}$ s^{-1}	[see section 3.2]

MOLECULAR DIFFUSION COEFFICIENT:

AIR	$D_g = 5.0 \cdot 10^{-6}$, m^2/s	[*Jury et al.*, 1983]
WATER	$D_w = 5.0 \cdot 10^{-10}$, m^2/s	[*Jury et al.*, 1983]

The following data are taken from [*Jacobs and van Pul*, 1996]

VOLUMETRIC FRACTION:

POROSITY $\varphi = 0.5$

VOLUMETRIC AIR CONTENT $a = 0.3$

VOLUMETRIC WATER CONTENT $\theta = 0.2$

SOIL BULK DENSITY $\rho_s = 1300$ kg/m^3

AERODYNAMIC RESISTANCE $$r_a = \frac{\ln(Z_r/Z_0) - \psi(Z_r/L) + \psi(Z_0/L)}{ku_*}$$

QUASI-LAMINAR BOUNDARY LAYER RESISTANCE $$r_b = \frac{2}{ku_*}\left(\frac{Sc}{Pr}\right)^{2/3}$$

DIFFUSION THICKNESS (WATER) $d_{zwm} = 4.0 \cdot 10^{-5}$, m

CHARACTERISTICS OF THE CALCULATION GRID FOR SOIL:

NUMBER OF LAYERS $K_{max} = 5$

DEPTHS OF LAYERS: DSZ(1) = 0.005, m
DSZ(2) = 0.005, m
DSZ(3) = 0.01, m
DSZ(4) = 0.02, m
DSZ(5) = 0.11, m

CHARACTERISTICS OF THE CALCULATION GRID FOR SEA: (see above in this section)

NUMBER OF LAYERS $K_{max} = 5$ -''-

DEPTHS OF LAYERS: DSZ(1) = 25, m -''-
DSZ(2) = 25, m -''-
DSZ(3) = 25, m -''-
DSZ(4) = 25, m -''-
DSZ(5) = 25, m -''-

EDDY DIFFUSIVITY IN SEA: K = 465, m^2/yr [*Strand and Hov*, 1996]

3.4 Input data

Emissions

In the model calculation emissions of PCBs estimated by *J.Berdowski et al.* [1997] for 1990 were used. These emission estimates are presented in table 3.4. Spatial distribution of emissions with the EMEP grid cells with resolution 150x150 km^2 is demonstrated in Figure 3.1. The total emissions for 1990 are about 116 tons. The emissions are distributed uniformly

during the year. Uncertainty factor of PCB emission estimates can be as high as 2-5 times [*Berdowski et al*., 1997].

Official data on PCB emissions were provided by only 8 countries (EB.AIR/GE.1/1997/3 EB.AIR/GE.1/1997/3/Add.1) (table 3.5). For the most part these data are close to estimates presented in table 3.4. Considerable discrepancies of the official data and estimates are observed for Finland.

At this stage estimates of emissions made by *J.Berdowski et al.* [1997] were used in the calculations.

Table 3.4 PCB emission estimates [*Berdowski et al.*, 1997]. Units: t/yr

Country	Emission	Country	Emission
Albania	0.034	Latvia	0.162
Austria	1.32	Lithuania	0.221
Belarus	0.600	Luxembourg	0.119
Belgium	5.20	The FYR of Macedonia	0.083
Bosnia & Herzegovina	0.128	Republic of Moldova	0.269
Bulgaria	0.317	Netherlands	0.251
Croatia	0.132	Norway	0.384
Cyprus	0.044	Poland	2.37
Czech Republic	1.99	Portugal	0.523
Denmark	0.987	Romania	0.515
Estonia	0.179	Russian Federation*	7.25
Finland	2.62	Slovakia	1.33
France	19.5	Slovenia	0.071
Germany	43.0	Spain	8.53
Greece	0.251	Sweden	1.93
Hungary	0.130	Switzerland	1.64
Iceland	0.047	Ukraine	3.74
Ireland	0.063	United Kingdom	3.45
Italy	5.83	Yugoslavia	0.435
TOTAL			116

* within the EMEP grid

Table 3.5 UN/ECE reported official PCBs emission data. Units: t/yr

Country	1990	1991	1992	1993	1994	1995
Bulgaria	0.2584					0.3822
Finland				5.3	1.1	15.8
France	13					
Germany	45					
Hungary	0.130	0.120	0.108	0.106	0.104	0.104
Netherlands	0		0.251			
Poland	2.373					2.338
United Kingdom				3.500		

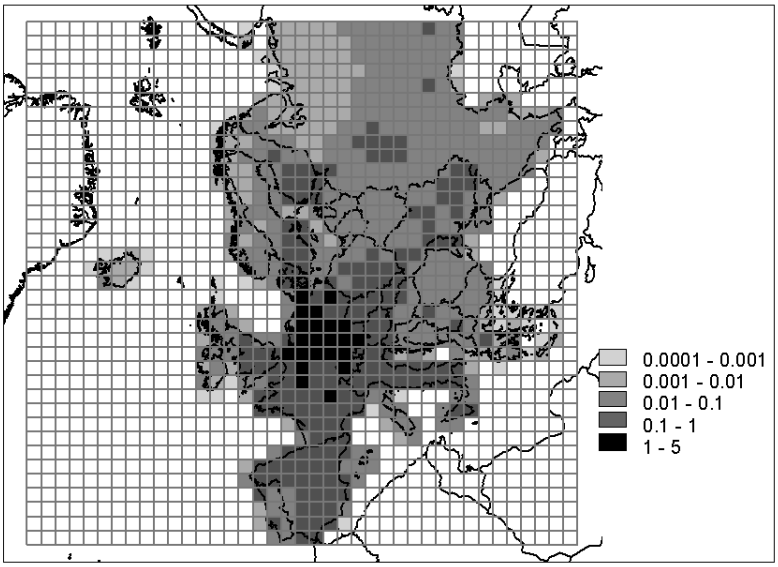

Figure 3.1 Map of PCB emission within EMEP grid for 1990 year.
Total emissions are 116 tons. Units: t/yr

Meteorology

Meteorological information prepared by Hydrometeorological Centre of the Russian Federation with the procedures described in [*Shapiro*, 1981] for 1987-1993 and in [*Frolov et al.*, 1994] for 1994-1996 is used in the calculations.

3.5 Calculations results

Modelling of PCBs transport for 40-year period was aimed at tracing PCB trends of accumulation in the soil and ocean waters, re-emission and degradation. In addition, study of PCBs behaviour in different environment compartments at the absence of emissions within the EMEP grid was also carried out.

Calculation results of PCBs transport for 40 year period

Figure 3.2 presents the map of total PCBs deposition on the surface inside EMEP grid after 40 years of simulations. The area of maximum deposition coincides with the region of maximum emissions in the centre of Europe. The other local maximum of deposition lies on the sea water along the coastal line. The maximum value of deposition on the continental surface is about 70 $\mu g/m^2$ after the whole period of integration (40 years). The maximum value of deposition on the surface of the Baltic Sea is about 50 $\mu g/m^2$, and about 25-50 $\mu g/m^2$ on the surface of the North Sea.

As it is clearly seen from the Figure 3.2 the sea surface is a powerful sink of PCBs. The soil surface adsorbs PCBs not so willingly as the sea surface.

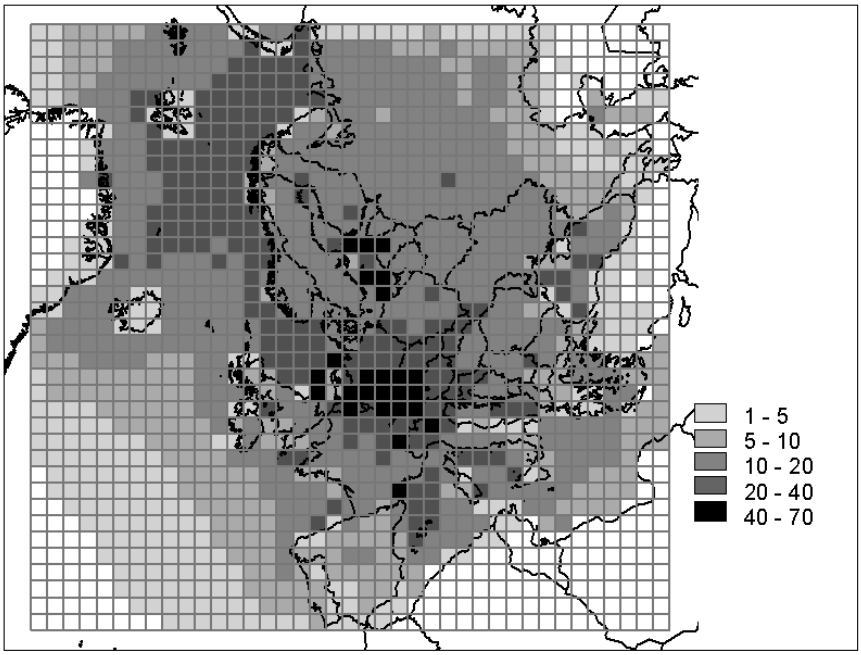

Figure 3.2 PCBs total deposition after 40-year of simulation period. Units: $\mu g/m^2$

As for high deposition on coastal regions, some comments are required.

1. For the atmospheric PCB concentrations (Figure 3.3a), the maximum is observed in the maximum emissions region. PCB concentrations decrease rather slowly (since both wet and dry deposition is relatively small), so that even near the western coast of Scandinavian peninsula they are just an order of magnitude lower than maximum concentrations.
2. In accordance with calculation results the rate of wet deposition is, on the average, lower than that of dry deposition.
3. Calculated dry deposition rates for land (0.004-0.01 cm/s) are considerably lower than those for sea (0.04-1.5 cm/s). These figures approximately coincide with the values presented in [*van den Hout*, 1994], i.e. 0.002-0.02 cm/s for land and 0.5 cm/s for sea.
4. A sharp change in dry deposition rates at the land-sea interface (coastal zone) leads to the increase in deposition on the sea.
5. A similar situation of the sharp increase in the deposition with the transition from land to sea across a coastal line is observed in model calculations for trifluralin and for 2.4-D particularly [*Baart et al.*, 1995]. In comparison with PCB-153 these substances have rather similar properties.

Figure 3.3 shows PCB air concentrations averaged over a year at the heights of 50 m (a) and 1600 m (b). Air concentrations are maximum in the region of maximum emissions and they are by 2 orders of magnitude lower at the borders of the EMEP grid. Directly over the emission region PCB concentrations at the height of 1600 m are 5 times lower than at the height of 50 m. In the remote regions the concentrations at these two heights are equal.

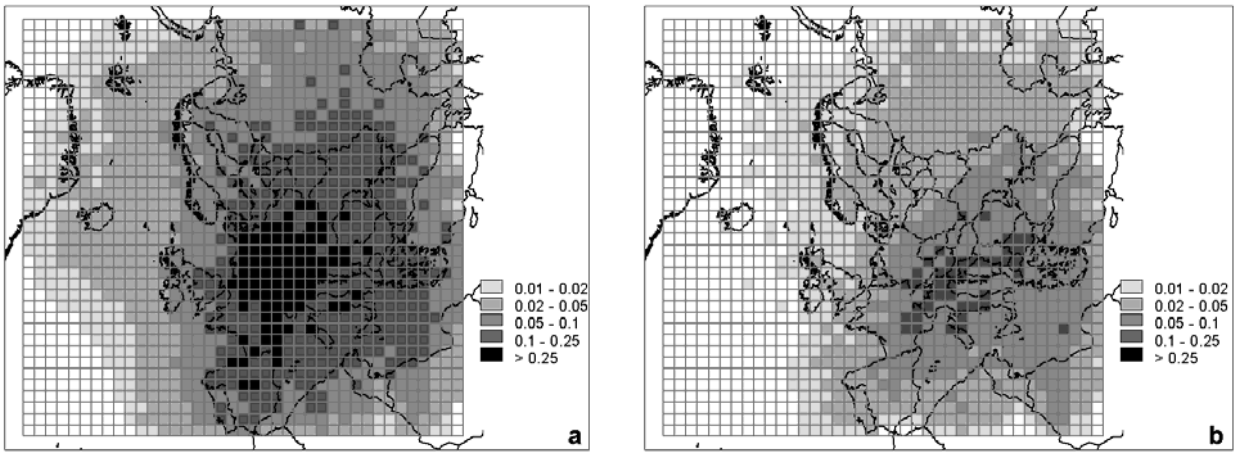

Figure 3.3 PCB mean annual concentrations in the atmosphere at the height of 50 m (a) and 1600 m (b). Units: ng/m^3

PCBs mass-balance for the last year of the calculation period is presented in Figure 3.4. As it can be seen from the diagram, steady state level in the soil and in the water is not fully reached: input of PCBs to the compartments due to deposition is not balanced in full measure by degradation and re-emission from the compartments. Amount of PCBs in the soil and water compartments is greater in the end of year than in the beginning of it. Partially it can be connected with yearly meteorological variability, which can generate oscillation near steady state level even on annual averaging.

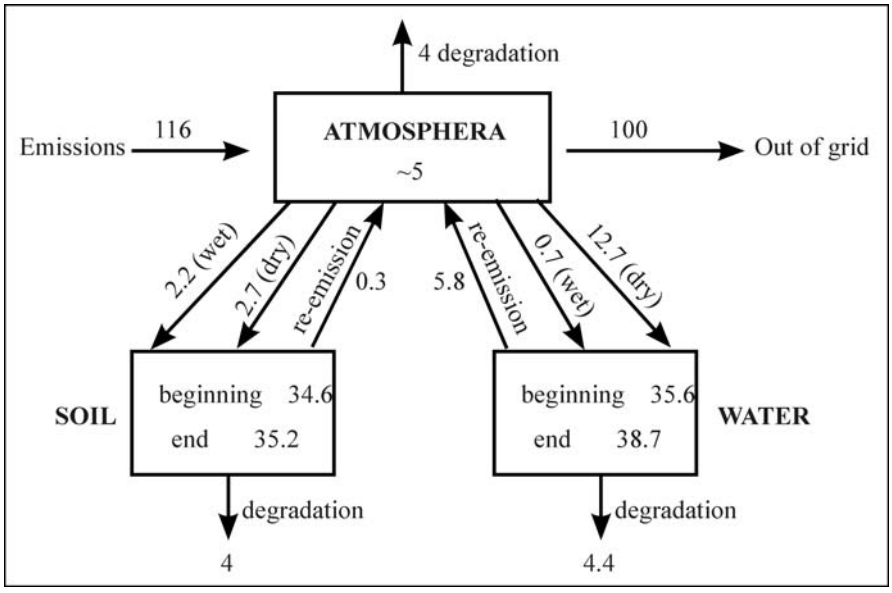

Figure 3.4 PCBs mass balance for 40th year of calculation. Units: tons

During the year the main part of emitted PCBs moves out of grid, about 5 tons of PCBs are deposited on the soil, nearly 13 tons – on the water. Re-emission of PCBs from the soil (about 0.3 tons) is less than that from the water (about 6 tons). Values of degradation in all the compartments are equal nearly to 4 tons each.

PCB mass variations in different compartments

As seen from Figure 3.5 PCBs mass in the water and soil is changed insignificantly after 10-years of calculations. PCB contents in the sea and soil vary with seasons. In the sea the variations are more distinctive.

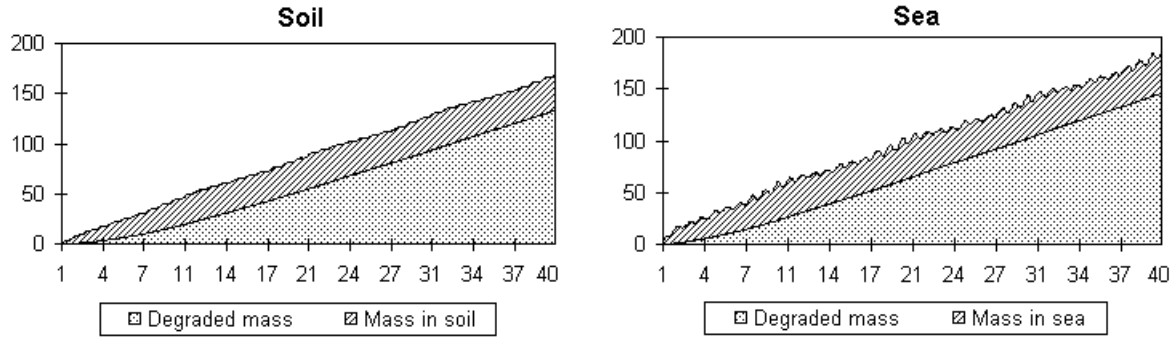

Figure 3.5 The changes of PCBs mass in the soil and in the sea during 40-year period. Units: tons

Figure 3.6 shows the change of PCBs mass in the air during 40-year period. PCBs amount in the air varies with seasons due to processes of re-emission from the soil and sea surfaces.

Figure 3.7 presents PCBs degradation in the air and their transport outside the calculation grid. These values increase practically linearly and the transport outside the grid is a substantial part of the total emissions.

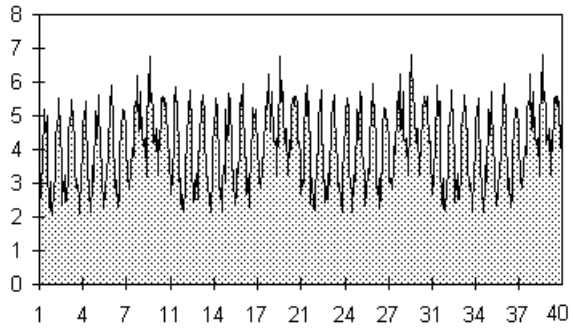

Figure 3.6 PCBs mass in the air during 40-year period. Units: tons

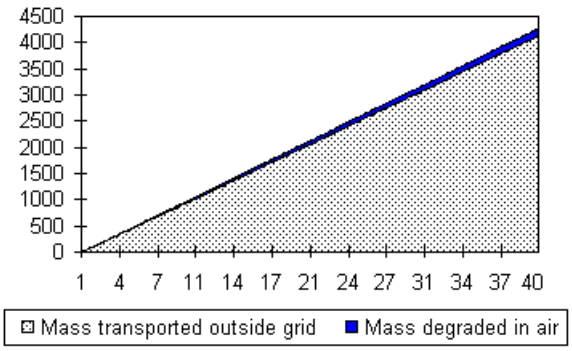

Figure 3.7 PCBs mass transported outside the EMEP grid and degraded in the air. Units: tons

The following diagrams (Figure 3.8) demonstrate PCBs mass balance within the EMEP grid for different simulation periods at the constant emissions equal to 116 t/yr.

Mass balance diagrams show that more than 80% of total mass of PCBs is transported out of EMEP grid, 3% degrades in the air, 2% is accumulated and 3% is degraded in sea, 1% is accumulated and 2% is degraded in the soil.

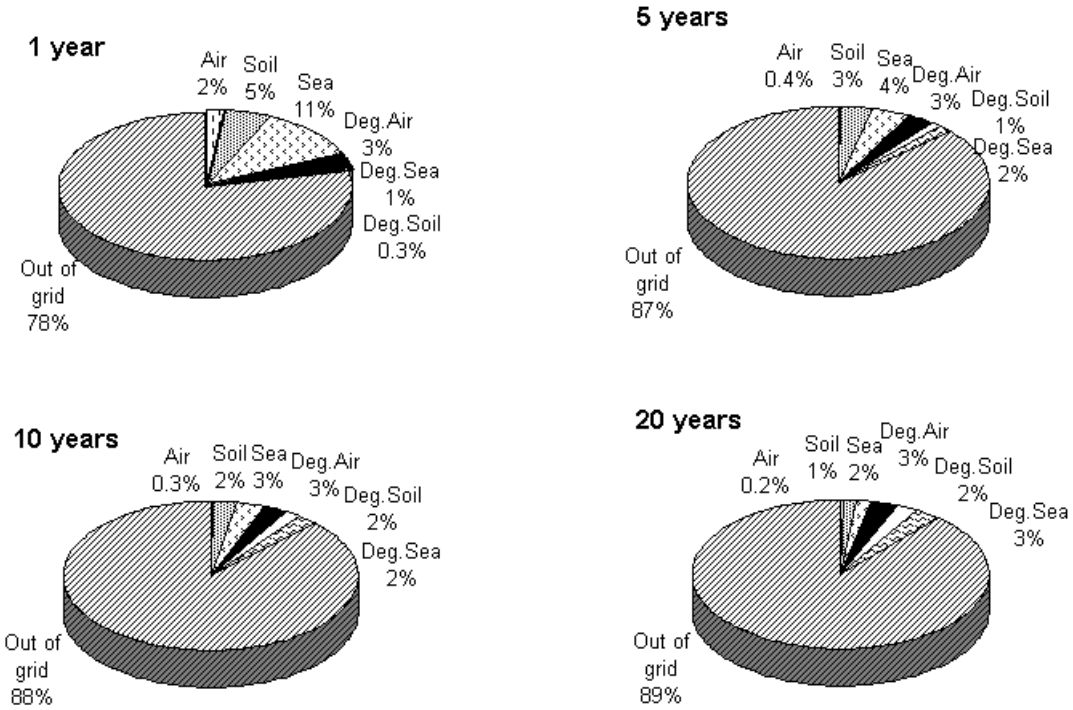

Figure 3.8 PCBs mass balance within the EMEP. Air%, Sea%, Soil% - mass fractions of PCBs in the air, marine water and soil relative to total emissions; Deg.Air%, Deg.Sea%, DegSoil% - PCB fractions degraded in the air, sea and soil; out of grid% - PCBs fraction transported outside the region of simulations.

Figure 3.9 presents diagrams of the input of wet and dry deposition on the land and sea and the relationship of accumulated, degraded and re-emitted amounts of PCBs in the soil and sea for 40-year simulation period.

As seen from diagrams the ratio of wet to dry deposition is approximately constant during the whole period of integration. As for the soil, wet deposition amounts to 40% and dry deposition – 60% of total deposition; and as for the sea, wet deposition amounts to 5% and dry deposition – 95% of total deposition.

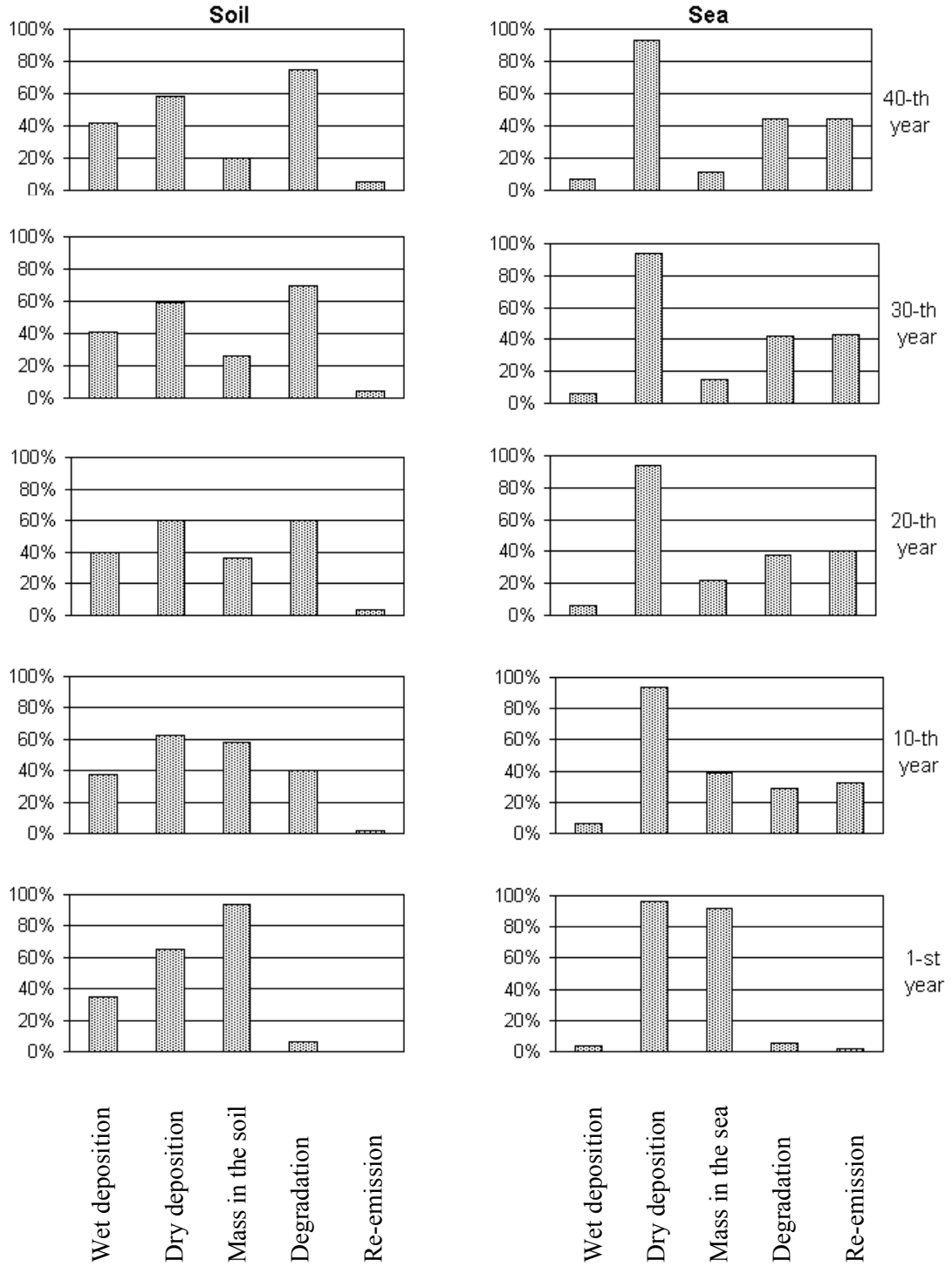

Figure 3.9 PCBs mass-balance in the soil and sea. Units:%

The ratio of wet to dry deposition for the 1st year is slightly different as compared with other years due to small re-emissions.

The percentage of re-emission from the soil and sea surfaces slightly increases from year to year. The re-emission from the soil is small and equals to nearly 5% in the 40th year of simulation. The percentage of re-emission from the sea is very high and reaches nearly 45% at the end of the simulation period.

The percentage of mass in the soil decreases slower than in sea. This is conditioned by the small rate of the re-emission from the soil. The main process that affects the removal of mass from the soil is degradation. Degradation in the soil reaches about 80% in the 40th year of simulation, and the remaining mass is about 20 %.

As for sea the both processes – degradation and re-emission – have near the same percentage. The percentages of degradation and re-emission are about 45% each for the 40th year of simulation.

Seasonal variations

Figure 3.10 shows monthly variations of the mean concentration (averaging is made over the whole EMEP grid) in the air over the land (a) and over the sea (b), $\mu g/m^3$ and monthly variations of net gaseous and wet deposition fluxes to the land (c,e) and to the sea surfaces (d,f), $\mu g/m^2$/month. The simulations were made for 1st, 4th and 10th years of the calculation period.

There is practically no concentration variation either over the land or over sea at constant emissions round the year. The mean concentration of PCBs over the land is 0.15 ng/m^3 and over the sea - 0.05 ng/m^3.

The net gaseous flux to the soil is positive everywhere during the 1st and 4th calculation year. In the 10th year during a warm period re-emission from the soil takes place. The absolute value of the net gaseous flux over the sea is at least by an order of magnitude higher than over the soil. Thus the atmosphere/sea exchange processes are more intensive than the atmosphere/soil ones and the sea more easily re-emits PCBs back to the atmosphere than soil.

Wet deposition fluxes over the sea and soil are 2 times higher in winter months of the year than in the summer ones at approximately equal PCB concentrations in the air round the year.

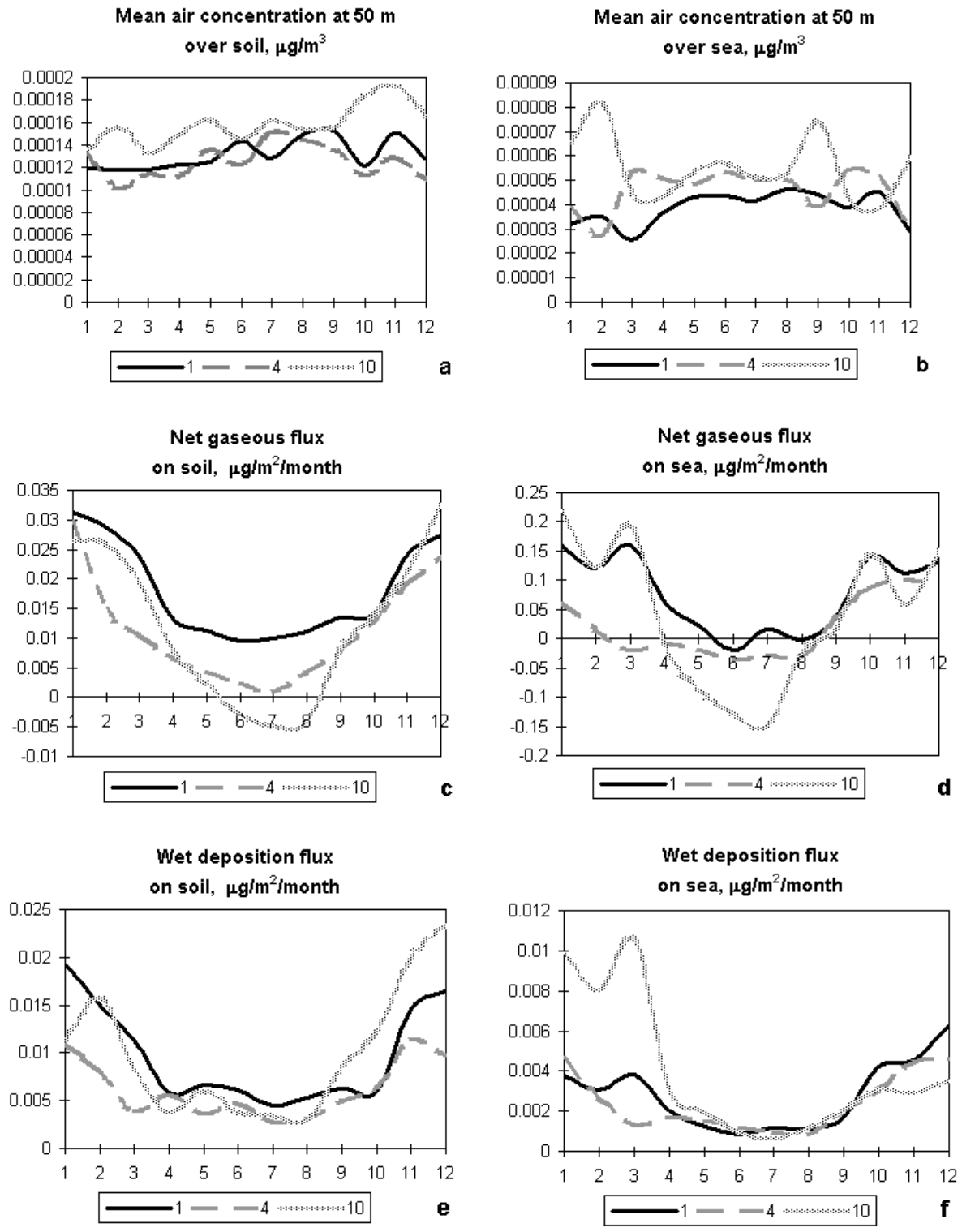

Figure 3.10 Annual variations of the mean concentration in the air over land (a) and over sea (b), $\mu g/m^3$, and annual variations of dry and wet deposition fluxes to the land (c,e) and to the sea surfaces (d,f), $\mu g/m^2$/month

Figure 3.11 presents PCB concentrations averaged over the EMEP grid on each calculation level in the soil and sea water for each of 12 months of 1996. The concentration in the surface soil layer has monthly variations. The monthly variations are connected with weather conditions and first of all with temperature regime. PCBs concentration decreases during the warm period and increases during the cold period of the year. Obviously it is explained by the fact that during the warm period net gaseous flux to the soil decreases and even becomes negative (the soil re-emits part of PCBs back to the atmosphere).

Monthly variations of PCB concentrations are more pronounced in the ocean surface layer than in the soil. The ocean more easily re-emits PCBs to the atmosphere during the warm period of the year.

In the deeper ocean layers PCB monthly variations are expressed very poorly. In soil deep layers PCB monthly variations are practically absent.

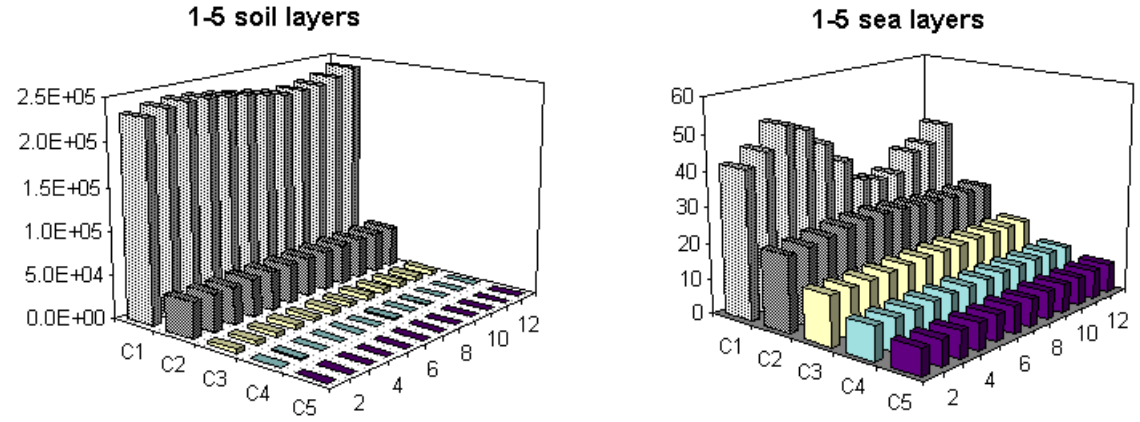

Figure 3.11 PCB mean concentrations in each calculation layer (C1-C5) of the soil and of the sea during January-December of 1996. Units: ng/m^3

Comparison with measurement data

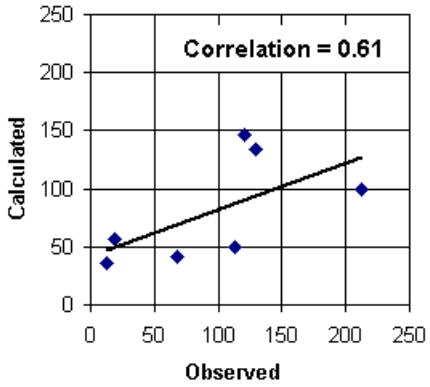

Calculation values were compared with available measurement data. In particular calculated PCB air concentrations were compared with observations. Results of the comparison are demonstrated in Figure 3.12.

Aggregated measurement data on mean annual concentrations are presented in table 3.6 [*Berg et al.*, 1996].

Figure 3.12 Comparison of calculated and measured data on PCB air concentrations. Units: pg/m^3

Table 3.6: Measurement and calculation data on PCB concentrations in the air*

Station code	Year	Mean concentrations of PCBs in the air. Units: pg/m^3	
		Measured	Calculated
IS91	95	18.26	56.6
NO42	93	13.11	35.5
NO42	94	112.57	49.9
NO42	95	68.19	41.2
NO99	92	211.96	98.9
NO99	93	129.71	133.7
NO99	94	120.98	145.9

* measurement data are taken from [*Berg et al.*, 1996]

Redistribution of PCBs in the environment after switching off the emissions

In order to follow the fate of PCBs accumulated in the environment compartments during 40-year period it was assumed that no further emissions took place during the next 10 years.

As evident from Figure 3.13 upon termination of emissions, PCBs mass in the soil during 10-year period cuts down from 35.2 tons to 7.63 tons (by 78%): due to degradation - by 57% and due to re-emission - by 7.28 tons (21%).

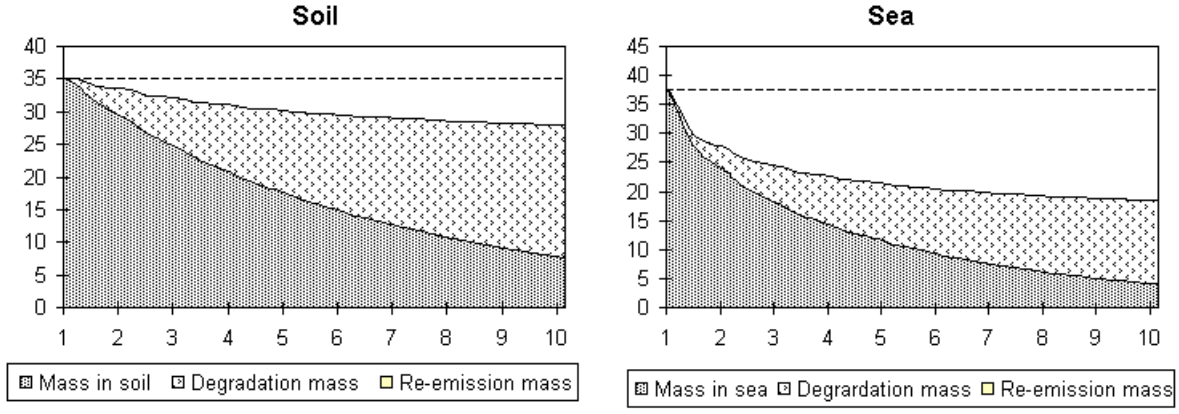

Figure 3.13 PCBs mass in the soil and sea with the allowance made for degradation and re-emission at the absence of emissions. Units: tons

Upon termination of the emissions, PCBs mass in the sea during 10-year period cuts down from 37.9 tons to 4.01 tons (by 89%): due to degradation - by 38% and due to re-emission - by 19.4 tons (51%). So the fluxes from the ocean surface are appreciably higher than from the soil.

As seen from Figure 3.14, during 10-year period (without emissions) PCBs mass in the air gradually decreases from year to year. PCBs content in the air varies with seasons due to re-emission from the soil and ocean surfaces during the warm period of the year. PCBs mass increases in the middle of the year. During calculation period PCBs mass in the air decreases by an order of magnitude from 700 kg to 50 kg.

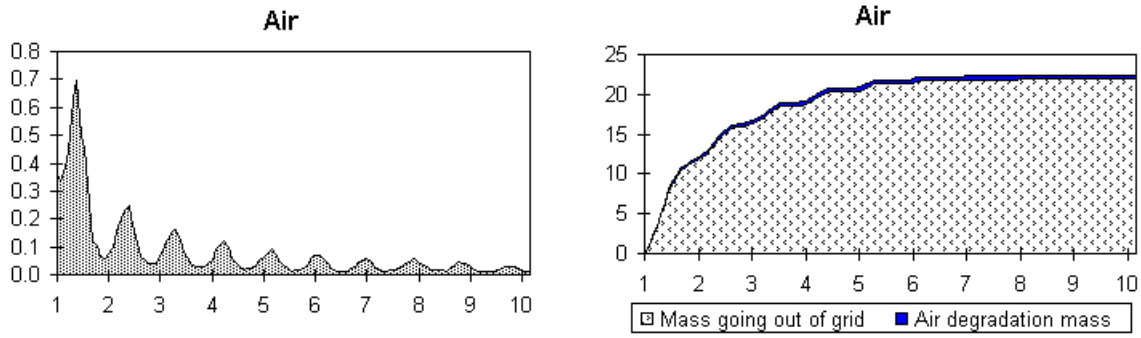

Figure 3.14 PCBs mass in the air. Units: tons

Figure 3.15a,b shows annual variations of PCB concentrations over the land and sea in the 1st, 4th and 10th years upon termination of emissions. Over the land and sea the concentration decreases during the first and subsequent years. In the middle of each year local concentration maximum connected with re-emission from the soil and sea is observed.

Figure 3.15c,d presents net gaseous fluxes over the land and sea. Basically these fluxes have negative sign (re-emission). Absolute values of these fluxes decrease with each year when there is no emissions. The fluxes have sharply pronounced monthly variations with maxima in the warm period of the years. Absolute values of re-emission fluxes over the sea are greater than those over the land.

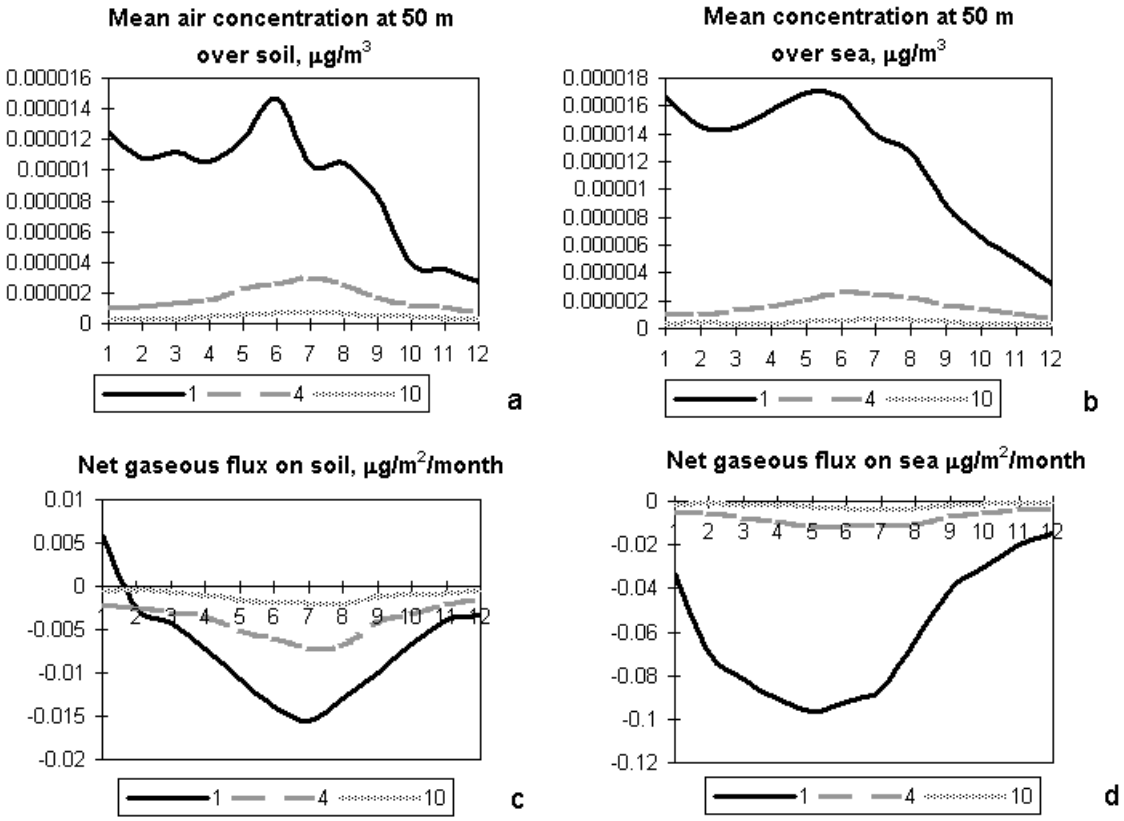

Figure 3.15 Annual variations of the mean concentration in the air over the land (a) and over the sea (b); annual variations of net gaseous fluxes on the land (c) and over the sea (d)

Conclusions

1. A modified 3-D regional Eulerian model [*Pekar*, 1996] coupled with exchange modules of [*Jacobs and van Pul*, 1996] was applied to the simulations of PCB transport and exchange with the underlying surface. Some additional assumptions concerning sea compartment were made. Physical-chemical parametrization of PCBs was adopted on the basis of the physical-chemical properties of PCB-153.
2. After 40-year simulation period about 80% of PCBs from European emissions was transported outside the EMEP grid and about 3% of PCBs was degraded in each of the compartments (air, soil and sea).
3. For PCBs dry deposition appears to prevail over wet deposition on the sea and on the land.
4. The annual re-emission flux is about 0.02 $\mu g/m^2$ per year for the land and 0.4 $\mu g/m^2$ per year for the sea.
5. Total deposition appears to be maximum in the maximum emissions zones and makes up around 2 $\mu g/m^2$ per year. The high level of deposition is also observed at the coastal line surrounding Europe and amounts to 1 $\mu g/m^2$ per year.
6. Mean concentrations in the air are around 0.15 ng/m^3 over the land and 0.05 ng/m^3 over the sea.
7. It was shown that the PCBs mass remaining after 10 years of modelling without emissions was about 22% for the soil and 10% for the sea.

References

Atlas E., Foster R., Glam C.S. [1982] Air-sea exchange of high molecular weight organic pollutants: Laboratory studies. *Environ. Sci. Technol*. v.16, pp.283-286.

Baart A.C., Berdowski J.J.M., van Jaarsveld J.A. and Wulffraat K.J., [1995] Calculation of atmospheric deposition of contaminants on the North Sea. TNO-MEP - R 95/138*, Delft, The Netherlands.

Background monitoring of land pollution by chlororganic substances [1990], ed. by Rovinsky F.Ya., Voronova L.D., Afanasiev M.I., Denisova A.V., Saint Petersburg, Hydrometeoizdat, 269, (in Russian).

Bayona J.M., Fernandez P., Porte G., Tolosa I., Albaiges J. [1991] Partitioning of urban micropollutants among coastal compartments. *Chemosphere* v.23, pp.313-326.

Berdowski J.J.M., Baas J., Bloos J.-P.J., Vesschedijk A.J.H. and Zandveld P.Y.J. [1997] The European Emission Inventory of Heavy Metals and Persistent Organic Pollutants. TNO, Report UBA-FB, UFOPLAN-Ref. No. 104.02 672/03, Apeldoorn, p.239

Berg T., Hjellbrekke A.-G. and Skjelmoen J.E. [1996]: Heavy metals and POPs within the ECE region. EMEP/CCC-Report 8/96. Norwegian Institute for Air Research.

Bergen B.J. [1993] *Environ.Sci.Technol*. v.27, pp.938-992.

Choiu C.T., Malcolm R.L., Brinton T.I., Kile D.E. [1986] Water solubility enhancement of some organic pollutants and pesticides by dissolved humic and fulvic acids. *Environ. Sci. Technol.* v.20, pp.502-508.

Doucette W.J., Andren A.W. [1988] Aqueous solubility of selected biphenyl, furan and dioxin congeners. *Chemosphere* v.17, pp.243-252.

Dunnivant F.M., Elzerman A.W. [1988] Aqueous solubility and Henry`s low constants for PCB Congeners for evaluation of quantitative structure-property relationships (QSPRs). *Chemosphere* v.17, pp. 525-541.

Estimating exposure to dioxin-like compounds [1994] EPA/600/6-88/005/Cb. *Washington* v.II, pp.5-9.

Fischer R. [1989] Fresenins Z. *Anal.Chem*. v.333, pp.731-737.

Frolov A., Vazhnic A., Astakhova E., Alferov Yu., Kiktev D., Rosinkina I., Rubinshtein K. [1994] System for diagnosis of the lower atmosphere state (SDA) for pollution transport model, EMEP/MSC-E Technical report 6/94.

Jacobs C.M.J. and van Pul W.A.J. [1996] Long-range Atmospheric transport of Persistent Organic Pollutants, 1: Description of surface - atmosphere exchange modules and implementation in EUROS. Report N722401013 RIVM, Bilthoven, The Netherlands.

Jury W.A., Spencer W.F. and Farmer W.J. [1983] Behavior Assessment Model for Trace Organics in Soil. *J. Environ. Qual*., v.12, pp.558-564.

Izrael Yu.A. and Tsyban A.V. [1989] Anthropogenic Ecology of the ocean. Hydrometeoizdat, Leningrad, (in Russian).

Haque R., Schmedding D.W. (1975) A method of measuring the water solubilities of hydrophobic chemicals: solubilities of five chlorinated biphenyls. Bull. Environ. Contam. Toxicol., v.14, pp.13-18.

Harner T., Mackay D., Jones K.C. [1995] Model of the long-term exchange of PCBs between soil and the atmosphere in the southern UK. *Environ. Sci. Technol*, v.29, pp.1200-1209.

Horzempa L.M., Di Tirro D.M. [1983] The extend of reversibility of polychlorinated biphenyl adsorption. Water Res., v.17, pp. 851-859.

van den Hout, ed. [1994] The impact of atmospheric deposition of non-acidifying Pollutants on the Quality of European forest soils and the North sea, Main report of the ESQUAD project, RIVM rep.722401003, IMW-TNO rep.R93/329.

Karikhoff S. W., Brown D.S., Scott T.A. [1979] Sorption of hydrophobic pollutants on natural waters. *Water Res.* v.13, pp.241-248.

Kisselev A.V., Khudoley V.V. [1997] *Poisoned cities*, M. Greenpeace, v.84, (in Russian).

Klissenko M.A. [1988] *Sanitation and Hygiene* v.7, pp.56-60 (in Russian).

Klyuev N.A., Brodsky E.C., et al. [1990] *J. of Analytical Chemistry* v. 45, № 10, p.1194, (in Russian).

Larsson P. [1984] *Environ.Pollut*. v.A34, № 3, pp.283-289.

Maistrenko V.N., Khamitov R.Z., Budinkov G.K. [1996] Ecological-Analytical monitoring of supertoxic substances, M. *Chemistry*, v.319 (in Russian).

Manchester O.H., Vikelsol J., et. al. [1990] *Chemosphere* v.16, № 10/12, pp.1779-1789.

Mackay D., Shiu W.Y. and Ma K.C. [1991] Illustrated Handbook of phisical-chemical properties and environmental fate for organic chemicals. USA, Lewis publishers, v.I.

Miller M.M., Ghodbane S., Wasik S.P., Tewari Y.B., Martire D.E. [1984] Aqueous solibulities, octanol-water partitioning coefficients, and entropies of wetting of chlorinated benzenes and biphenyls. J. *Chem. Eng. Data* v.29, pp. 84-190.

Moscow Workshop [1996] Workshop on the Assessment of EMEP Activities Concerning HMs and POPs and Their Further Development (24-26 September, 1996). MSC-E Report 1/97

Murphy T.J., Mullin M.D., Meyer J.A. [1987] Equilibration of polychlorinated biphenyls and toxaphen with air and water. *Environ. Sci. Technol.* v.21, pp.155-162.

van Oss R.F. and J.H. Duyzer [1996] Deposition of persistent organic pollutants; a Literature survey. TNO-report R 96/409.

Pal D., Weber J.B., Overcash M.R. (1980) Fate of polychlorinated biphenyls (PCBs) in soil-plant systems. Residue Reviews, 1980, v. 74, pp. 45-98.

Risby T.H., Hsu T.-B., Sehnert S.S., Bhan P. [1990] Physico-chemical properties of individual hexachlorobiphenils congeners. *Environ. Sci. Technol.*v. 24, pp.168-187.

Rovinsky F.Ya., Afanasiev M.I., Buivolov Yu.A. etc. [1992] *J. of Ecological Chemistry* v.1, pp.46-64 (in Russian).

Rovinsky F.Ya., Afanasiev M.I., Voronova L.D., A.V.Denisova, I.G.Pushkar [1990] Background monitoring pollution of chloro-organic compounds. L., Hydrometeoizdat, (in Russian).

Prokofiev A.K. [1990] *Progress in Chemistry* v.59, № 11, pp.1799-1818 (in Russian).

Schlatter C. [1994] *Sci.Total Environment* v.143, pp.93-101.

Shapiro M.Ya. [1981] Wind field objective analysis based in geopotential and wind data, EMEP/MSC-E Technical report 3/1981.

Shiu W.Y., Mackay D. [1986] A critical review of aqueous solibulities, vapor pressures, Henry`s low constants and octanol-water partitioning coefficients of the polychlorinated biphenyls. J. *Phys. Chem. Ref. Data* v.15, pp.911-935.

Strand A. and Hov Ø. [1996] A model Strategy for the Simulation of Chlorinated Hydrocarbon Distribution in the Global Environment. Water, Air and Soil Pollution, v.86, pp.283-316.

Surnina V. and Tarasov V. [1992] *J. of Ecological Chemistry* v. 2, pp.5-20 (in Russian).

Travis C.C., Hattemer-Frey H.A. [1987] *Chemosphere* v.16, № 10/12, pp.2331-2342.

Vit Long [1992] *Chromatog.*, v.95, pp.1-43.

Vozhzennikov O.I., Bulgakov A.A., Popov V.E. et al. [1997] Review of migration and transformation parameters of selected POPs, EMEP/MSC-E Report 3/97.

Yalkowsky S.H., Valvani S.C., Mackay D. [1983] Estimation of the aqueous solubility of some aromatic compounds. *Residue Reviews* v.85, pp.43-55.

Chapter 4 Benzo(a)pyrene (B(a)P) modelling

Introduction

Benzo(a)pyrene belongs to a group of polycyclic aromatic hydrocarbons (PAH). This group also incorporates such compounds as pyrene, fluoranthene, benzoperylene, chrysene etc. Low solubility of these compounds in the water rules out their mobility in soils and bottom sediments [*Yufit et al*., 1997]. Many of PAH are regarded to be hazardous compounds. Due to their properties PAH are accumulated in tissues of plants and animals. Although PAH are rapidly metabolized in the fatty tissues of animals and man, the products of their metabolism can be even more hazardous than initial compounds. B(a)P is one of the most carcinogenic compound among PAH. B(a)P was recommended by EMEP workshop on heavy metals (HM) and persistent organic compounds (POP) for long-range transport modelling [*Moscow Workshop*, 1996].

B(a)P are emitted both by anthropogenic (fuel combustion, metallurgy, wood preservation [*Berdowski et al*., 1997]) and natural sources [*Holoubec et al*., 1993]. In the atmosphere B(a)P can occur in gaseous and aerosol phases and the latter is likely to be predominant. B(a)P has the property of accumulation in the environment compartments. In addition, B(a)P gaseous phase can be re-emitted from underling surface. Due to coplanarity of the B(a)P molecules sorption on surface is very high and B(a)P can not penetrate into deep soil layers [*Yufit et al*., 1997]. B(a)P can be removed from the atmosphere by dry and wet deposition. In accordance with model calculations [*Baart et al*., 1995] gaseous phase of B(a)P dry deposition may be the main pathway (over 80% of the total deposition). Wet deposition is more important for aerosol fraction. Since deposition processes are different for aerosol and gaseous fractions the description of phase redistribution is of great importance. B(a)P degradation in the atmosphere is mainly due to oxidation [*Rovinsky et al*., 1988].

4.1 Physical-chemical properties of B(a)P

Some of physical-chemical characteristics of B(a)P determine its behavior in the atmosphere, so they are important for modeling calculations. Unfortunately, many of them are known to be of low accuracy. Below the estimates of critical parameters are a given on a quantitative basis.

Saturated vapor pressure (P_{0L})

The value of saturated vapor pressure determines a compound maximum concentration in the air and gas/aerosol partitioning. In the last case vapor pressure for the subcooled liquid P_{0L} is used.

Its value as a temperature function can be calculated by the formula [*Hincley at al.*, 1990]:

$$\log P_{0L}\,(\text{Pa}) = -4989/T(\text{K}) + 11.59$$

Henry`s law constant

Henry's law constant determines the equilibrium exchange between water-phase (including rain drops and clouds) and the gas-phase substances. This value affects the washout rate by precipitation and interaction. According to *D.Mackay et al.* [1991] Henry's law constant for

B(a)P is equal to 0.05 Pa m^3/mol at 25^0C. A temperature dependence of the parameter for fresh water can be determined by the formula:

$$\log H \text{ (Pa } m^3\text{/mol)} = -4529/T(K) + 13.89$$

B(a)P degradation rate in the atmosphere

The rate of B(a)P degradation in the ambient atmosphere can depend on many environmental parameters - solar radiation intensity, oxidant concentrations, temperature, aggregate state of B(a)P occurrence. Thus, it can vary in the real atmosphere in a very wide range. Many authors believe that B(a)P stability in the particulate phase is much higher than that for a gas phase. *Y.Cohen and R.E.Clay* [1994] used the value of degradation half-life of B(a)P in the gas-phase equal to 1.1 hr while in the particulate phase - 8 days. According to the calculations made by *L.Blau and H.Güster* [1981] calculated that the degradation half-life under daily average intensity of the summer sun radiation in central Europe was equal to 5 hr. In the model calculations *D.Mackay et al.* [1991] recommend to use the value of 170 hr as an annual mean half-life degradation rate.

Gas/aerosol partitioning in the atmosphere

Gas/aerosol partitioning of B(a)P depends mainly on temperature. In winter the share of the aerosol fraction increases with the decreasing of mean temperature [*Finlayson-Pitts et al.,* 1986]. *M.Afanasiev et al.* [1982] measured the benzo(a)pyrene gas/particle distribution in rural areas of the European USSR in 1982. The gas fraction varied from 2.3 to 18.2%. The similar results (6-20% of the gas fraction) were obtained in the suburbs of large cities in Belgium and the Netherlands [*Broddin et al.,* 1980]. A coefficient of the equilibrium distribution of B(a)P between the phases can be estimated on the basis of *C.Junge's* approach [*Junge,* 1977] as a function of the total aerosol particle surface and saturated vapor pressure. This approach shows that for mean European temperatures and aerosol concentrations, about 10% of B(a)P should occur in the gas phase. The open question is how quick the process of gas/aerosol partitioning can be.

Size distribution of particulate B(a)P

Size distribution is a factor of critical importance, which determines the rate of dry and wet deposition. It was found in a transport tunnel experiment [*Venkataraman et al.,* 1994] that more than 85 % of PAH was sorbed on fine particles.

Washout ratio

A lot of experimental data on B(a)P concentrations both in the air and precipitation were obtained by *F.Rovinskiy et al*. [1988] in the background regions of the European part of former USSR. On this basis it is possible to assume that the washout ratio can be 10^4 -10^5 in summer and 10^3 - 10^4 in winter. It is naturally that washout ratio values should be different for gaseous and particulate phases of B(a)P. For the particulate phase *A.Baart et al.* [1995] used the value of $3 \cdot 10^5$. The value for the gaseous phase can be estimated as a function of Henry's law constant and temperature. Under typical European conditions, it should be in the range of 10-100.

Diffusion coefficients

Molecular diffusion determines the intensity of the B(a)P exchange between air, water and soil. As estimated by *R.Schwarzenbach et al.* [1993] B(a)P diffusion coefficients in the air are 6.9×10^{-6} m^2/s and in the water - 7.5×10^{-10} m^2/s. In model calculations *D.Bakker and W. de Vries* [1996] recommend to use the values of 4×10^{-6} and 4×10^{-9} m^2/s, respectively.

4.2 Model assumptions and parametrization

At a given stage of the developing of the model for B(a)P, the following processes are taken into account: anthropogenic emissions, advective transport and diffusion in the atmosphere, re-distribution of gaseous and aerosol B(a)P in the atmosphere, wet and dry deposition of B(a)P in the two phases from the atmosphere, B(a)P degradation in the atmosphere.

Re-emission from and degradation in the water and soil are not allowed for. This version of the model does not use atmosphere-surface exchange modules.

Here it is assumed that in the atmosphere the equilibrium between gaseous and aerosol B(a)P is set instantaneously. The fact that the mixing processes are more active in the atmosphere than in the soil is taken into account here. It is assumed that specific aerosol surface is constant in space and time.

Particle-bound B(a)P is assumed to be on the particles which median mass diameter (MMD) is 0.84 μm, as taken for cadmium in the ASIMD model [*Pekar*, 1996]. In the course of B(a)P transport and deposition this diameter remains unchanged.

In the present work the estimation of the B(a)P lifetime in the air due to degradation is 10 days as recommended by *D.Mackay et al.,* [1991]: seasonally it changes from 5 days in summer, to 10 days in autumn and spring and to 15 days in winter. The period indicated refer to both of the phases.

On the base of the data considered above model parametrization, represented in Table 4.1 was carried out.

Table 4.1 Model parametrization

Parameter	Parametrization	Reference
HENRY`S LAW CONSTANT Pa·m^3/mol	$\lg_{10} H = -\frac{4529}{T} + 13.89$	[*Vozhzennikov et al*, 1997]
DIFFUSION COEFFICIENT: m^2/s		
ATMOSPHERE	$D_A = 6.9 \cdot 10^{-6}$	[*Schwarzenbach et al*, 1993]
WATER	$D_W = 7.5 \cdot 10^{-6}$	[*Schwarzenbach et al*, 1993]
RESISTANCES (s/m): **AERODYNAMIC**	$r_a = \frac{\ln(Z_1 / Z_0) - \Psi(Z_1 / L) + \Psi(Z_0 / L)}{0.4 u_*}$	[*Jacobs and van Pul*, 1996]
QUASY-LAMINAR BOUNDARY LAYER	$r_b = \frac{2}{0.4\ u_*}\left(\frac{Sc}{Pr}\right)^{2/3}$	[*Jacobs and van Pul*, 1996]
WATER SURFACE	$r_{c\ sea} = \frac{d_{zwm}}{D_w}\frac{H}{RT}$	[*Jacobs and van Pul*, 1996]
SOIL SURFACE	$r_{c\ soil} = \frac{0.5 dz_{soil}}{D_a a^{10/3}(1-l-a)^{-2} + D_w l^{10/3}(1-l-a)^{-2} W_g}$	[*Strand and Hov*, 1996]
WASHOUT RATIO GAS	$W_g = \frac{RT}{H}$	[*Strand and Hov*, 1996]
PARTICLES	$W_p = 5 \cdot 10^5$	[*Pekar*, 1996]
DIFFUSION THICKNESS, m **WATER**	$d_{zwm} = 4 \cdot 10^{-5}$	[*Jacobs and van Pul*, 1996]
SOIL DIFFUSION LAYER DEPTH, m	$dz_{soil} = 5 \cdot 10^{-3}$	[*Jacobs and van Pul*, 1996]
RATE OF DEGRADATION IN ATMOSPHERE, s^{-1}	$K_a = \begin{cases} 2.315 \cdot 10^{-6} & (summer) \\ 1.157 \cdot 10^{-6} & (spring,\ autumn) \\ 7.716 \cdot 10^{-7} & (winter) \end{cases}$	[*Mackay et al.*, 1991, hand-book],
AIR-PARTICLE PARTITIONING COEFFICIENT	$K_{p,g} = \frac{C_{part}}{C_{tot}} = \frac{c\theta}{P_{0l} + c\theta}$	[*Junge*, 1977]
CONSTANT OF PROPORTIONALITY, Pa · m	$c = 0.17$	[*Junge*, 1977]
SPECIFIC AEROSOL SURFACE AREA, m^2/m^3	$\theta = 1.5 \cdot 10^{-4}$	[*Whitby*, 1978]
SATURATED VAPOR PRESSURE FOR SUBCOOLED LIQUID, Pa	$\lg_{10} P_{0l} = -\frac{4989}{T} + 11.59$	[*Hincley et al*, 1990]

4.3 Input data

Emissions

The contribution to anthropogenic emissions of polycyclic aromatic hydrocarbons (PAH) including B(a)P makes organic fuel combustion for electricity and heat production, iron and steel industry, non-ferrous industry, mobile sources, wood preservation and others.

Table 4.2 summarizes the UN/ECE reported official data on PAH emissions for 11 countries (EB.AIR/GE.1/1997/3, EB.AIR/GE.1/1997/3/Add.1) but only some of them indicated the composition of total emissions. Data on B(a)P emissions are available only for Bulgaria (17 t for 1990) and Denmark (2.7 t for 1994).

Table 4.2 UN/ECE reported official PAH emission data. Units: t/yr

Country	1990	1991	1992	1993	1994	1995
Austria					458.0	
Bulgaria	677.3					521.4
Denmark					37.2*	
Finland						556
France	3480					
Germany	420					
Hungary	192.3*	193.9*	119.7*	113.6*	96.1*	
Netherlands	172.0		1120 *			
Poland	372*					536*
Sweden	182		153			153
United Kingdom				770		

* 6 Borneff PAH (fluoranthene, benz(a)pyrene, benzo(b)fluoranthene, benzo(k)fluoranthene, benzo(ghi)perylene, indeno(1,2,3-c,d)pyrene)

The emissions of 6 Borneff PAH in Europe has been estimated by *J.Berdowski et al*. [1997] within the EMEP grid with spatial resolution 50 x 50 km^2. In order to evaluate B(a)P emission field the percentage of B(a)P in the total emissions of 6 Borneff PAH from [*Baart et al*., 1995] was used. The initial data and obtained results are presented in Table 4.3. Spatial distribution of B(a)P emissions is showed in Figure 4.1.

The uncertainty of PAH emission estimates can be large, ranging a factor 2-5 [*Berdowski et al*., 1997]. It is mainly due to the uncertainty of data on consumption of wood as a fuel and data on wood preservation.

According to the estimate of *J.Berdowski et al*. [1997] the per cent contribution of different sources to the total emissions of 6 Borneff PAH is as follows: fuel combustion for heat production by small stationary sources – 42%; wood preservation – 31%; mobile sources – 11%; iron and steel industry – 6%; non-ferrous metal industry – 4%; other sources – 6%. Hence, in the first approximation it can be assumed that about 90% of emissions enters the lower atmospheric layer (< 100 m) and the rest to the second (100 - 400m) model layer.

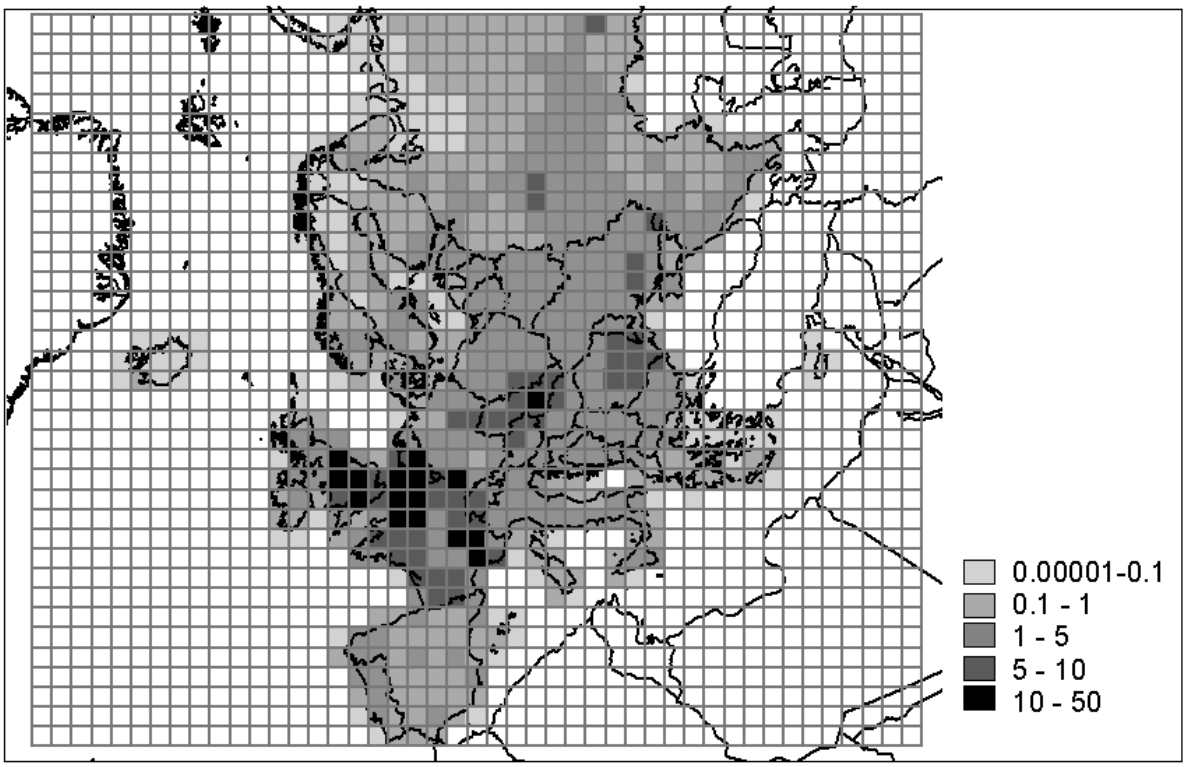

Figure 4.1 B(a)P emission distribution within the EMEP grid for 1990. Units: t/year

In the model calculations temporal variability of B(a)P input to the atmosphere was equal to that of work by *A.Baart et al*. [1995]: in the cold season (from October to March) - 60% of total emissions, from April to September – 40%.

Table 4.3 PAH emission data. Units: t /yr.

Country	Estimates for 1990 [*Baart et al.*,1995]			Estimates for 1990 [*Berdowski et al., 1997]*	B(a)P emissions used in calculations
	6 Borneff PAH	B(a)P	B(a)P, %	6 Borneff PAH	
Albania	32	2	6	36	2
Austria	210	20	10	243	24
Belgium	143	12	8	818	65
Bulgaria	126	10	8	55	17***
Cyprus				0.2	0.01
former Czechoslovakia	369	37	10		
Czech Republic				259	26
Slovakia				310	31
Denmark	64	4	6	77	3***
Finland	102	8	8	104	8
France	1230	108	9	3479	313
Germany	1340	103	8	420	32
Greece	146	10	7	153	11
Hungary	198	16	8	192	15
Iceland				6	0.5
Ireland	73	6	8	74	6
Italy	688	47	7	694	49
Luxembourg	6	<1		6	0.5
Netherlands	183	14	8	184	15
Norway	106	9	8	140	11
Poland	704	69	10	372	37
Portugal	138	10	7	138	10
Romania	456	46	10	723	72
Spain	449	28	6	521	31
Sweden	105	7	7	282	20
Switzerland	238	28	12	96	12
United Kingdom	730	54	7	1437	101
former USSR *	5330	465	9		
Belarus				191	17
Estonia				28	3
Latvia				38	3
Lithuania				52	5
Republic of Moldova				58	5
Russian Federation**				1938	174
Ukraine				1137	102
former Yugoslavia	346	27	8		
Bosnia&Herzegovina				48	4
Croatia				54	4
The FYR of Macedonia				22	2
Slovenia				51	4
Yugoslavia				172	14
Total	13510	1140	8	14607	1251

* to 60^{o}E ** within the EMEP grid *** official data

Meteorology

Meteorological information for 1995 is used in calculations.

Geophysical information

Organic matter content is not taken into account.

4.4 Calculation results

Total and gas-phase B(a)P deposition

Deposition of total (gas plus particles) B(a)P and B(a)P associated with the gas phase is presented in Figures 4.2 (a) and 4.2 (b), respectively. As seen from Figure 4.2 (a) distribution of total B(a)P deposition reproduce its emissions rather exactly. Maximum values of deposition are about 300 μg/m^2/yr. For comparison, B(a)P deposition in Budapest in the 60-s made up 200 μg/m^2/yr [*Kertesz-Saringer et al*, 1969]. Deposition density decreases with distance from regions of maximum emissions, but even near the eastern boundary (58 degree of e.l.) of computational domain level of deposition remains rather high (up to 50 μg/m^2/yr), indicating a significant outflow of B(a)P through this boundary. Minimum calculated values of deposition within the domain are practically about 0.1 μg/m^2/yr. We note that B(a)P deposition in Lithuania in the 70- s were not less than 5 μg/m^2/yr [*Milukaite and Galvonaite*, 1991].

The pattern of gaseous B(a)P deposition distribution is also similar to that of emission distribution, and, hence, the pattern of total B(a)P deposition. Ranging of values and isoline steps were chosen in such a way, that their values were exactly one order less than ones in Figure 4.2 (a). Both these figures show that in general gas-phase B(a)P deposition is less than 10% of total B(a)P deposition, i. e., particulate B(a)P deposition makes up more than 90% of total B(a)P deposition.

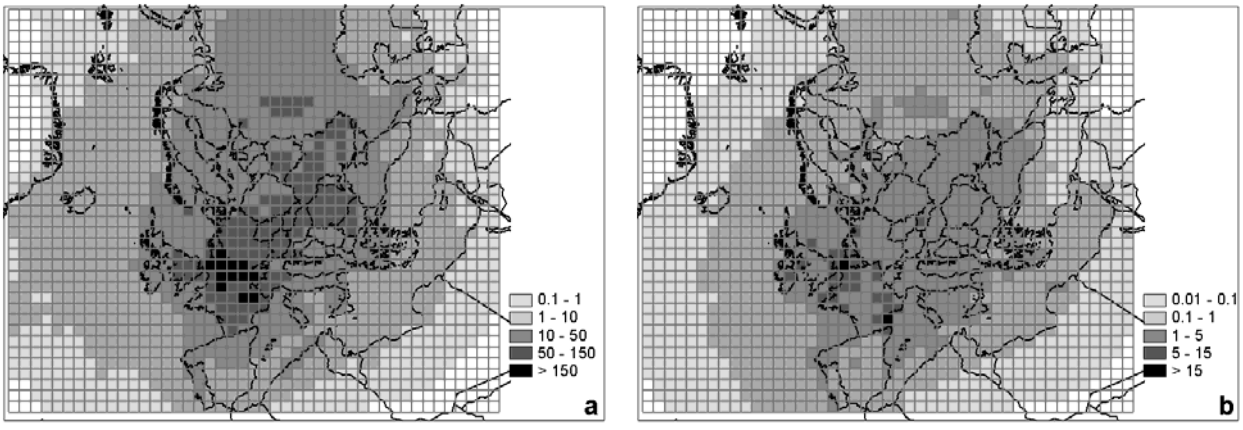

Figure 4.2 Benz(a)pyrene deposition density: (a) - total deposition and (b) - gas-phase deposition. Units: μg/m^2/yr

Dry and wet deposition of particulate and gas-phase B(a)P

Pattern of particulate-phase B(a)P scavenging from the atmosphere is presented in Figure 4.3 (a) for wet and 4.3 (b) for dry depositions. As seen from these figures, values of dry and wet deposition have the same order of magnitude, although on the average the ratio of wet deposition to dry deposition amounts to about 60:40 for land and 80:20 for sea. These ratios seem to be reasonable, though, contribution of dry deposition on land might be overestimated.

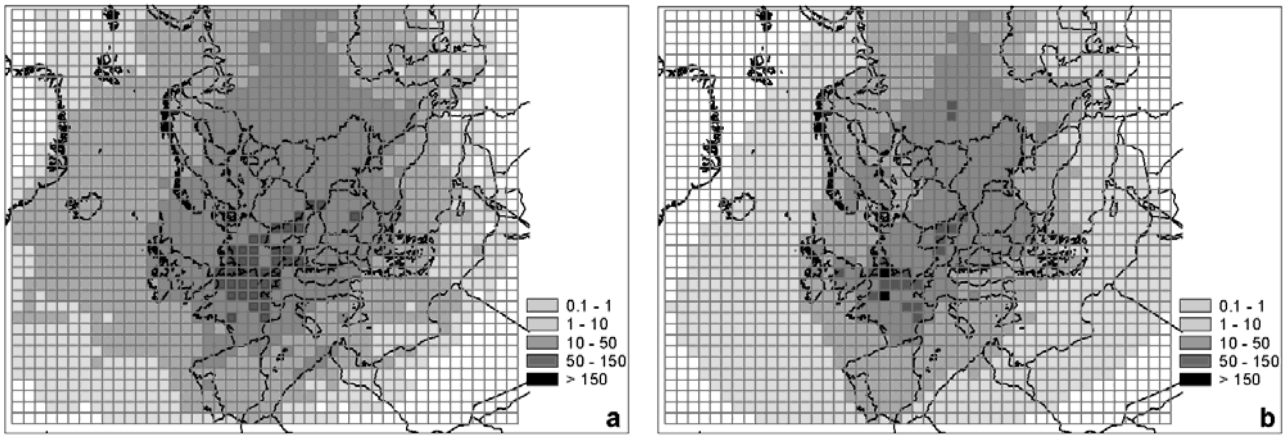

Figure 4.3 Wet (a) and dry (b) deposition density of particulate-phase benzo(a)pyrene. Units: μg/m^2/yr

Values of wet and dry deposition of particulate and gas-phases for January, July and round the year are presented in Table 4.4.

Table 4.4 Depositions of particulate and gas phase of benzo(a)pyrene within the EMEP grid in various periods. Units: tons

Period	Particulate phase				Gas phase			
	Wet		Dry		Wet		Dry	
	On sea	On land	On sea	On land	On sea	On land	On sea	On land
January	11.8	28.8	2.2	20.13	0.18	0.43	0.54	0.61
July	3.2	12.2	0.7	7.99	0.06	0.26	1.45	0.85
Year	83.6	261.4	19.2	181.33	1.43	4.46	12.80	10.10

As follows from the table, wet to dry deposition ratio for particulate phase makes up about 1.5 for land and 4 for sea inessentially changing from winter to summer when annual averaging is used. Ratio of deposition on land to deposition on sea for the particulate phase makes up about 4 at annual averaging, for January it is 3, for July it is 5. The reason for such noticeable differences between winter and summer is to be explained.

From the table one can see that dry deposition of the gas-phase exceeds (at annual averaging) wet deposition as much as 2 times for land and 10 times for sea. On the whole deposition of the gas-phase on sea is nearly equal to deposition on land, because dry deposition velocities over sea assumed in this model version are greater than those over land (see Table 4.5).

Table 4.5 Range of dry deposition velocities derived from model calculations. Units: cm/s

	July	January
$V_{d\ soil}$	0.02 - 0.6	0.09 - 0.58
$V_{d\ sea}$	0.05 - 2.2	0.07 - 2.9

Dry deposition velocities for sea are greater than for land probably because of the influence of vegetation on B(a)P scavenging is not taken into account at this stage and the assumed top soil layer thickness for which diffusion flux from the atmosphere considered might be exaggerated ($dz_{soil} = 5 \cdot 10^{-3}$ m).

B(a)P concentration in precipitation

Mean annual total and gas-phase B(a)P concentrations in precipitation are shown in Figure 4.4. As seen from Figure 4.4 (a), the domain of maximum total B(a)P concentrations in precipitation (more than 100 ng/l) coincides with the region of maximum emissions. On the main part of the calculation domain concentrations are less than 50 ng/l. As in the case of total deposition, remarkable concentrations in precipitation (more than 5 ng/l) are observed near the eastern boundary of the calculation domain, indicating a significant transport outside the domain. Concentrations in precipitation of gas-phase B(a)P (see Figure 4.4, b) are about two decimal orders less than the concentration of total B(a)P, i. e. practically all B(a)P in precipitation is represented by aerosol phase.

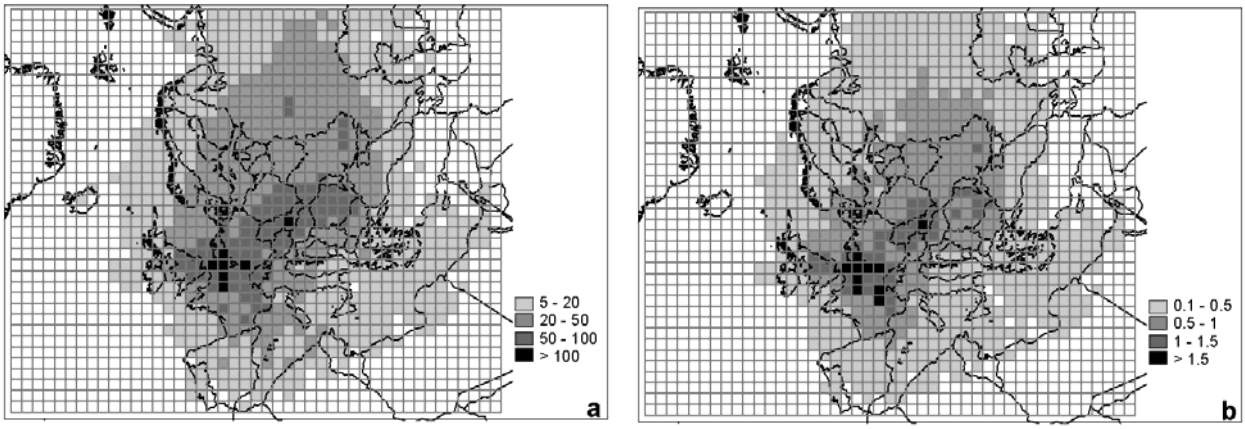

Figure 4.4 Concentration of total benzo(a)pyrene (a) and gas-phase benzo(a)pyrene (b) in atmospheric precipitation. Units: ng/l

B(a)P air concentrations

Air total B(a)P concentrations in the 1st (0 - 100 m) and 4th (1100 - 2100 m) model layers are presented in Figures 4.5 (a) and 4.5 (b). The region of maximum concentrations in 1st calculation layer - 8 ng/m^3 - coincides with the location of maximum emissions. First of all it is explained by the model assumption that 90% of emissions occurs in the 1st model layer. Maximum concentrations to some extent agree with the range of concentrations measured in Western Europe - up to 4.3 ng/m^3 [*Rovinsky et al*, 1988]. With the distance from emission sources concentrations in the 1st calculation layer decrease but remain rather high even near the eastern boundary of the calculation domain (more than 0.2 hg/m^3). On the whole the 1st

calculation layer concentration decreases from 8 ng/m^3 to about 0.01 ng/m^3. There are no concentrations more than 1 ng/m^3 in the 4th layer and concentrations ranging from 0.2 ng/m^3 to 1.0 ng/m^3 take place over a very small region corresponding approximately to the region of maximum emissions. The isoline with minimum value - 0.01 ng/m^3 in both figures practically coincide. It means that with the distance from sources concentrations in the whole calculation layer from 0 to 2100 meters are practically become equal.

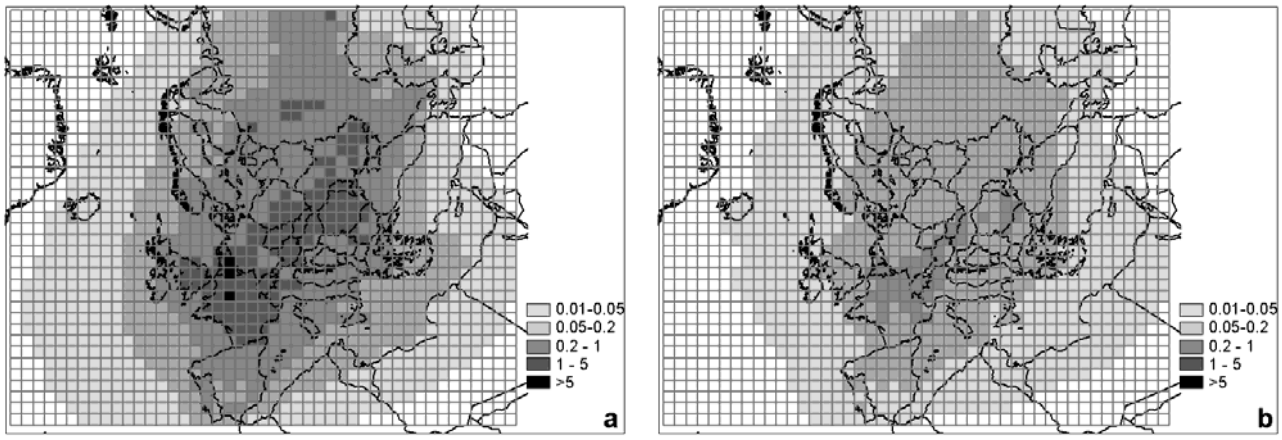

Figure 4.5 Mean annual total benzo(a)pyrene air concentration at 1st (a) and 4th (b) model layers. Units: ng/m^3

In Figures 4.6 (a) and 4.6 (b) gas-phase B(a)P concentrations in the 1st and 4th calculation layers are presented. The pattern of gas-phase B(a)P distribution is similar to that of total B(a)P, but ranging of isoline values used for gas-phase is 20 -30 times less than analogous values for total B(a)P i. e., contribution of the gas phase to the total concentration makes up per cent, and total B(a)P in air is represented mainly by particulate phase.

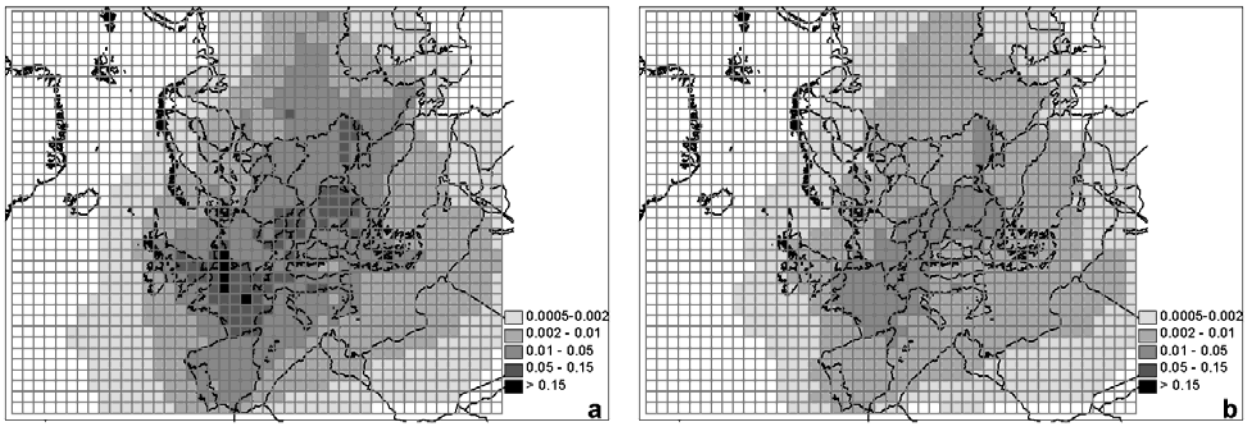

Figure 4.6 Mean annual gas-phase benzo(a)pyrene air concentration at 1st (a) and 4th (b) model layers. Units: ng/m^3

Seasonal variations of air B(a)P concentrations and percentage of the gas-phase

The contribution of the gaseous component to total B(a)P will differ in different seasons and in different points of calculation domain. Per cent contributions of gaseous component to total B(a)P in 1st model layer for January and July are presented in Figures 4.7 (a) and 4.7 (b). As one can see from the figures, gas phase content does not exceed few per cent in January while it can reach nearly 50% in July even at monthly averaging. Such relationships are directly connected with temperatures during month in each grid point. As it is known from a number of experimental data [*Rovinsky et al.*, 1988] surface concentrations of B(a)P in winter exceed its summer concentrations in several times. In the Figure 4.8 total B(a)P concentrations in the 1st model layer in January (Figure 4.8, a) and July (Figure 4.8, b) are presented. The comparisons of figures indicate that in the region of comparatively high pollution winter concentrations are mainly 2 - 3 times higher than summer ones. It is connected both with the emissions which is assumed 1.5 time higher in winter than in summer and with slower B(a)P scavenging in winter.

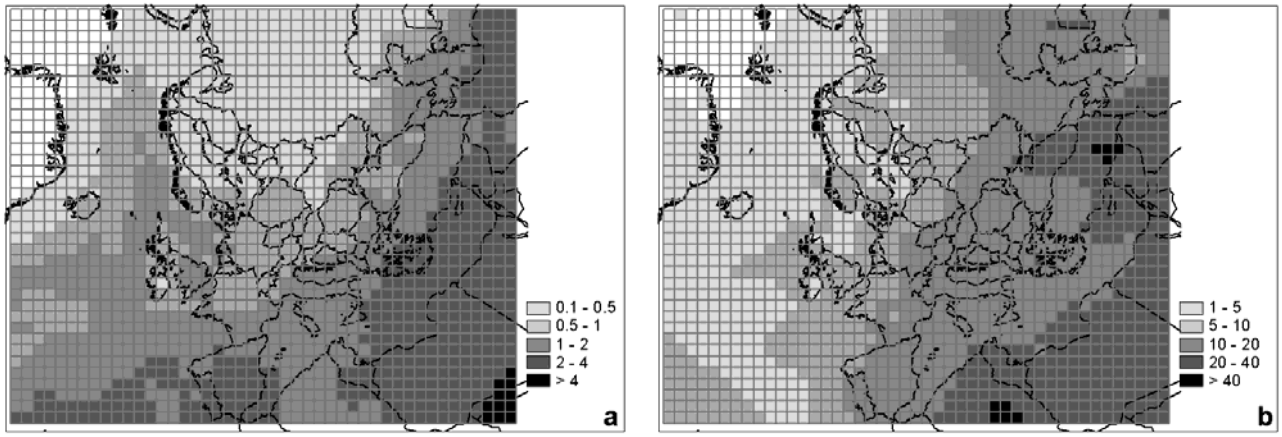

Figure 4.7 Percentage of benzo(a)pyrene gas-phase in January (a) and July (b)

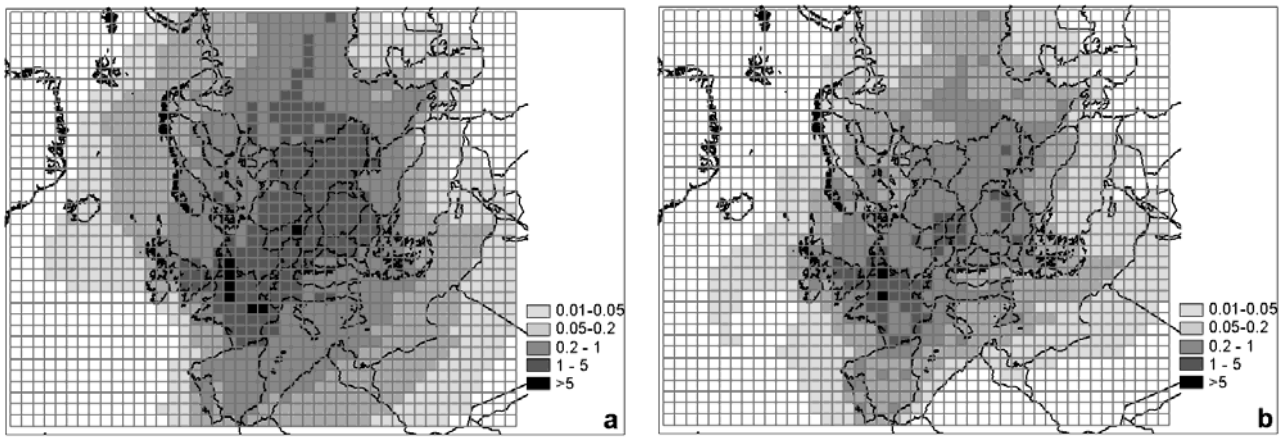

Figure 4.8 Total air concentrations of benzo(a)pyrene at 50m level in January (a) and July (b). Units: ng/m^3

B(a)P balance relationships for 1995

Basic B(a)P balance relationships for one calculation year are presented in Figure 4.9. As one can see from the figure, deposition on the land amounts to about 37% of the emitted B(a)P, on the sea surface - about 9% and degradation and transport outside the domain makes up 26% and 27% respectively.

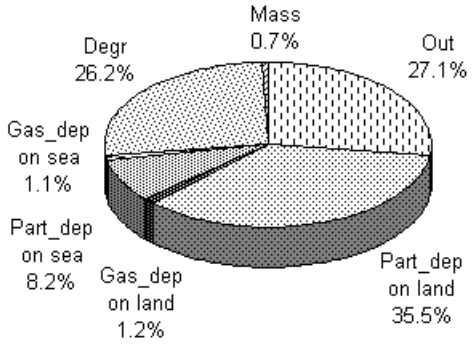

Gaseous B(a)P deposition on the land amounts to about 1% of the annual total B(a)P emissions, or about 3% of the total deposition on the land. Gaseous B(a)P emissions deposition on the sea also amounts to 1% of the total B(a)P, or about 10% of total B(a)P deposition on the sea.

Figure 4.9 Mass balance of B(a)P within EMEP region for 1995

0.7% of annually emitted B(a)P remained in the air by the end of the calculation period. It can be supposed that this value characterized the annually averaged steady state of B(a)P in the atmosphere when B(a)P input with emissions is balanced by B(a)P deposition, degradation and transport outside the calculation domain. B(a)P atmospheric effective life-time within the EMEP region can be assessed on the annual level. It is approximately equal to 2 days since 0.7% of the annual emissions is nearly a two-day «portion» of the emitted B(a)P.

Comparison with measurement data and other modelling results

Measurement data on B(a)P are quite scarce. In a number of cases it is difficult to determine if they regard to total B(a)P or to some of its phase. The obtained results agree with available literature data within an order of magnitude. Some results of the comparison are given in Tables 4.6 - 4.8.

Table 4.6 Air concentrations, ng/m^3

Location	Time	Measured value	Calculated value	References
Baltic	1983-1985	0.4 - 0.5	0.2 - 1.0	[*Rovinsky*, 1988]
Belarus	1980-1985	0.5	0.2 - 1.0	[*Rovinsky*, 1988]
Central part of Russia	1984-1985	0.2 - 0.6	0.7 - 2.0	[*Rovinsky*, 1988]
Astrakhan	1985-1986	0.03	0.05 - 0.2	[*Rovinsky*, 1988]
Netherlands	1989-1990	0.4 - 0.6	1 – 5	[*Baart et al.*, 1995]
Poland, Upper Silesia	1994	2.3	1 – 5	[*Bodzek et al.*, 1998]

Table 4.7 B(a)P deposition, μg/m^2/yr

Location	Time	Measured value	Calculated value	References
Lithuania	1973/1974, 1976/1977	5 - 60	10 - 50	[*Milukaite and Galvonaite*, 1991]
Budapest	1960-s years	2 - 200	50 - 150	[*Kertezs-Saringer et al*., 1969]

Table 4.8 B(a)P concentrations in precipitation, ng/l

Location	Time	Measured value	Calculated value	References
Belarus	1980 - 1983	2 - 6	20 - 50	[*Rovinsky* 1988]
Tver region	1985	1 - 8	20 - 50	[*Rovinsky* 1988]
Moscow region.	1984 - 1985	2 - 28	20 - 50	[*Rovinsky* 1988]
Astrakhan region	1985	3	5 - 20	[*Rovinsky* 1988]
Southern Norway	1983 - 1984	50 - 300	20 - 50	[*Rovinsky* 1988]
Norway, Netherlands	1985	20 - 150	50 – 100	[*Rovinsky* 1988]

B(a)P deposition pattern described in [*van den Hout*, 1994] is similar to obtained in this work. Thus, according to [*van den Hout,* 1994] deposition ranges from 20 to 200 μg/m^2/yr in Great Britain and from 15 to 150 μg/m^2/yr in France. Deposition on the southern part of Great Britain obtained in [*Baart et al.,* 1995], lie mainly within 25 - 200 μg/m^2/yr range.

Conclusions

1. A preliminary model version of the B(a)P atmospheric transport, deposition and transformation was developed. The processes considered are: gaseous and particulate B(a)P partitioning in the atmosphere, dry and wet removal from the atmosphere of gaseous and particulate and degradation in the atmosphere. The influence of vegetation on the B(a)P deposition on land, re-emission from the underling surface and degradation in the soil and water were not taken into account. Tentative calculations were carried out.
2. The calculations showed that during a year 27% of the emitted B(a)P is transported outside the domain, 26% is degraded, about 46% is deposited within the calculation domain and 0.7% remains in the air. Thus, the B(a)P life-time within the calculation domain makes up about two days at annual averaging.
3. Deposition on the underling surface takes place largely due to the particulate phase of B(a)P. The role of gaseous B(a)P is relatively small.
4. Calculation results revealed peculiarities of B(a)P seasonal variations: elevated concentrations in the air and lower content of the gas-phase in winter versus summer.
5. A comparison of calculation results obtained with available measurement data and results of other models showed their reasonable agreement.
6. When developing the model for the operational calculation of the atmospheric B(a)P transport, a number of investigations should be carried out in order to answer the following most important questions:
   a) What dependence does the particulate and gaseous B(a)P partition obey? How rapid is the equilibrium set; what is the fraction of the B(a)P sorbed irreversibly on the particles?
   b) What is B(a)P distribution with particle size in emissions; how does the B(a)P distribution change in the course of the transport and what is the efficient model description of this process?
   c) What is B(a)P degradation rate in the atmosphere; how does it depend on a season, time of day and B(a)P phase?

d) What is the role of sub-cloud and in-cloud washout and what are washout ratios for gaseous B(a)P and particles - carriers?

e) What is the role of vegetation in dry deposition of B(a)P on land and how can it be taken into account?

f) How significant is B(a)P re-emission in the process of the underling surface - atmosphere exchange; can particulate B(a)P once entered the land or water be transported into the gas-phase?

g) What is the B(a)P degradation rate in various compartment, including vegetation?

In addition it should be noted that emissions and measurement problems are required to be solved concurrently with those indicated above.

References

Afanasiev M.I., Alexeeva T.A., Teplitskaya T.A. [1982] The estimation of 3,4-benzo(a)pyrene in the air on background monitoring stations. In: The background pollution monitoring of the environment. Issue 1, L., Hydrometeoizdat (In Russian).

Baart A.C., Berdowski J.J.M., van Jaarsveld J.A. and Wulffraat K.J. [1995] Calculation of atmospheric deposition of contaminants on the North Sea. TNO-MEP - R 95/138*, Delft, The Netherlands.

Bakker D.J., de Vries W. [1996] Manual for calculating critical loads of persistent organic pollutants for soils and surface waters.- TNO-MEP report R 96/509, The Netherlands.

Berdowski J.J.M., Baas J., Bloos J.-P.J., Vesschedijk A.J.H. and Zandveld P.Y.J. [1997] The European Emission Inventory of Heavy Metals and Persistent Organic Pollutants. TNO, Report UBA-FB, UFOPLAN-Ref. No. 104.02 672/03, Apeldoorn, p.239

Blau L., Güster H. [1994] Quantum yields of the photodecomposition of polynuclear hydrocarbons adsorbed on silica gel. In: Polynuclear aromatic hydrocarbons: Phys. and biol. chem.6th Int. Symp., Columbus, 23-19 oct.1981, pp. 133-144.

Bodzek D., Luks-Betlej K. and B. Janoszka [1998] Occurrence of PAHs in various elements of environment in zabrze (upper Silesia, Poland). Water, Air and Soil Pollution, v.103, pp.91-100.

Broddin G., Cautreels W., Van Cauwenberghe K. [1980] On the aliphatic and poliaromatic hydrocarbon levels in urban and background aerosols from Belgium and Netherlands. Atm. Environ., v. 14, pp. 895-910.

Cohen Y. and Clay R.E. [1994] Multimedia Partitioning of Particle-Bound Organics. *J Hazard Mater v.* 37, pp. 507-526

Finlayson-Pitts B. J., Pitts J.N. Jr. [1986] Atmospheric chemistry: Fundamentals and experimental techniques. Willy, New York.

Frolov A., Vazhnic A., Astakhova E., Alferov Yu., Kiktev D., Rosinkina I., Rubinshtein K. [1994] System for diagnosis of the lower atmosphere state (SDA) for pollution transport model, EMEP/MSC-E Technical report 6/94.

Jacobs C.M.J. and van Pul W.A.J. [1996] Long-range Atmospheric transport of Persistent Organic Pollutants, 1: Description of surface - atmosphere exchange modules and implementation in EUROS. Report N722401013 RIVM, Bilthoven, The Netherlands.

Junge C.E. [1977] Basic considerations about trace constituent in the atmosphere is related to the fate of global pollutant. In: Fate of pollutants in the air and water environment. Part I, I.H. Suffer (ed.) (Advanced in environmental science and technology, v.8), Wiley-Interscience, New York.

Hincley D.A., Bidleman, T.F., and Foreman W.T. [1990] Determination of vapor pressures for nonpolar and semipolar organic compounds from gas chromatographic retention data. Journal of Chemical and Engineering Data v. 35, № 3, pp. 232-237

Holoubek I. et al. [1993] Methodologies for the estimation of the emission of POP's to the atmosphere.- Project TOCOEN.

van den Hout, ed. [1994] The impact of atmospheric deposition of non-acidifying Pollutants on the Quality of European forest soils and the North sea, Main report of the ESQUAD project, RIVM rep.722401003, IMW-TNO rep.R93/329.

Kertesz-Saringer M., Morik J., Morlin Z. [1969] On the atmospheric benzo(a)pyrene pollution in Budapest//Atmospheric Environment, v.3, pp.417-422.

Mackay D., Shiu W.Y., Ma K.C. [1991] Illustrated handbook of physical-chemical properties and environmental fate for organic chemicals. CRC. Press. Boca Raton, FL., vol. II.

Milukaite A. and A. Galvonaite [1991] Monitoring of benzo(a)pyrene fallout and evaluation of its concentrations in atmospheric air in Lithuania.

Moscow Workshop [1987] Workshop on the Assessment of EMEP Activities Concerning HMs and POPs and Their Further Development (24-26 September, 1996). MSC-E Report 1/97

Pekar M. [1996] Regional models LPMOD and ASIMD. Algorithms, parametrization, and results of application to Pb and Cd in Europe scale for 1990. EMEP/MSC-E Report 9/96.

Rovinsky F.Ya., Afanasiev M.I., Vulih N.K. [1988] Background concentration of chloro-organic compounds and 3,4 benzo(a)pyrene in natural compartments (according to world data). Report 1,2,3,4,5. J.Monimong of backgroud pollution. L., Hydrometeoizdat, (in Russian).

Rovinsky F.Ya., Afanasiev M.I., Buivolov Yu.A. etc. [1992] *J. of Ecological Chemistry* v.1, pp.46-64 (in Russian).

Schreitmüller J., Ballschmiter K. [1994] Fresenius *Anal.Chem.* v.348, pp.226-239.

Schwarzenbach R.P., Gschwend P.M., [1993] Imboden D.M. Environmental organic chemistry. John Wiley&Sons Inc., New York.

Strand A. and O. Hov [1996] A model Strategy for the Simulation of Chlorinated Hydrocarbon Distribution in the Global Environment. Water, Air and Soil Pollution, v.86, pp.283-316.

Venkataraman, C. and S.K. Friedlander [1994] Size distributions of polycyclic aromatic hydrocarbons and elemental carbon. 2. Ambient Measurements and Effects of Atmospheric Processes. Environ. Sci. Technol., v. 28, pp. 563-572,

Vozhzennikov O.I., Bulgakov A.A., Popov V.E. et al. [1997] Review of migration and transformation parameters of selected POPs, EMEP/MSC-E Report 3/97.

Yufit S.S., Klyuev N.A. [1997] Analytical review of physical-chemical processes responsible for the input to and removal from the atmosphere of persistent xenobiotics, Moscow, (in Russian).

Whitby K.T. [1978] The physical characteristics of sulphur aerosols. Atmospheric Environment, v.12, pp.135-195.

Chapter 5 Sensitivity analysis of the model to variations of physical-chemical parameters of gaseous POPs

Introduction

Persistent organic pollutants include substances with a wide spectrum of physical-chemical properties determining their behaviour in different environmental compartments. Modelling of these pollutants behavior in the atmosphere and other compartments is connected with the necessity of devising models adequately responding to variations in key-parameters. In this study we considered the sensitivity of the POP transport model described in Chapter 1 to variations in the following parameters: distribution coefficient K_{da}; dimensionless Henry coefficient K_H; relative moisture content θ; degradation coefficients in the atmosphere k_a, in the soil k_s and in the water k_w; soil temperature T_s; temperature gradient along the atmosphere height; convective water flux in the soil J_w; water surface molecular diffusion depth ΔZ_{wm}.

The most important stage of this study is an investigation of POP exchange processes between the atmosphere and the underlying surface in the course of the long-range transport.

5.1 Surface-atmosphere exchange

A great number of parameters describing the mathematical model of the long-range transport of POPs (see, for example, [*Progress report MSC-E-RIVM*, 1997]), does not allow to use directly three-dimensional version of ASIMD [*Pekar*, 1996] for the sensitivity analysis. Therefore like [*Jacobs and van Pul,* 1996] we limited ourselves by the consideration of vertical exchange processes in the atmosphere with well-defined initial and boundary conditions.

Mathematically, the problem can be formulated in the following way:

$$\frac{\partial C}{\partial t} = \frac{\partial}{\partial z} D_z \frac{\partial C}{\partial z} - (k_a + \Lambda)C + Q \tag{5.1}$$

$$\frac{\partial C_T}{\partial t} + \frac{\partial J_T}{\partial z} = -k_s C_T \tag{5.2}$$

where: $J_T = V_E C_T - D_E \frac{\partial C_T}{\partial z}$

$$\frac{\partial C_w}{\partial t} = \frac{C_r - C_{surf}}{\Delta z_w \Sigma r} - k_w C_w + \frac{F_w}{\Delta z_w} \tag{5.3}$$

In equations (5.1)-(5.3): t - time; z -vertical co-ordinate; $C(z,t)$, $C_T(z,t)$, $C_w(t)$ - POP concentration in the atmosphere, total concentration in the soil and in the water, respectively; $D_z=D_z(z,t)$, D_E - vertical coefficient of diffusion in the atmosphere and effective coefficient of diffusion in the soil respectively; k_a, k_s, k_w - POP degradation rates in the atmosphere, soil and water; Λ - coefficient of washout by atmospheric precipitation; $Q = Q(z,t)$ -emission; J_T - POP total flux in the soil; V_E - effective velocity of dissolved matter; C_r, C_{surf} - POP concentration in the lower atmospheric layer and on the soil surface (water surface), respectively; ΔZ_w - depth of the accumulating water layer; Σr - integrated resistance of the lower atmospheric layer.

Equation (5.1) describes POP distribution with the atmosphere, equation (5.2) - POP distribution with the soil, equation (5.3) - POP distribution with the water.

As initial conditions the following is used:

$$C_0(z) = 0;$$
$$C_{T0}(z) = 0; \quad (5.4)$$
$$C_{w0} = 0.$$

As the condition at the interface atmosphere-underlying surface it is assumed that POP total flux in the soil is equal to POP total flux in the atmosphere (5.5). POP total flux in the atmosphere is equal to a sum of dry deposition and wet deposition fluxes:

$$J_T(z=0) = \left(V_E C_T - D_E \frac{\partial C_T}{\partial z} \right)_{z=0} = \frac{C_r - C_{surf}}{\Sigma r} + R_l C \quad (5.5)$$

where: R_l - precipitation intensity.

POP total concentration in the soil is usually presented as [*Jury et al.*, 1983]:

$$C_T = \rho_s C_s + \theta C_l + (\varphi - \theta) C_g, \quad (5.6)$$

where: ρ_s - volumetric bulk density of the soil; θ - volumetric water content; φ - soil porosity; C_s, C_l, C_g - absorbed phase, liquid phase and gas phase concentrations.

Following [*Jacobs and van Pul,* 1996] relationship:

$$D_E = \frac{\xi_g D_g}{R_g} + \frac{\xi_l D_l}{R_l} \quad (5.7)$$

was used as an effective diffusion coefficient, where

$\xi_l = \frac{\theta^{10/3}}{\varphi^2}, \xi_g = \frac{(\varphi - \theta)^{10/3}}{\varphi^2}$ - tortuosity factors for liquid and gas, respectively;

$R_l = \rho_s K_{da} + \theta + (\varphi - \theta) K_H; R_g = R_l / K_H; R_s = R_l / K_{da}$ - are the liquid-phase partition coefficient, gas-phase partition coefficients and the adsorbed-phase partition coefficient, respectively; D_g, D_l - molecular diffusion of POP in the air and in the water respectively; K_{da} - adsorption isotherm slope called also distribution coefficient; K_H - Henry dimensionless coefficient. In case of lindane for the calculation of K_H the equation [*Jacobs and van Pul,* 1996]

$$K_H = \frac{0.073}{RT} \exp\left(-7329 \left(\frac{1}{T} - \frac{1}{283.15} \right) \right), \quad (5.8)$$

was used where R = 8.314 J mol^{-1} K^{-1} - gas constant; T- absolute temperature (K).

While computing the distribution coefficient K_{da} relationship [*Jury et al.*, 1983]

$$K_{da} = f_{oc} \cdot K_{oc}, \quad (5.9)$$

was used, where f_{oc} - percentage of the organic carbon content in the soil; K_{oc} - organic distribution coefficient which correlates well with the waterorganic distribution coefficient [*Mackay et al.*, 1992].

The effective transport velocity of dissolved substance is calculated from the relationship:

$$V_E = \frac{J_w}{R_l}, \tag{5.10}$$

where J_w - convective water flux.

The following relationship was used in the calculation of the surface - atmospheric exchange of gaseous POPs [*Jacobs and van Pul,* 1996].

$$F_g = \frac{C_r - C_{surf}}{r_a + r_b + r_s}, \tag{5.11}$$

where F_g - gaseous POP flux across the boundary of the interface (atmosphere-soil or atmosphere-water); r_a - aerodynamic resistance between reference levels at the height Z_r (in our case 50 m) and aerodynamic roughness size at the height Z_0, r_b - resistance of the quasi-laminar boundary layer; r_s -surface resistance.

Values r_a and r_b in these experiments were given as input data. For calculations of surface resistance r_s and POP surface concentration C_{surf} relationships for the interface atmosphere-soil [*Jacobs and van Pul,*1996] were used:

$$r_s = \frac{1}{R_g\left(\frac{2D_E}{\Delta Z_1} + pV_E\right)};\ C_{surf} = \frac{C_{T,1}}{R_g}\frac{\frac{2D_E}{\Delta Z_1} - qV_E}{\frac{2D_E}{\Delta Z_1} + pV_E}, \tag{5.12}$$

where ΔZ_1 - depth of the first calculation layer in the soil; $C_{T,1}$ - POP total concentration in the first calculation layer of the soil; p, q - weight coefficients such as $p + q = 1$. For the interface atmosphere-water:

$$r_s = K_H \cdot r_w, \qquad C_{surf} = K_H\, C_w, \tag{5.13}$$

where K_H - dimensionless Henry coefficient; $r_w = \Delta Z_{wm}/D_l$ - molecular layer resistance; ΔZ_{wm} - molecular layer depth (it is assumed that $\Delta Z_{wm} \approx 4 \cdot 10^{-5}$ m); D_l - molecular diffusion coefficient of a pollutant in the water; C_w - pollutant concentration in the water.

5.2 Spatial discretization

Spatial discretization of eq. (5.1) along spatial co-ordinate z is the same as in [*Pekar*, 1996]. The co-ordinate z is directed upward, four layers with depths 100 m, 300 m, 700 m and 1000 m were considered. The calculated point is in the middle of each layer, coefficients of vertical macrodiffusion $D(z,t)$ were calculated using the procedure described in [*Pekar*, 1996] for 6-hour meteorological period.

Spatial discretization of eq.(5.2) followed the procedure described in [*Jacobs and van Pul,* 1996]. Co-ordinate z is directed vertically downward, five levels with different depths: ΔZ_1 = 0.5 cm; ΔZ_2 = 0.5 cm; ΔZ_3=1 cm; ΔZ_4 = 2 cm; ΔZ_5 = 11 cm and total depth $\Sigma\Delta Z$ = 15 cm were considered. As the boundary condition at the lower boundary, it was taken that POP flux is assumed to be equal to zero.

Equation (5.3) is one-dimensional and in the sensitivity analysis it was assumed that the accumulating water depth is ΔZ_w = 1m. The pollutant does not penetrate below it.

5.3 Peculiarities of sensitivity analysis

Following the procedure of sensitivity study performed by [*van Pul,* 1996] two kinds of analysis were carried out:

- an analysis without atmospheric feedback, i.e. a fixed set of conditions at the reference level was used;
- an analysis with atmospheric feedback, when the processes of vertical exchange in the atmosphere were taken into account.

For the first kind of the analysis it is not necessary to solve equation (5.1) among other equations considered. Only the characteristics of underlying surface and physico-chemical parameters of the pollutant determine the value of gaseous fluxes and concentration distribution with the soil.

For the second kind of the analysis the formulation (5.1)-(5.5) with closing dependencies (5.6)-(5.13) is fully realized.

In this work the effect of the following parameters was studied: distribution coefficient K_d; dimensionless Henry coefficient K_H; relative moisture content θ; influence of POP degradation coefficients in the atmosphere (k_a), in the soil (k_s) and in the water (k_w); influence of soil temperature (T_s) ; influence of temperature gradient along the atmosphere height; influence of convective flux of water in the soil J_w.

In calculations of the effect of a certain parameter only studied parameter was changed whereas the rest of parameters were kept unvaried. In the discussion of the results the attention was focused on the parameters of annual fluxes of dry and wet deposition.

In calculation runs the interacting system atmosphere-soil or atmosphere-water should reach a quasi-stationary state. When it is reached a stable annual cycle, appropriate concentrations and fluxes should be practically unchangeable from year to year. Meteorological data for one year are used for all years of modelling. Modelling duration depends, for instance, on degradation coefficient values in interacting media. In the system atmosphere-soil a quasi-stationary state is reached in 10-15 years if parameters of a pollutant are similar to those of lindane. For the system atmosphere-water, if the degradation coefficient for water is taken to be zero, the period over which the attainment of a quasi-stationary state is established is very great (thousands of years [*Jacobs and van Pul,* 1996]).

5.4 Initial data

Physical-Chemical parameters

Physical-chemical parameters of γ-HCH lindane [*Jacobs and van Pul,* 1996] were used as basic. As a rule, investigated parameters were taken in a relative form. For example, for the dimensionless Henry coefficient it will be of the form (K_H/K_H(HCH)), where K_H(HCH) is the standard value of K_H for γ-HCH lindane.

Meteorological information

In order to have a possibility to compare indirectly our results with the data of Dutch authors we used MSC-E meteodata for 1989 in the square ix = 20, iy = 15 of the EMEP grid with gridsize 150x150 km^2. This square contains a point with geographical co-ordinate 52^{O}06` N, 5$^O$11` E. Meteorological data observed at this point in 1989 were used in the Dutch study [*Jacobs and van Pul,* 1996] as initial information. Our initial information averaged over 6-hour period included: precipitation intensity P, temperature T_r (2 m above the ground surface), resistance of aerodynamic and quasi-laminar boundary layer (r_a and r_b). Plots of annual variation (1989) in precipitation intensity (P), temperature (T_r) and resistance sum ($r_a + r_b$) are in Figure 5.1.

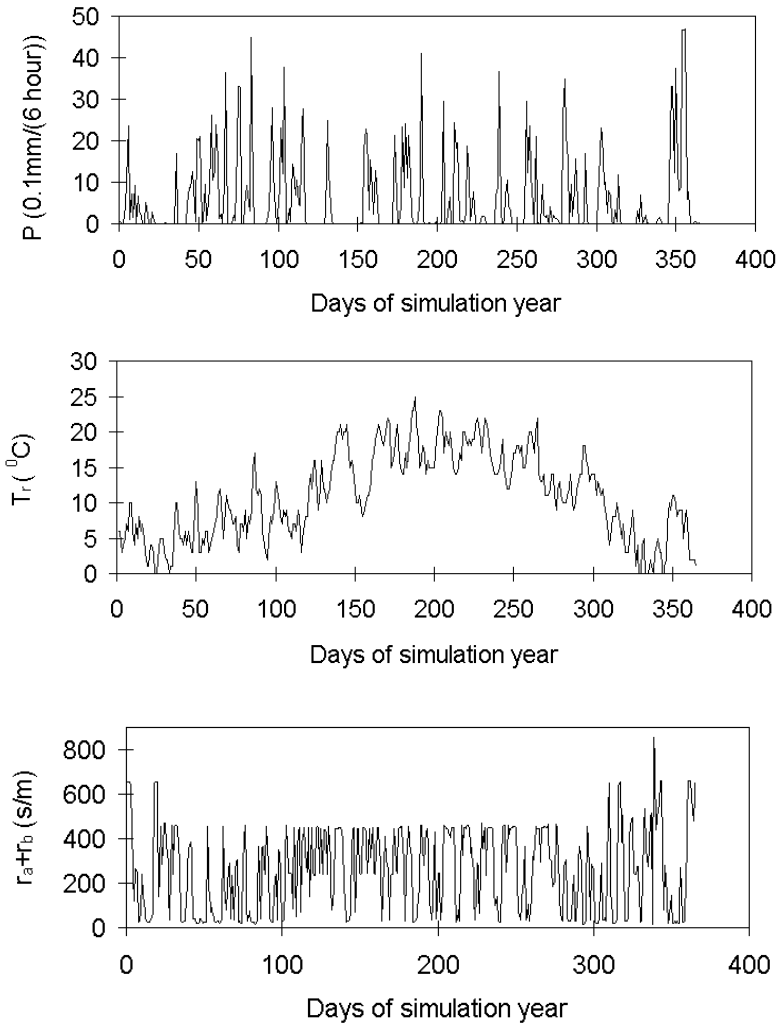

Figure 5.1 Precipitation (P, upper), temperature (T_r, middle) at ix = 20; iy = 15 of 150×150 km^2 EMEP-grid for 1989, and sum of aerodynamic and boundary layer resistances ($r_a + r_b$, lower)

From the comparison of our initial data with those of [*Jacobs and van Pul,* 1996] it follows that estimates of annual precipitation of Dutch authors were 2-2.5 times lower than those used in our study (841 mm); annual temperature variations in both cases are approximately the same; values of aerodynamic resistance r_a vary within the same limits.

Soil characteristics

The lower boundary of the fifth layer was taken to be impermeable for POP. Soil porosity φ was assumed to be 0.5, volumetric bulk density of the soil ρ_s was taken to be equal to 1350 kg/m^3. Initial concentrations of a pollutant were zero. Non-applicable regions were considered. All data discussed in this section completely coincide with the data presented in [*Jacobs and van Pul,* 1996].

Characteristics of water surfaces

In calculations of sensitivity it was assumed that the depth of accumulating water layer was equal to 1 m. Meteorological conditions were assumed to be the same as over the soil surface. The initial concentration of a pollutant in the water was zero.

5.5 Experiments

The effect of adsorption coefficient

The adsorption coefficient K_{da} is calculated as $K_{da} = K_{oc}{\cdot}f$, where K_{oc} – parameter of POP adsorption on organic components of the soil, f_{oc} – per cent content of the organic matter in the soil. The value of f_{oc} can vary from 1 to 30%. K_{oc} value is different for different POPs. Therefore in experiments K_{da} value varied in a wide range: from 10^{-3} K_{da} to 10^3 K_{da}, where K_{da} is a standard value of K_{da} for lindane. Calculations were made for various coefficients of the soil moisture (0.15, 0.30, 0.45). For the value of surface resistance r_s at J_w=0 it is possible to obtained the ratio:

$$r_s = \frac{\Delta Z_1 \varphi^2 K_H}{2\left((\varphi-\theta)^{10/3} D_g \cdot K_H + \theta^{10/3} D_w\right)}. \qquad (5.14)$$

Under the same condition we have the expression:

$$\frac{C_{surf}}{C_{T1}} = \frac{K_H}{\rho_s K_{da} + \theta + (\varphi-\theta)K_H}. \qquad (5.15)$$

These relationships help to understand the experiment results.

The Figure 5.2 shows the increase of gaseous flux of lindane with the increase of organic carbon content in the soil. When the content of organic matter in the soil is low, the gaseous flux of lindane is directed to the atmosphere, at the high content – to the soil. Total annual flux is equal to zero at f_{oc} = 13.6%. This result is different from that obtained in [*Jacobs and van Pul*, 1996], where F_g = 0 at f_{oc} = 6.3%. This discrepancy is explained by the difference in the rate of lindane input to the surface with atmospheric precipitation (445 μg/m^2/yr in this work and 188.4 μg/m^2/yr in [*Jacobs and van Pul*, 1996]). In further experiments, unless specially mentioned, the following assumption is made: f_{oc} = 13.6%.

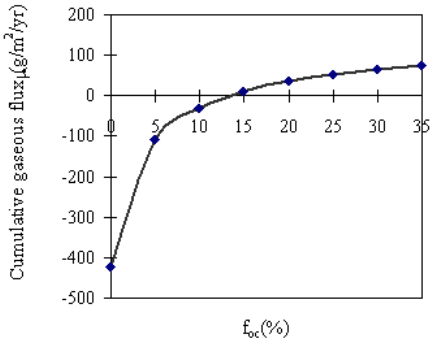

Figure 5.2 Dependence of total annual gaseous flux of lindane in gas-phase through the atmosphere-soil interface (F_g в μg/m^2/yr) on organic carbon content in the soil (f_{oc}) at fixed content of lindane in the lower atmospheric layer (0.01 μg/m^3)

Effect of linear partitioning coefficient, K_{da}

The ratio C_{surf}/C_{T1} depends to a considerable extent on K_{da} and almost does not depend on the soil moisture (Figure 5.3). It can be explained by the evaluation of analytical dependence C_{surf}/C_{T1} (5.15). Relative values of terms in the denominator are 10^2:1:10^{-5} at standard values of K_H and K_{da}. At high and mean values of K_{da} the value of C_{surf}/C_{T1} can be considered to be proportional to $1/K_{da}$. At low values of K_{da} the second term θ in the denominator becomes important. The value of surface resistance r_s at J_w = 0 is described by expression (5.14). Hence r_s does not depend on K_{da}.

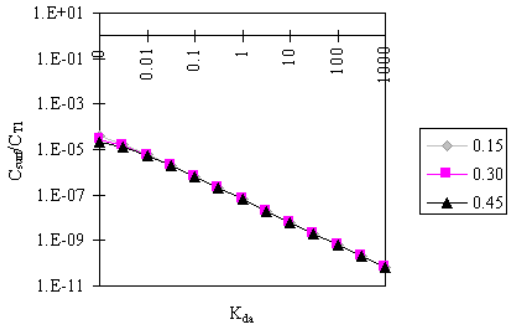

Figure 5.3 Dependence of C_{surf}/C_{T1} on the adsorption coefficient of lindane in the soil K_{da} at different values of the soil moisture coefficient

Gaseous flux of lindane is directed to the atmosphere through the surface at K_{da} lower than lindane K_{da} and to the soil at K_{da} higher than lindane K_{da} (Figure 5.4). The flux values strongly depend on the soil moisture in the range of positive values of F_g and practically do not depend on it in the range of negative values. The experiment results quantitatively differ from those presented in [*Jacobs and van Pul,* 1996]. This difference is explained by the difference in annual wet deposition amounts (445 μg/m^2 in this work versus 188.4 μg/m^2 in [*Jacobs and van Pul,* 1996]).

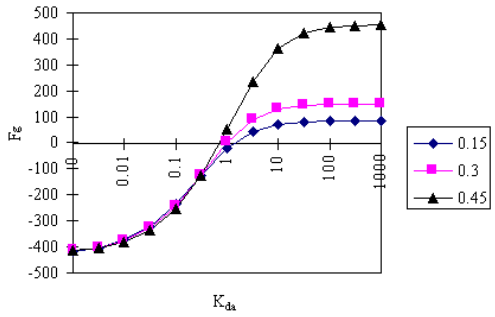

Figure 5.4 Dependence of total annual gaseous flux of lindane through the atmosphere-soil interface (F_g μg/m^2/yr) on the adsorption coefficient of the soil at fixed lindane content in the lower atmospheric layer (0.01 μg/m^3) and different values of the soil moisture coefficient (0.15, 0.30, 0.45)

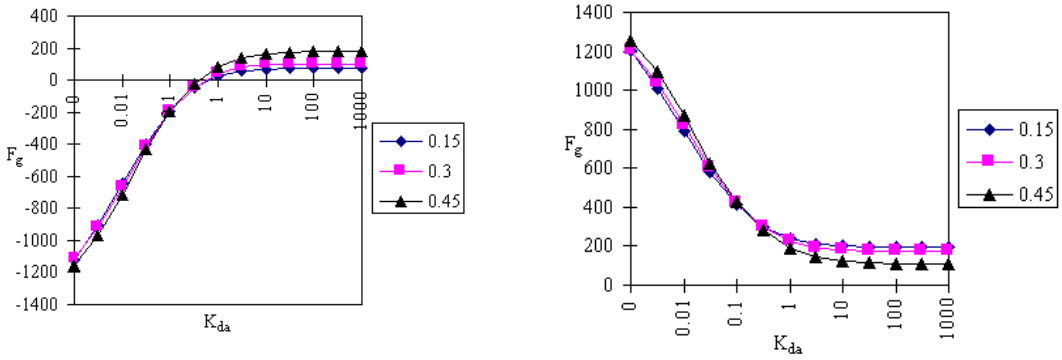

Figure 5.5 Dependence of total annual flux of lindane in gas and liquid forms through the atmosphere-soil interface (μg/m^2/yr) on soil adsorption coefficient at the interaction with the atmosphere and different values of soil moisture coefficient (0.15, 0.30, 0.45)

Like in the previous test the gaseous flux of lindane through the surface is directed to the atmosphere at K_{da} lower than K_{da} of lindane and to the soil at K_{da} higher than K_{da} lindane (Figure 5.5). K_{da} value appreciably affects the flux value. Lindane flux in the liquid phase

through the surface decreases with K_{da} increase. The rate of the flux decrease slows down with the K_{da} increase.

The effect of Henry coefficient: atmosphere-soil

Since Henry coefficient is difficult to be determined in experiments it was changed by 6 orders of magnitude: from 10^{-3} K_{H0} to 10^{3} K_{H0}, where K_{H0} – K_H of lindane. Calculations were made with different soil moisture coefficients (0.15, 0.30, 0.45). The experiments showed that K_H substantially influences processes in the model. This influence is expressed by surface resistance variation r_s, surface concentration C_{surf} and coefficient of lindane washout from the atmosphere with precipitation (Figure 5.6).

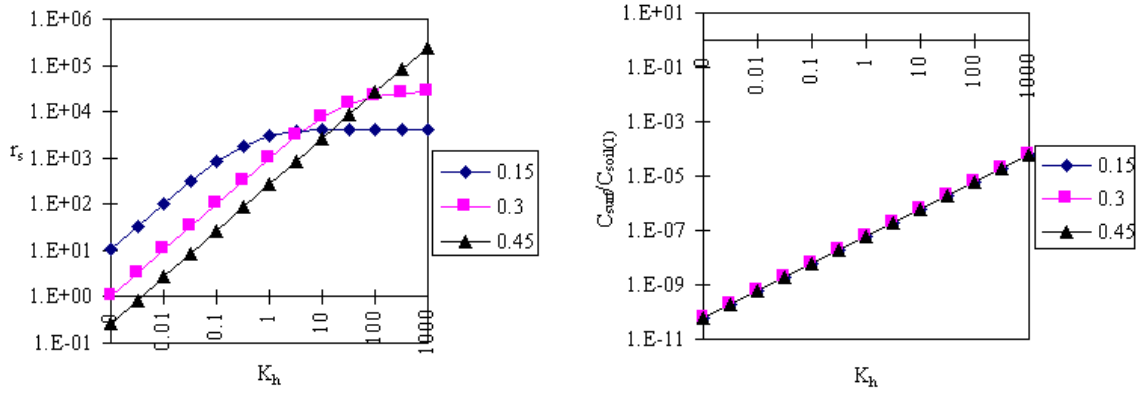

Figure 5.6 Dependence of surface resistance and ratio C_{surf} to lindane concentration in the soil near the surface on Henry coefficient value at different values of soil moisture coefficient (0.15, 0.30, 0.45)

The value of surface resistance increases with the K_H increase. At high values of soil moisture, this dependence is more pronounced. As it was mentioned above for the case of J_w =0, the value r_s is expressed by ratio (5.14). At low values of K_H (1.14) can be substituted for the expression $\Delta Z_1 \varphi^2 K_H/(2\theta^{10/3} D_l)$ linearly increasing with K_H. At high values of K_H, the second term in the denominator becomes important distorting the linear dependence on K_H at low θ. C_{surf}/C_{T1} linearly increases with the K_H increase. In fact, as shown above, at J_w=0, the value C_{surf}/C_{T1} is expressed by dependence (5.15). Under standard conditions $\rho_s K_{da} >> \theta >> (\varphi-\theta)K_H$, i.e. C_{surf}/C_{T1} is estimated by the expression $K_H/\rho_s K_{da}$ proving the linear dependence of C_{surf}/C_{T1} on K_H.

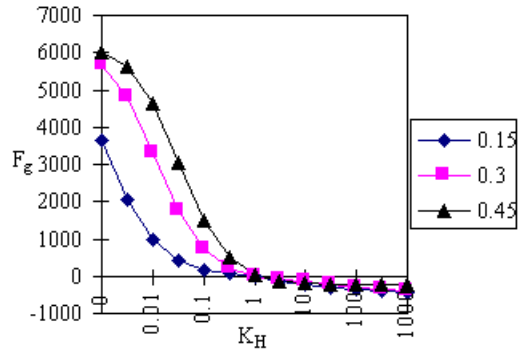

Lindane flux in the gaseous form through the surface is directed to the soil and it is high at low values of K_H (Figure 5.7). At high values of K_H the flux is directed to the atmosphere and it is inessential. In the range of positive values the flux increases with soil moisture increase. At negative values of the flux the effect of moisture is small.

Figure 5.7 Dependence of total annual gaseous flux of lindane through the atmosphere-soil interface (F_g μg/m²/yr) on Henry coefficient value at fixed lindane content in the lower atmospheric layer (0.01 μg/m³) and different values of soil moisture coefficient (0.15, 0.30, 0.45)

The lindane flux in the gaseous form through the surface is high and directed to the soil at low values of the Henry coefficient (Figure 5.8). At high values of K_H the flux is inessential. In this experiment the flux is appreciably lower than in the previous case due to damping effect of the atmosphere. The lindane flux in the liquid form through the atmosphere is not high at low values of K_H. It has the maximum at intermediate values of K_H and it decreases to zero at high values of K_H. The dependencies shown in Figures 5.7 and 5.8 are similar to those given in [*Jacobs and van Pul,* 1996]. However, numerical values are different. It can be explained by the difference in both input data and model formulation.

Figure 5.8 Dependence of total annual flux of lindane in gas and liquid forms through the

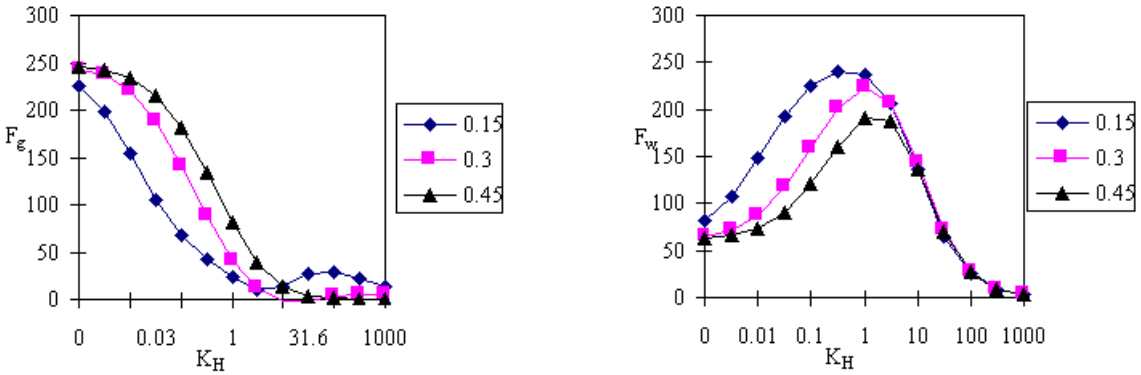

atmosphere-soil interface (μg/m^2/yr) on Henry coefficient value at the interaction with the atmosphere and different values of soil moisture coefficient (0.15, 0.30, 0.45)

The effect of the Henry coefficient: atmosphere-surface water

In the formulation of a given model it is assumed that at the interface of atmosphere-water the surface resistance $r_s = K_H \Delta Z_w D_l$, surface concentration - $C_{surf} = K_H \cdot C_w$, where ΔZ_w – layer depth of POP molecular diffusion in the water, C_w – POP concentration in the subsurface water layer. It follows that at low K_H, the surface resistance and concentration are also low and vice versa, they are high at high K_H. In the atmosphere POP washout with precipitation increases with the K_H decrease.

At high values of the POP degradation coefficient in the water the dependence of total POP flux in the gaseous form is poorly expressed (Figure 5.9). At low values of the degradation coefficient, this dependence has the distinctive minimum. At low K_H POP concentration in the water is high, the interface does not re-emit. At high K_H the resistance coefficient of the surface is high, the coefficient of washout with precipitation is low and processes in the system are not rather intensive. At the intermediate K_H and low degradation coefficient, POP concentration is high in the water, at the same time POP washout coefficient is sufficiently high. In this case the interface is re-emitting. The intensity of the gaseous flux from the water to the atmosphere should be sufficiently high since POP inflow with the liquid phase but the sink due to degradation is inessential.

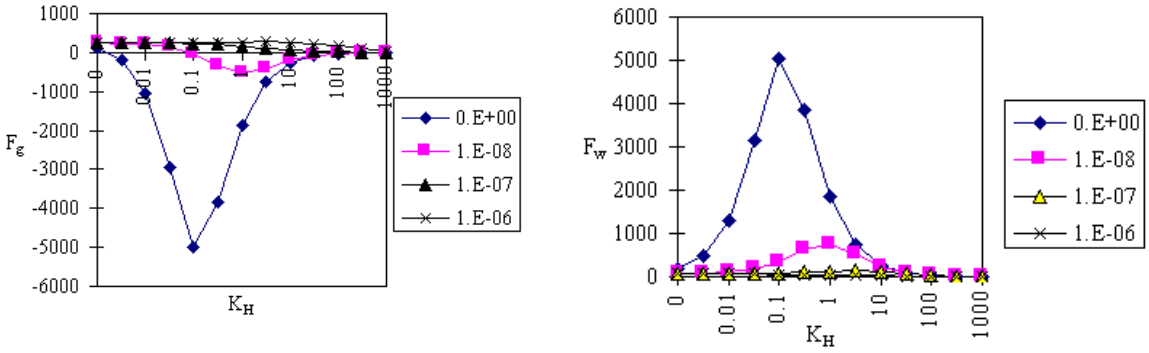

Figure 5.9 Dependence of total annual flux of lindane in gas and liquid forms through the atmosphere-soil interface (μg/m^2/yr) on K_H at the interaction with the atmosphere and different values of the degradation coefficient in the water (0, 10^{-8}, 10^{-7}, 10^{-6})

Effects of degradation coefficients

Effects of POP degradation in different compartments are poorly studied. Here, a linear dependence of degradation rate of the matter on its concentrations is assumed. The accuracy of degradation coefficient values is low. In numerical experiments values k_a, k_s, k_w from 10^{-9} to 10^{-5} 1/s are considered. Experiments were made with different K_H and for the soil in addition different values of K_{da} were additionally used.

At the standard K_{da} the flux of lindane is not so sensitive to the variation in the degradation coefficient in the air (Figure 5.10). At low values of K_{da}, flux variations are appreciable. In this case, at low values of the degradation coefficient, the interface is re-emitting in order to balance downward POP flux.

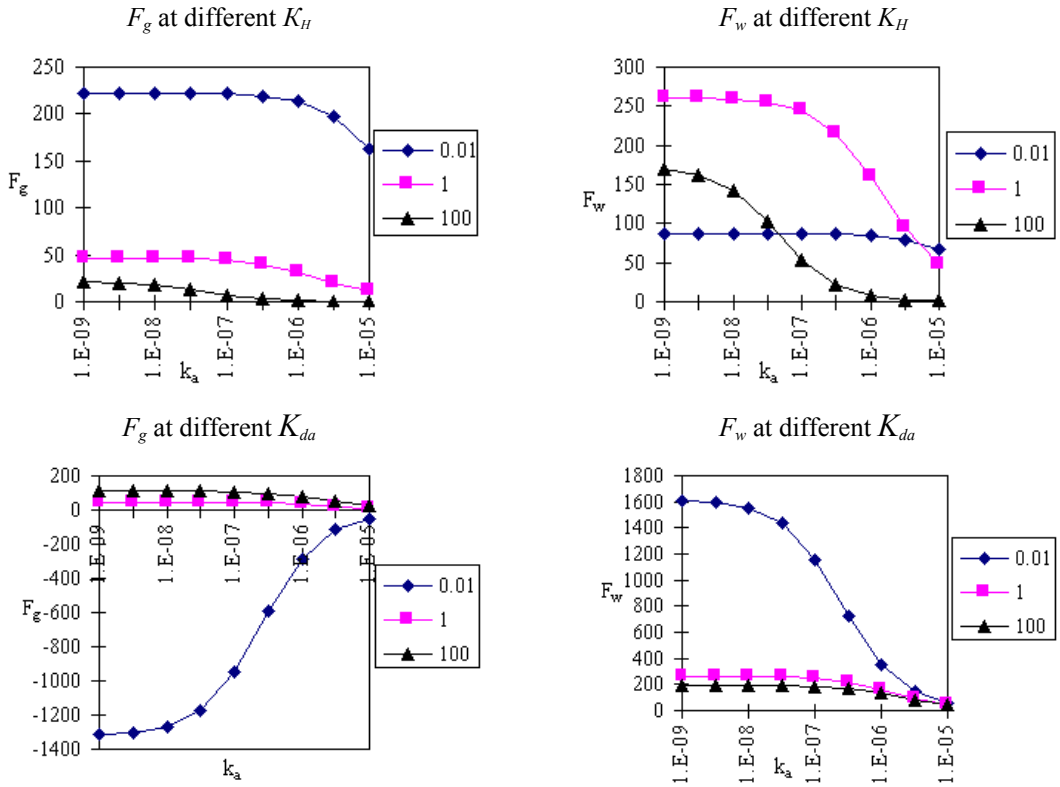

Figure 5.10 Dependence of total annual flux of lindane in gaseous and liquid forms through the atmosphere-soil interface (μg/m^2/yr) on the degradation coefficient in the atmosphere at different values of K_H (10^{-2} K_H lindane, K_H lindane, $10^2 K_H$ lindane) and different values of the adsorption coefficient in the soil (10^{-2} K_{da} lindane, 10^2 K_{da} lindane)

At the variation in the degradation coefficient in the soil, the flux intensity also changes as a rule inessential (Figure 5.11). The case with low K_{da} is an exception. In this case a relative value of concentrations of gaseous component in the soil is great. At low degradation coefficient mass balance in the soil is maintained by the inflow of POP with the liquid phase and outflow with the gas-phase.

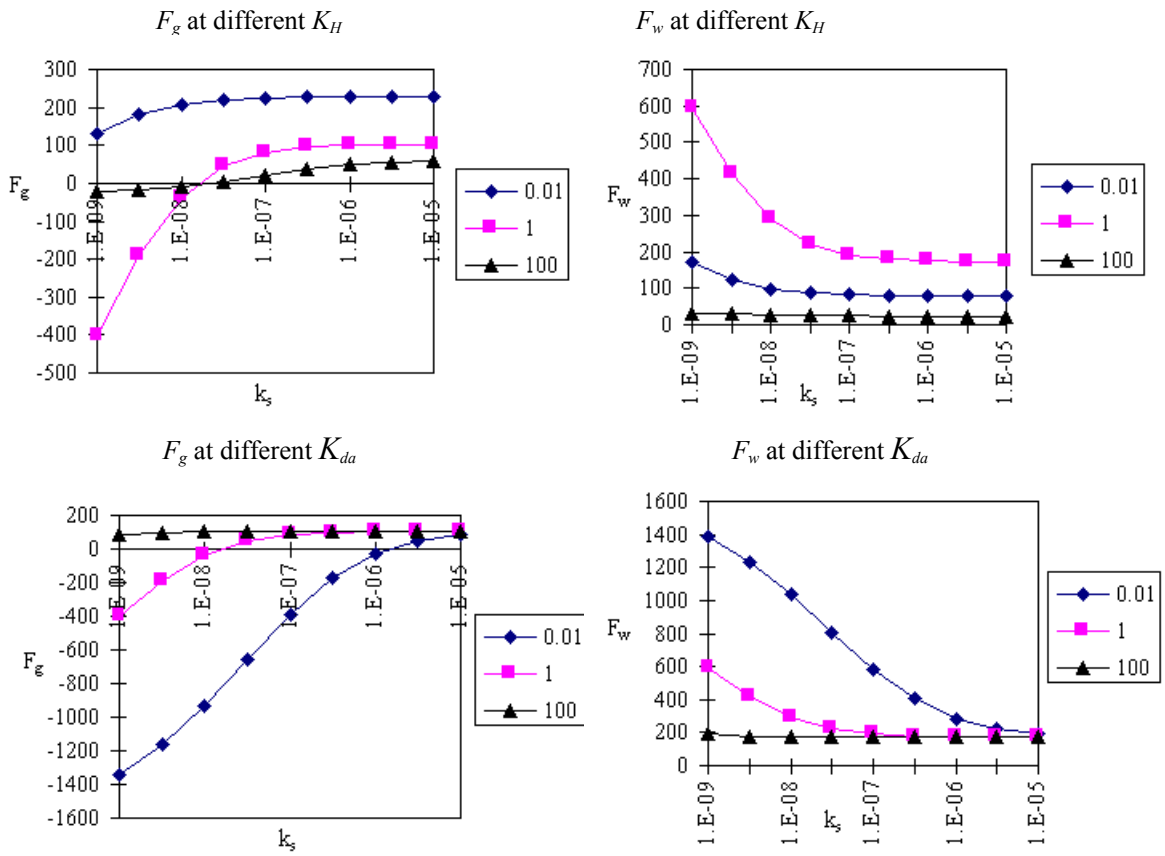

Figure 5.11 Dependence of total annual flux of lindane in gaseous and liquid forms through the atmosphere-soil interface (μg/m^2/yr) on the value of the degradation coefficient in the soil at the interaction with the atmosphere and different K_H (10^{-2} K_H lindane, K_H lindane, $10^2 K_h$ lindane) and different adsorption coefficient in the soil (10^{-2} K_{da} lindane, K_{da} lindane, 10^2 K_{da} lindane)

The increase of the degradation coefficient of lindane in the water is followed by the increase of gaseous flux through the interface atmosphere-soil. This effect is insignificant at low K_H (Figure 5.12). The increase of the gaseous flux is easy to explain. In fact the increase of the degradation coefficient in the water results in additional mass consumption. In this case, to maintain the system equilibrium it is necessary to increase the mass inflow. It is realized by the increase of the gaseous flux of lindane through the surface. An insignificant effect at high K_H is explained by the fact that in this case lindane mass in the atmosphere is small and its flux from the atmosphere to the water can not be appreciably increased.

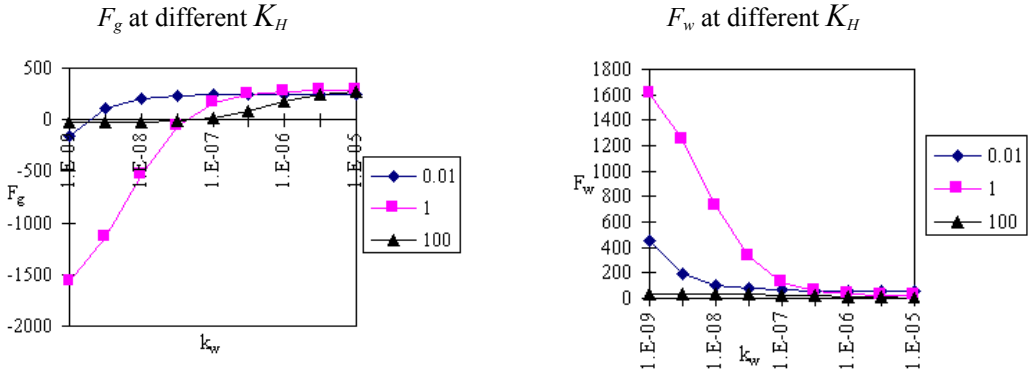

Figure 5.12 Dependence of total annual flux of lindane in gaseous and liquid forms through the atmosphere-water interface (μg/m^2/yr) on the degradation coefficient in the water at the interaction with the atmosphere at different values of K_H ($10^{-2}K_H$ lindane, K_H lindane, 10^2K_H lindane)

Effect of soil temperature

In order to investigate the effect of temperature differences in the atmosphere and in the soil layer, experiments with soil temperature $T_s=T_a+dT$ were carried out. Here T_a – atmospheric temperature near the surface, dT – experimental temperature difference varying from -10^0K to $+10^0$K with step 2^0K. Experiments were made with different K_H and K_{da}.

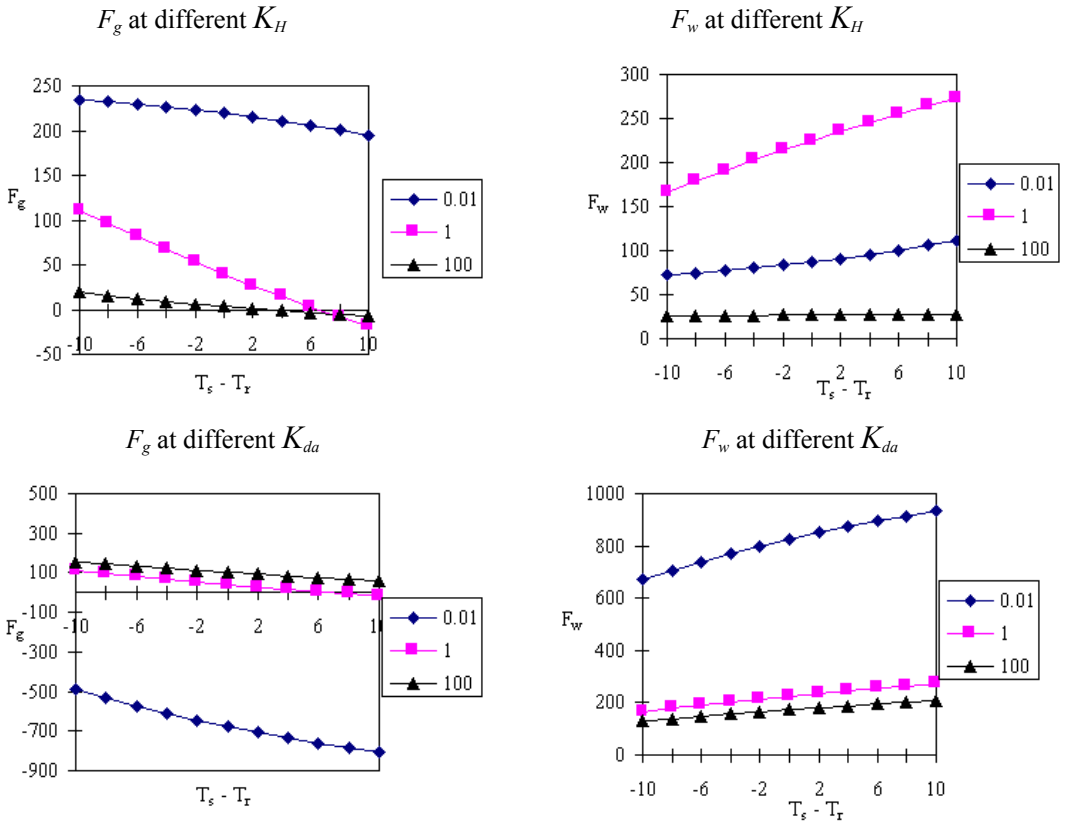

Figure 5.13 Dependence of total annual flux of lindane in gaseous and liquid forms through the atmosphere-soil interface (μg/m^2/yr) on the value of temperature difference in the soil and the atmosphere at the interaction with the atmosphere, different K_H (10^{-2} K_H lindane, K_H lindane, 10^2 K_H lindane) and different adsorption coefficient in the soil (10^{-2} K_{da} lindane, K_{da} lindane, 10^2 K_{da} lindane)

Flux values vary inessentially with the variation in temperature difference in the soil and in the atmosphere (Figure 5.13). Therefore this temperature difference is neglected and soil temperature considered is to be equal to the temperature of surface air.

Soil moisture effect

The effect of soil moisture coefficient on system parameters is manifested by surface resistance variation r_s. The surface resistance r_s depends on K_H, too. Under the condition J_w=0, r_s can be expressed as (5.14).

The surface resistance decreases with the moisture increase at low Henry coefficient and it increases at high values of the Henry coefficient (Figure 5.14). The difference in surface resistance at various K_H is small in the range of low moisture values and it is great at high moisture values. This effect can be explained by the formula for r_s given above. At low K_H the estimate of r_s (5.14) can be expressed as $\Delta Z_1 \varphi^2 K_H/(2\theta^{10/3} D_l)$. In this case surface resistance value decreases with the soil moisture increase. For high K_H values the estimate is expressed by the formula $\Delta Z_1 \varphi^2/(2(\varphi-\theta)^{10/3} D_g)$. In this case the surface resistance increases with the soil moisture increase.

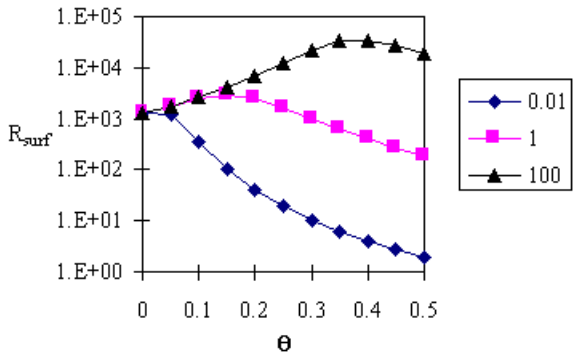

Figure 5.14 Surface resistance coefficient dependence on soil moisture value at different values of the Henry coefficient ($10^{-2}K_H$ lindane, K_H lindane, $10^2 K_H$ lindane)

The effect of water convective flux in the soil

The flux of POP in the soil can be transported with water convective fluxes. The convective flux can be directed both upward and downward. According to estimates of [*Jacobs and van Pul,* 1996] the value of convective flux can vary from –0.5 m/yr to +0.5 m/yr. Obviously the effect of the convective flux is more essential at low K_H (POP concentration great in the water) and at low values of the adsorption coefficient (a small part of POP mass is bound in the soil). At low value of K_H, the flux value through the surface is affected by the increase of POP washout from the atmosphere with precipitation.

The gas flux increases with the liquid convective flux increase (Figure 5.15). The convective flux is an additional means of lindane transport in the soil. When the convective flux increases from negative (from the depth to the surface) to positive values (from the surface to the depth) the intensity of lindane transport from the surface to the depth increases and lindane concentration near the surface decreases, thus enhancing the intensity of gaseous flux from the atmosphere due to the increase of the difference.

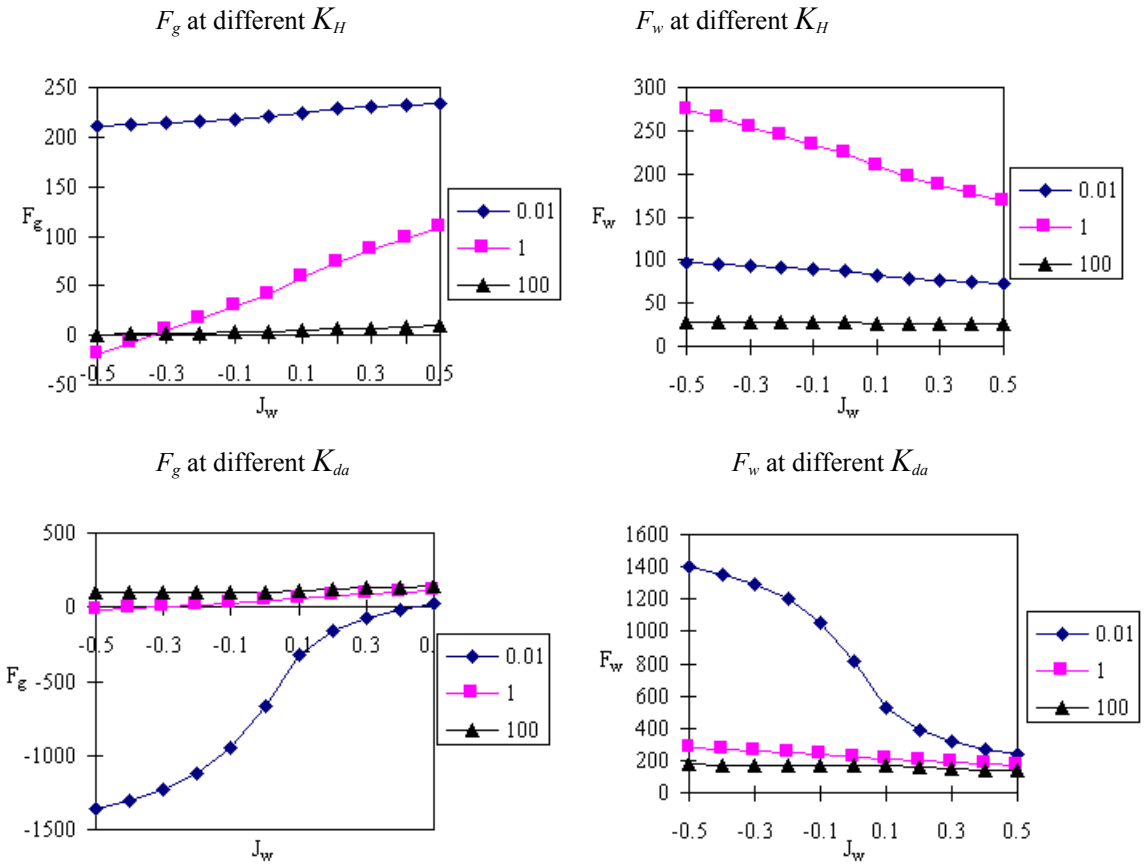

Figure 5.15 Dependence of total annual flux of lindane in gaseous and liquid forms through the atmosphere-soil interface (μg/m^2/yr) on the value of liquid convective flux in the soil at the interaction with the atmosphere and different Henry coefficients ($10^{-2}K_H$ lindane, K_H lindane, 10^2K_H lindane) and different adsorption coefficient in the soil (10^{-2} K_{da} lindane, 10^2 K_{da} lindane).

Discussion of the results

As it was mentioned above, the aim of this study was to assess the sensitivity of the ASIMD model coupled with surface modules, developed in RIVM, to the variation in main physico-chemical properties of POP and environmental conditions. The results obtained show quite complicated nature of POP exchange processes between considered compartments.

Like in the work [*Jacobs and van Pul*, 1996] the results have pointed out the major role of wet deposition in input of lindane into the soil. In order to present obtained results and to give an extent of their uncertainty, they are summarized in Table 5.1.

Table 5. 1

Parameter ***Soil***	Parameter deviation	F_w deviation (in this work)	F_w deviation in work [*Jacobs and van Pul,* 1996]
K_{da}	0.25/4	+42/-16	+34/-10
K_H	0.5/2	-5/-2	+24/-10
k_a	0.5/2	+7/-12	+23/-22
k_s	0.5/2	+17/-10	+22/-11
T_s-T_a	-5/+5^{0}K	-13/+11	-12/+11
θ	-0.15/+0.15	+6/-14	+6/-21
J_w	-0.2/+0.2	+9/-12	+13/-17
Water			
K_H	0.5/2	+60/-41	+107/-62
k_w	$+10^{-9}$/$+10^{-7}$	-13/-93	-5/-82

In general results of this work qualitatively coincide with the results presented in [*Jacobs and van Pul*, 1996] (3rd and 4th columns in the table). At the same time, some differences can be noted. In particular, the deviations of F_w due to the variation in K_H (in case of soil surfaces) are different in both works. One of the reasons, explaining these discrepancies, is connected with the obvious differences in the atmospheric models applied. The other one - with different initial conditions of the tests (annual precipitation amount was 2-2.5 times higher in this work). In this work much attention was paid to the evaluation of impact of physical-chemical properties on the exchange processes. Regarding the environmental conditions, only the effect of variation in soil moisture was tested.

Conclusions

1 The obtained results allow us to draw the following conclusion. In spite of the considerable range of variations in the considered parameters the model adequately reflects these variations.

2 The obtained results are similar to those obtained in [*Jacobs and van Pul,* 1996].

3 Inessential discrepancies obtained in a number of experiments (especially at K_H coefficient variations) are basically connected with the differences in the atmospheric models used and initial conditions.

References

Mackay D., Shiu W.Y., Ma K.C. [1992] Illustrated handbook of physical-chemical properties and environmental fate for organic chemicals. CRC. Press. Boca Raton, FL., vol. II

Jacobs C.M.J. and van Pul W.A.J. [1996] Long-range atmospheric transport of persistent organic pollutants, I: Description of surface-Atmosphere exchange modules and implementation in EUROS. National Institute of Public Health and the Environment, Bilthoven, The Netherlands. Report No.722401013

Jury W.A., Spencer W.F. and Farmer W.J. [1983] Behavior Assessment Model for Trace Organics in Soil. *J. Environ. Qual*., v.12, pp.558-564

Pekar M. [1996] Regional models LPMOD and ASIMD. Algorithms, parametrization and results of application to Pb and Cd in Europe scale for 1990 MSC-E Report 9/96, September

Progress report MSC-E-RIVM [1997] Modelling of long-range transport of lindane and PCB with implementation of RIVM model of atmosphere-surface exchange, August